Quantitative Analysis of DNA Repair and p53 in Individual Human Cells

Galit Lahav Ketki Dinesh Verkhedkar

Quantitative analysis of DNA repair and p53 in individual human cells

Abstract

The goal of my research was to obtain a quantitative understanding of the mechanisms of DNA double-strand break (DSB) repair, and the activation of the tumor suppressor p53 in response to DSBs in human cells.

In Chapter 2, we investigated how the kinetics of repair, and the balance between the alternate DSB repair pathways, nonhomologous end-joining (NHEJ) and homologous recombination (HR), change with cell cycle progression. We developed fluorescent reporters to quantify DSBs, HR and cell cycle phase in individual, living cells. We show that the rates of DSB repair depend on the cell cycle stage at the time of damage. We find that NHEJ is the dominant repair mechanism in G1 and in G2 cells even in the presence of a functional HR pathway. S and G2 cells use both NHEJ and HR, and higher use of HR strongly correlates with slower repair. Further, we demonstrate that the balance between NHEJ and HR changes gradually with cell cycle progression, with a maximal use of HR at the peak of active replication in mid-S. Our results establish that the presence of a sister chromatid does not affect the use of HR in human cells.

Chapter 3 examines the sensitivity of the p53 pathway to DNA DSBs. We combined our fluorescent reporter for DSBs with a fluorescent reporter for p53, to quantify the level of damage and p53 activation in single cells. We find that the probability of inducing a p53 pulse increases linearly with the amount of damage. However, cancer cells do not have a distinct threshold of DSBs above which they uniformly induce p53 accumulation. We demonstrate that the decision to activate p53 is potentially controlled by cell-specific factors. Finally, we establish that the rates of DSB repair do not affect the decision to activate p53 or the dynamical properties of the p53 pulse.

Collectively, this work emphasizes the importance of collecting quantitative dynamic information in single cells in order to gain a comprehensive understanding of how different DNA damage response pathways function in a coordinated manner to maintain genomic integrity.

Table of Contents

List of Figures

Acknowledgements

Completing this PhD has been an incredible journey that would not have been possible without the support and contributions of a whole raft of people.

I will begin by expressing my deepest gratitude to my PhD advisor, Galit Lahav for her excellent advice and guidance throughout my dissertation work. Her uncanny ability to ask searching, difficult questions has undoubtedly strengthened my critical abilities, not to mention this work. Galit was a fabulous mentor: Perceptive, dynamic, approachable, and mindful of the things that truly matter.

I express my sincere thanks to the professors on my dissertation advisory committee, Tim Mitchison, Steve Elledge and Roy Kishony, for their invaluable scientific advice and encouragement throughout my graduate studies. I also thank the professors on my PhD committee, Ralph Scully, Angela DePace and Mike Springer for their time and effort in evaluating my work.

During my PhD I have collaborated with many colleagues for whom I have great regard. I extend my warmest thanks to Ran Kafri and Alexander Loewer for their contributions to my dissertation work. Ran and Alex are gifted scientists, and working closely with them has been instrumental in molding my personal scientific perspective. The 'Lahavians' are smart, effervescent people who are always enthusiastic to discuss science, research and life in general. I thank them for helping me with all aspects of science and for making my time at Harvard memorable. Dave Nelson took me under his wings as an inexperienced

rotation student and taught me many techniques I used in my research. Jeremy Purvis introduced me to the creative side of science and patiently taught me how to make scientific data look visually appealing. Caroline Mock ensured that the lab always ran smoothly and took on the formidable task of keeping us organized. A special thanks to them all.

My sincere gratitude goes out to all the people who took wonderful care of the logistical aspects of my PhD. I thank Samantha Reed for handling all the bureaucracy and paperwork related to graduate school. Thanks to Kathy Buhl, Tenzin Phulchung, Laura Lamp and other members of the lab-ops team for their help with reagents, ordering and product deliveries. I often called upon the prompt and excellent service provided by the Systems Biology IT personnel, Mason Miranda, Pam Needham and Zach Minton for all computer-related issues (and there were many!). I thank them for their support.

I am grateful to all my friends for making life as good as it is. Sara and Michael gave me a sense of home when I was new to Boston. I thank them for their hospitality and kindness and I will always remember our friendship with fondness. I thank Sudhakaran and Ruchi for their wonderful companionship, and little Soham for his unending supply of smiles and hugs. I am indebted to my life long friends and fellow PhD crusaders, Jayashree, Purbasha, Sindu and Vasanta, for their support and on-demand counseling sessions that kept up my enthusiasm for science on the days I wasn't feeling the love for it.

Last, and most importantly, heartfelt love and thanks to my mum and dad, Rohini and Dinesh Verkhedkar, for believing I could do it; my in-laws Bharathi and Subbarao Karanam for their encouragement; and my dear husband Sitaram for tirelessly supporting me in the pursuit of my dreams.

Chapter 1: Introduction

Part of the content in this chapter will be published as an invited review article in a special issue of:
Briefings in Functional Genomics (2013)

Authors: Ketki Karanam, Alexander Loewer, and Galit Lahav

Introduction to DNA double strand breaks

Even under the best of circumstances, our genetic material constantly incurs damage from a variety of endogenously generated and external agents. Every human cell can accumulate up to 10^5 spontaneous DNA lesions per day (Hoeijmakers, 2009). Of the diverse lesions that can be generated on a DNA molecule, DNA double strand breaks (DSBs), formed when both phosphodiester strands are broken at sites usually less than ten nucleotides apart, are considered the most harmful. Unrepaired DSBs can result in cell death and mis-repair of DSBs can generate gross chromosomal alterations that compromise our genetic integrity. Failure to detect and address DSBs in a timely and accurate manner can lead to developmental defects, immunodeficiency, sterility, radiosensitivity and cancer predisposition (Jackson and Bartek, 2009).

Inside cells, DNA is exposed to nucleases and metabolic products such as reactive oxygen and nitrogen species. These products introduce chemical modifications in the DNA, including modified bases and sugars, DNA intra- and inter-strand crosslinks, DNA-protein adducts, base-free sites and tandem lesions. DNA can also undergo spontaneous hydrolytic reactions and non-enzymatic methylations that generate thousands of base lesions per cell per day. DNA single strand breaks (SSBs) are commonly generated by free radical attack on DNA or when nucleases cut the phosphodiester backbone for the removal and repair of damaged bases. DSBs arise as an indirect consequence of two closely located SSBs, or when the DNA replication machinery attempts to replicate past SSBs and blocking lesions. SSBs and DSBs are also

occasionally introduced during DNA replication due to aborted topoisomerase I and topoisomerase II activity. Additionally, DSBs are directly generated as intermediates in developmentally regulated genome rearrangements such as meiotic recombination in germ cells (Richardson et al., 2004) and class switch recombination in maturing lymphocytes (Rooney et al., 2004). Other cellular processes including apoptotic DNA fragmentation (Rogakou et al., 2000), retroviral integration (Skalka and Katz, 2005), senescence (Sedelnikova et al., 2004) and dysfunctional telomeres (Hao et al., 2004) also provoke DSBs. Cellular stresses such as hyperosmotic stress (Kultz and Chakravarty, 2001), hypoxia (Hammond et al., 2003) and heat shock (Kaneko et al., 2005; Takahashi et al., 2004; Takahashi et al., 2008) induce the classical indicators of DSBs, however the mechanisms by which they generate DNA breaks is not clear.

Environmental agents such as ionizing radiation (IR), ultraviolet light (UV), and radiomimetic and chemotherapeutic drugs alter the chemical composition of the DNA backbone. IR, particularly X-rays, was the first environmental agent shown to be mutagenic in *Drosophila melanogaster* (Muller, 1927). We are constantly exposed to background levels of IR from cosmic radiation and from medical uses employing X-rays and radiography. IR can directly interact with and modify components of the DNA molecule. It also ionizes water molecules in the vicinity of DNA, producing free radicals that attack the hydrogen bonds in the DNA molecule. Drugs such as bleomycin and tirapazamine also act *via* the production of free radicals while etoposide and doxorubicin, which are commonly used in chemotherapy, are topoisomerase poisons that prevent topoisomerase II mediated DNA re-ligation. Other agents such as U.V. light which

produces SSBs, cyclobutane pyrimidine dimers and 6-4 photoproducts, crosslinking reagents such as cisplatin and actinomycin D, as well as alkylating agents such as N-methyl N'-nitro-N-nitrosoguanidine and adozelesin generate DSBs by impeding DNA replication.

The cellular response to DNA double strand breaks

To avoid the deleterious consequences of DNA DSBs, eukaryotic cells have evolved a complex response that works swiftly to address these potentially cytotoxic lesions. In the DNA damage response (DDR), several signaling pathways co-ordinate the rapid detection of DNA lesions, with the activation of repair machinery and the establishment of cellular checkpoints that temporarily delay the cell cycle (Figure1.1, Ciccia and Elledge, 2010; Harper and Elledge, 2007). In certain contexts, the DDR also initiates apoptotic programs to eliminate severely damaged cells that fail to restore genomic integrity and re-establish cellular homeostasis. Various sensors (proteins that detect the lesion), mediators (proteins that amplify the damage signal) and effectors (proteins that function in repair and checkpoint initiation) are recruited to chromatin regions surrounding the break site (Zhou and Elledge, 2000). Some proteins, particularly those involved in checkpoint signaling, re-localize to the DSB transiently for activation and subsequently diffuse to transmit the damage signal throughout the nucleus (Bekker-Jensen et al., 2006). Other proteins are recruited more stably and accumulate in large numbers to form macromolecular structures (called foci) around the break sites. Foci are microscopically discernible and serve as convenient markers for the location and number

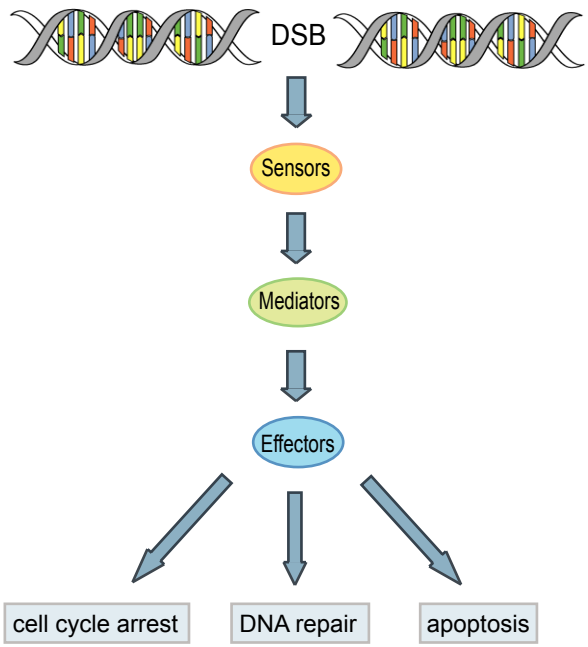

Figure 1.1: The general organization of the DNA damage response.

DSBs are recognized by a sensor, which transmits the signal downstream to mediator proteins. Mediator proteins amplify the damage signal and initiate signal transduction cascades that activate effector molecules to induce repair and execute cell cycle arrest or cell death if the damage is irreparable.

---

of DSBs. They are dynamic structures, in which numerous DDR factors assemble and disassemble in a precise spatio-temporal sequence that provides a kinetic choice of repair options (Polo and Jackson, 2011). During recruitment of DDR factors to the break site, large segments of chromatin are restructured in the vicinity of the DSB. This is mediated by a broad spectrum of post-translational modifications including phosphorylation, ubiquitination, sumoylation, acetylation and methylation. These modifications increase the accessibility of the damaged regions and allow the DDR proteins to be stably maintained at the break site (Ciccia and Elledge, 2010; Polo and Jackson, 2011).

The DDR is initiated when the primary sensor - the MRN (Mre11-Rad50-NBS1 in humans) complex, recognizes the DSB (Lavin, 2007). MRN then recruits ATM (ataxia-telangiectasia mutated), a member of the phosphatidylinositol 3-kinase related kinase (PIKK) family of serine/threonine kinases, to the break. ATM is activated by autophosphorylation at the DSB (Bakkenist and Kastan, 2003; Lee and Paull, 2007). It then phosphorylates and activates several proteins involved in repair, signaling and checkpoint activation (Derheimer and Kastan, 2010; Lavin, 2008; Lavin and Kozlov, 2007). The histone variant H2AX is a primary substrate of ATM; it is phosphorylated at serine 139 to generate a chromatin mark (γ-H2AX) that spreads to several megabases around the break (Rogakou et al., 1999; Rogakou et al., 1998; Stiff et al., 2004). γ-H2AX is subsequently bound by the mediator protein MDC1 (Lee et al., 2005; Lou et al., 2006; Stucki et al., 2005) which interacts with ATM and NBS1 (Chapman and Jackson, 2008; Lou et al., 2006; Melander et al., 2008; Spycher et al., 2008) to generate a positive feedback loop that amplifies the γ-H2AX signal and promotes additional recruitment of the interacting proteins (Lou et al., 2006). MDC1 itself is phosphorylated in an ATM-dependent manner (Goldberg et al., 2003; Stewart et al., 2003), and this modification stimulates binding by the E3 ubiquitin ligase RNF8, which initiates a ubiquitination cascade that further modifies γ-H2AX (Huen et al., 2007; Kolas et al., 2007; Mailand et al., 2007). Once phosphorylated and ubiquitylated, H2AX facilitates the stable recruitment of mediator proteins such as 53BP1 and BRCA1 that amplify the damage signal and regulate the DSB repair pathways (Ciccia and Elledge, 2010; Polo and Jackson, 2011). In addition to enabling chromatin-modifying activities and mediator protein recruitment; activated ATM also phosphorylates and activates the checkpoint

protein Chk2 (checkpoint kinase 2) and the tumor suppressor p53 (Lavin and Kozlov, 2007). Activation of these proteins elicits the rapid establishment of the G1/S and the G2/M cell cycle checkpoints and the execution of cellular programs that co-ordinate DNA repair with cell fate decisions.

A fully active DDR sets into motion DNA repair activities that work to restore an intact DNA molecule. Eukaryotic cells utilize two main pathways for DSB repair – nonhomologous end-joining (NHEJ) and homologous recombination (HR). These pathways are described below.

Double strand break repair by nonhomologous end-joining

The nonhomologous end-joining pathway is abundantly used for repairing DSBs in somatic cells of higher eukaryotes including mammals. Although the NHEJ machinery has been identified in bacteria (Weller et al., 2002) and in lower eukaryotes such as the yeasts *Saccharomyces cerevisiae* and *Saccharomyces pombe* (Boulton and Jackson, 1996; Feldmann et al., 1996; Herrmann et al., 1998; Manolis et al., 2001; Ramos et al., 1998; Schar et al., 1997; Teo and Jackson, 1997; Wilson et al., 1999), it is only considered to be a backup system for repairing DSBs in these organisms. NHEJ joins the two ends of a DSB through a largely homology independent process that proceeds through three stages: detection of the DSB and tethering/protection of the DNA ends; DNA end processing to remove damaged or non-ligatable groups and DNA ligation (Hartlerode and Scully, 2009; Lees-Miller and Meek, 2003; Lieber et al., 2003; Mahaney et al., 2009). Depending on

the specific sequences and chemical modifications generated at the DSB, NHEJ may be precise or mutagenic. The core NHEJ factors comprise the Ku70-Ku80 heterodimer (collectively called Ku), DNA-PKcs, and the XRCC4-Ligase IV complex.

NHEJ is initiated by the binding of Ku to both ends of the broken DNA molecule (Figure 1.2). Both Ku70 and Ku80 subunits of the Ku heterodimer contribute to a central, toroidal DNA binding core that slides over dsDNA in a sequence independent manner (Walker et al., 2001). Association of Ku with DNA ends serves as a scaffold for the assembly of the NHEJ synapse, and the Ku-DNA complex recruits DNA-PKcs, a member of the PIKK family of protein kinases (Gottlieb and Jackson, 1993). Ku then translocates inward on the DNA strand, allowing two DNA-PKcs molecules to contact DNA and interact across the DSB, forming a molecular bridge between the two DNA ends (DeFazio et al., 2002; Yoo and Dynan, 1999). The DNA-PKcs-Ku-DNA complex collectively forms the DNA-PK holoenzyme, which serves to tether the ends of the DSB together and is thought to protect the DNA ends from nuclease attack. The association of DNA-PKcs with both DNA and Ku leads to the activation of its serine/threonine kinase activity (Yaneva et al., 1997), promoting its autophosphorylation in trans across the DSB (Chan et al., 2002; Meek et al., 2007). This phosphorylation is essential for the release of the large DNA-PKcs molecules from the DNA ends, which promotes access to the termini and sets the stage for re-ligation of the broken DNA molecule (Block et al., 2004; Ding et al., 2003; Weterings et al., 2003). Before ligation can take place effectively, non-complementary ends must be processed into 5'-phosphorylated, ligatable ends. Since DSBs can occur with a variety of different ends, a number of processing enzymes may be required to

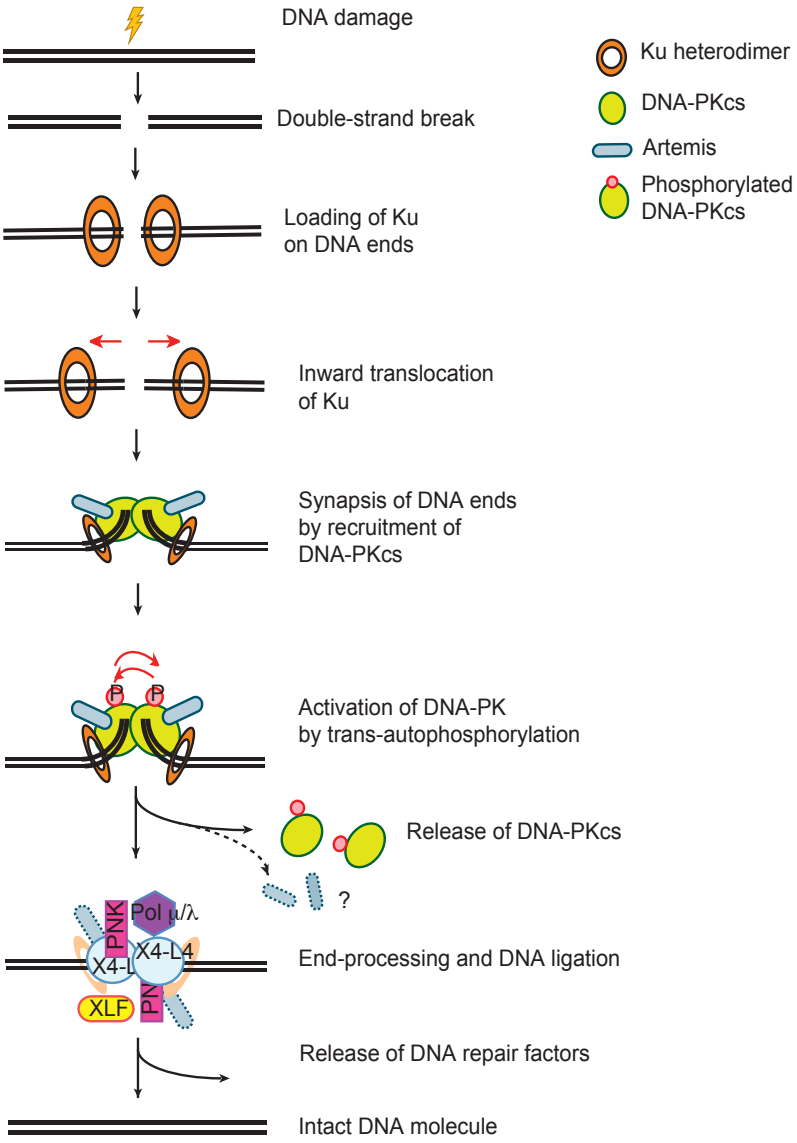

Figure 1.2: The Nonhomologous end-joining pathway of DNA double-strand break repair.

Induction of a DSB forms DNA ends that are bound by the Ku heterodimer. Bound Ku translocates inwards, allowing recruitment of DNA-PKcs to the extreme termini of the break. The end-processing enzyme Artemis is also recruited to the DSB in a complex with DNA-PKcs. Two DNA-PK molecules (DNA-PKcs bound to DNA-bound Ku) interact to tether the DSB ends together in synaptic complex. This triggers autophosphorylation of DNA-PKcs in trans, inducing a conformational change that causes a release of phosphorylated DNA-PKcs from the complex. It is unclear if Artemis is also released from the break site at the same time. Dissociation of DNA-PKcs from the DNA termini permits DNA end-processing enzymes such as polynucleotide kinase (PNK), DNA polymerases μ / λ and potentially others, to access the DNA ends and process them into compatible ends. The XRCC4-Ligase IV (X4-L4) complex in conjunction with XLF subsequently ligates the compatible ends to yield an intact DNA molecule.

remove blocking end groups, fill in gaps, and/or remove damaged DNA or secondary structure elements surrounding the break. In case of single-stranded overhangs, DNA termini can be made ligatable by either filling in the missing nucleotides or by resection of the overhang. DNA polymerases μ and λ, terminal deoxyribonucleotidyltransferase, polynucleotide kinase, and several nucleases have been shown to play a role in this processing (Mahaney et al., 2009). Another key enzyme Artemis, is recruited to the DSB in a complex with DNA-PKcs and plays a role in removal of single-stranded overhangs and hairpin structures in the DNA (Mahaney et al., 2009). Since NHEJ occurs in the absence of a DNA template or extended regions of homology, processing of the DNA ends has the potential to result in an alteration of the nucleotide sequence, making NHEJ an inherently error-prone process. After correct processing, the two tethered DNA termini can finally be ligated. The Ligase IV-XRCC4 complex mediates ligation, possibly in conjunction with XLF/Cernunnos to restore an intact DNA molecule (Grawunder et al., 1997; Gu et al., 2007).

An alternative end-joining pathway that directly ligates DNA ends in the absence of core NHEJ factors has been recently identified, however, whether this pathway functions in normal cells or only when classical NHEJ is deficient is not clear. This pathway, called alternative-NHEJ (alt-NHEJ) or microhomology mediated end-joining (MMEJ) involves distinct repair proteins including Poly-(ADP-ribose) polymerase-1 (PARP-1), DNA Ligase I/IIIα and XRCC1 and utilizes small sequence (5-25 nucleotide) microhomologies around the DSB to align broken strands of DNA (Hartlerode and Scully, 2009; McVey and Lee, 2008). After microhomology mediated annealing, the remaining non-

complementary DNA segments are removed prior to ligation resulting in deletions flanking the original break. Alt-NHEJ is therefore frequently associated with large chromosomal abnormalities such as deletions, translocations, inversions and other complex rearrangements.

Homology dependent pathways of double strand break repair

Repair of DSBs by HR involves an exchange or transfer of information between the damaged DNA molecule and an identical sequence located on another intact homologous partner which can be a sister chromatid, homologous chromosome or direct repeat on the same or different chromosome. HR is the oldest pathway of DSB repair and is conserved from bacteria to humans. It is also the primary DSB repair pathway in prokaryotes and lower eukaryotes (Dudas and Chovanec, 2004). A large proportion of the genes essential for HR were initially identified in the budding yeast *Saccharomyces cerevisiae* by employing classical genetic methods – isolation of mutants based on their sensitivity to DNA damaging agents such as IR, followed by in-depth epistasis analyses and cloning of the corresponding genes by complementation of the mutant phenotype. These genes are collectively referred to as the Rad52 (*Rad* stands for *radiation sensitivity*) epistasis group. HR mutants are extremely radiosensitive and embryonic lethal in mice (Dudas and Chovanec, 2004). Mutations in several HR proteins have also been directly linked with cancer predisposition and human disease (Ciccia and Elledge, 2010; Heyer et al., 2010).

HR is initiated by nucleolytic resection of the 5' DNA strands at the break site to generate single-stranded 3' overhangs (Figure 1.3, Paques and Haber, 1999). This is a complex and critical step involving helicase and nuclease activity. In humans, the MRN complex and CtIP trim the DNA to an intermediate form, followed by more extensive trimming by the Exo1 and Dna2 nucleases (Mimitou and Symington, 2009). The BLM helicase provides the essential helicase activity and the recruitment of CtIP to the damaged sites in humans is facilitated by the action of the E3 ubiquitin ligase BRCA1 (Breast cancer susceptibility gene 1, (Huen et al., 2010). The 3' single-stranded overhangs generated by resection are first coated by replication protein A (RPA) that eliminates secondary structures in these regions and protects them from degradation (Sung and Klein, 2006). RPA is subsequently replaced by multimers of the main recombinase enzyme Rad51 to form the recombinase filament. Loading Rad51 on the RPA coated single-stranded DNA (ssDNA) requires several accessory factors as RPA forms a kinetic barrier against Rad51 filament assembly. In mammals, six mediator proteins that promote Rad51 loading on the ssDNA have been identified – five of these are Rad51 paralogs RAD51B, RAD51C, RAD51D, XRCC2, XRCC3 and the sixth protein is the human Breast Cancer susceptibility protein BRCA2 (Heyer et al., 2010; Jensen et al., 2010; Li and Heyer, 2008). The exact function and interplay between the Rad51 paralogs in still poorly understood. BRCA2 promotes Rad51 filament nucleation at the ssDNA-dsDNA junction of the resected end (Jensen et al., 2010).

Once formed, the Rad51 coated recombinase filament mediates the core reactions of HR, which are homology searching and invasion of homologous duplex DNA to form a D-

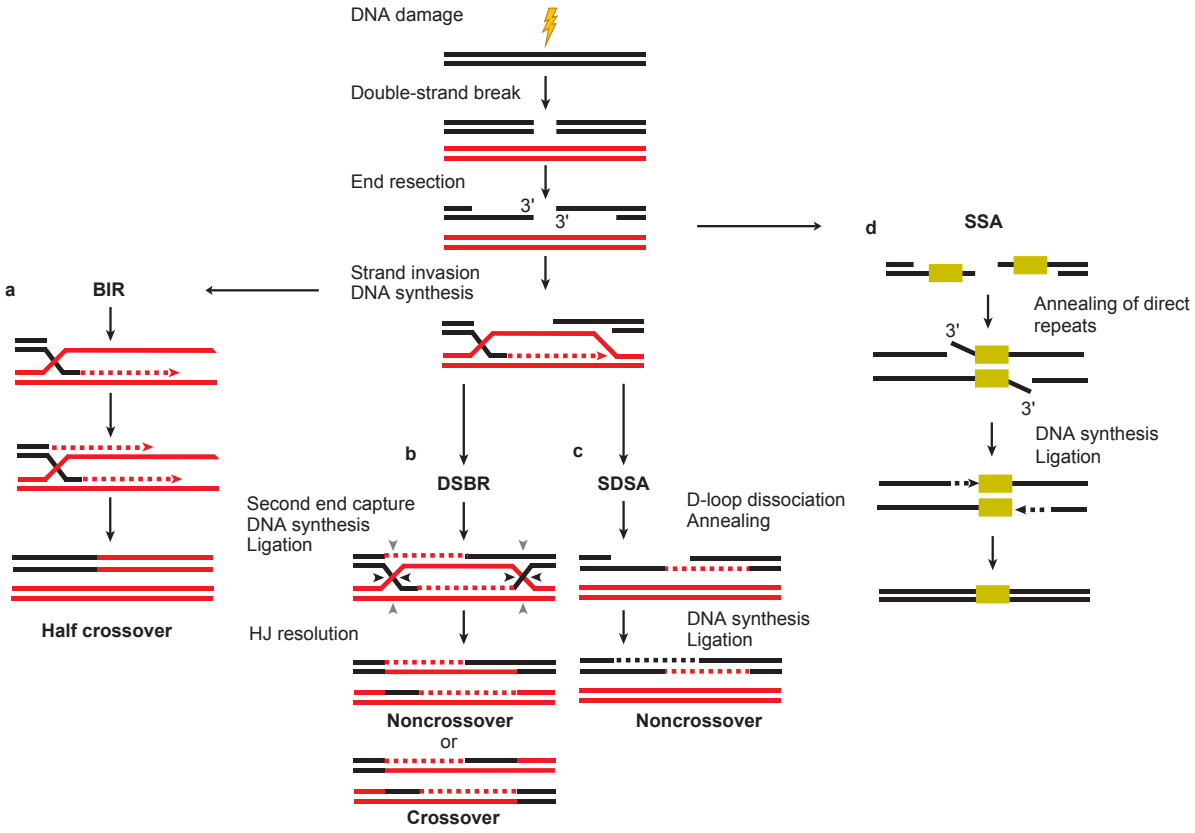

Figure 1.3: Pathways of homology-dependent DNA double-strand break repair.

DSBs can be repaired by distinct homology-dependent repair pathways, such as break induced replication (BIR, a), double-strand break repair (DSBR, b), synthesis-dependent strand annealing (SDSA, c), and single-strand annealing (SSA, d). After DSB formation, the DNA ends are resected to yield 3′ single-strand DNA (ssDNA) overhangs, which become the substrate for the HR protein machinery to execute strand invasion of a partner chromosome. After a successful homology search, strand invasion occurs to form a nascent D-loop structure. DNA synthesis then ensues. (a) In the absence of a second DNA end, the D-loop may become a full-fledged replication fork that proceeds till the end of the DNA molecule. This generates half-crossover products. (b) In the DSBR pathway, the second DSB end is captured to form an intermediate that harbors two Holliday junctions (HJ)s, accompanied by gap-filling DNA synthesis and ligation. The resolution of HJs by a specialized endonuclease can result in either noncrossover (black triangles) or crossover products (gray triangles). (c) Alternately, in the SDSA pathway, the D-loop is unwound and the freed ssDNA strand anneals with the complementary ssDNA strand that is associated with the other DSB end. The reaction is completed by gap-filling DNA synthesis and ligation. Only noncrossover products are formed. (d) When end-resection uncovers tandem repeats, they anneal together directly without requiring strand-invasion and D-loop formation. This is followed by trimming of the excess 3' tails, gap filling and ligation to yield an intact DNA molecule that has one less repeat than the original sequence.
Figure and legend adapted from (San Filippo et al., 2008).

loop intermediate (Heyer et al., 2010; West, 2003). Studies of the bacterial recombinase protein RecA suggest that the homology search probably occurs by random collisions between the nucleoprotein filament and duplex DNA where segments of the dsDNA are probed in an iterative fashion until homology is found (Bianco et al., 1998). When homology is established, the invading strand is used to prime repair synthesis by DNA polymerase (likely polymerase η in humans, McIlwraith et al., 2005). This leads to the formation of a D-loop intermediate. The Rad54 motor protein plays a key role in first stabilizing the Rad51 filament and enhancing D-loop formation and later for promoting the transition from DNA strand invasion to DNA synthesis by dissociating the Rad51 multimers from heteroduplex DNA (San Filippo et al., 2008). After the D-loop intermediate is formed, repair can proceed via many sub-pathways (Heyer et al., 2010; San Filippo et al., 2008). In the double strand break repair (DSBR) pathway, the invading strand captures the second DSB end by annealing to the extended D-loop and leads to the formation of two crossed strands or Holliday junctions (Figure 1.3, pathway b). The Holliday junctions may move along the DNA by branch migration to extend or shrink the region of heteroduplex DNA and are eventually resolved to generate crossover or non-crossover products. Alternately, the invading strand may be displaced to anneal with the second resected DSB end. This pathway of HR, called synthesis dependent strand annealing (SDSA), does not result in crossover products (Figure 1.3, pathway c). Under some circumstances, only one end of a DSB can be used for repair. This occurs when only one of the DSB ends shares homology with another region in the genome or when one end of a broken DNA molecule is lost. One-ended DSBs are also generated at collapsed replication forks in S phase and at telomeres that have lost their protective

telomeric repeats. In these cases, HR repair proceeds through the break-induced replication (BIR) pathway where the resected DSB end invades a homologous sequence and initiates unidirectional DNA synthesis from the site of strand invasion (Figure 1.3, pathway a). BIR usually proceeds for long distances, often covering the entire chromosome and may result in a large-scale loss of heterozygosity.

The last sub-pathway of homology-dependent repair does not require Rad51 filament formation and functions independent of strand invasion, D-loop extension and Holliday junction resolution. This pathway, known as single-strand annealing (SSA) occurs when 5' resection of DSB ends uncovers direct repeats flanking the break site (Figure 1.3, pathway d). In such cases, complementary strands from each repeat sequence can anneal together to repair the break in a reaction catalyzed by the Rad52 protein. This results in the deletion of one of the repeats. Protruding single-stranded tails that are not involved in annealing may be further trimmed by nucleases and the resulting gaps or nicks are filled in by DNA synthesis and ligation. As approximately 50% of the mammalian genome comprises repeat sequences (Lander et al., 2001), DSB repair by SSA, may potentially be a frequent source of mutagenesis.

Regulation of the DNA double strand break repair pathway choice

NHEJ and HR are both critical for maintaining genomic integrity and the two pathways cooperate to enhance the overall efficiency of DNA repair. Mutants in either pathway show increased radiosensitivity, and single knockouts of multiple proteins functioning in

either pathway (for e.g., Rad51, BRCA1, BRCA2, and XRCC2 in HR and DNA ligase IV and XRCC4 in NHEJ) are embryonic lethal in mice (Pierce et al., 2001b). Additionally, a concurrent loss of a protein from each pathway generates a more severe phenotype than the knockout of a single pathway alone. For example, chicken cells mutated for Rad54 and Ku70 or DNA-PKcs are acutely radiosensitive compared to single mutants (Fukushima et al., 2001; Takata et al., 1998) and embryonic fibroblasts deficient for both Rad54 and DNA ligase IV accrue high levels of spontaneous DNA damage and chromatid breaks (Mills et al., 2004). Similarly, mice with mutations in Rad54 and Ku80 exhibit decreased survival, increased accumulation of unrepaired DSBs and extreme radiosensitivity, while single mutants are viable (Couedel et al., 2004).

While both NHEJ and HR are crucial for DSB repair and survival, the two pathways are not always activated at the same time and are not completely redundant in the DSB substrates they repair. Several factors including the cell type and organism, nature of the lesion, the surrounding chromatin complexity and cell cycle phase regulate the activation of, and choice between pathways (Jeggo et al., 2011; Kass and Jasin, 2010; Shrivastav et al., 2008). Lower organisms such as bacteria and yeast rely heavily on HR, while NHEJ is the preferred pathway for repair in humans. Even within an organism, different tissues vary in their use of NHEJ and HR and the same tissue may employ different pathways depending on its developmental stage. This is particularly eminent in neuronal tissues, where developing neurons require functional HR in the early proliferative stages but switch to a greater use of NHEJ in the post-mitotic stages (Orii et al., 2006). Programmed DSBs are channeled into specific repair pathways in a regulated manner: DSBs generated

during V(D)J recombination in lymphocytes are repaired by NHEJ (Dudley et al., 2005) while DSBs generated during meiosis in eukaryotes are repaired exclusively by HR (Cole et al., 2010) .

More generally, cell cycle is the primary determinant of pathway choice. NHEJ operates throughout the cell cycle while HR is restricted to the S/G2 phases (Rothkamm et al., 2003). This restriction makes sense from the standpoint that the sister chromatid, which is the primary repair template, particularly in mammals, is not present in G1 cells. The earliest evidence of the differential usage of NHEJ and HR through the cell cycle was obtained from studies of mutant chicken DT40 cells. Cells deficient in NHEJ factors were found to be highly sensitive to IR in the G1 and early S phase of the cell cycle, whereas HR mutants were sensitive primarily in the S and G2 phases (Takata et al., 1998). This was further corroborated by the observation that mammalian cells deficient in NHEJ factors demonstrated reduced repair in all cell cycle stages, while HR deficient cells had a minor defect in G1, and a greater impairment in S/G2/M phases (Hinz et al., 2005; Rothkamm et al., 2003). Additionally, it was observed that DNA end-resection, accumulation of proteins in ssDNA compartments and Rad51 foci formation, which are key steps of the HR pathway, are temporally restricted to the S and G2 phases in yeast and in mammalian cells (Bekker-Jensen et al., 2006; Jazayeri et al., 2006; Lisby et al., 2004; Tashiro et al., 2000). Recent work suggests that this restriction of HR to post-replicative cell cycle phases is actively mediated by cylin dependent kinase (CDK) activity. Failure of G1 arrested yeast cells to initiate efficient end resection and load HR factors at an HO induced DSB locus correlates with low levels of active CDK1 (Aylon et

al., 2004). Consistent with this, inhibiting CDK1 activity in G2 cells also prevents end resection in this phase. Interestingly, in yeast, CDK1 activity is sufficient to initiate HR even in the absence of DNA replication, suggesting that the presence of replicated sister-chromatids does not influence the use of HR in these cells (Aylon et al., 2004). It is presently unclear if this is also the case in mammalian cells.

CDK1 controls HR by regulating a core protein of the DNA resection machinery - Sae2 in *Saccharomyces cerevisiae* / CtIP in humans (Huertas et al., 2008; Huertas and Jackson, 2009; Sartori et al., 2007). Cells expressing a non-phosphorylatable Sae2/CtIP protein demonstrate delayed HR; conversely, cells expressing constitutively phosphorylated Sae2/CtIP forms initiate end resection even in the absence of CDK activity and demonstrate accelerated HR in post-replicative cell cycle phases (Huertas et al., 2008; Huertas and Jackson, 2009). Phosphorylation of CtIP by CDK1 promotes its interaction with BRCA1 and facilitates its recruitment to break sites (Yu and Chen, 2004; Yun and Hiom, 2009). Additionally, CDK1 activity also regulates BRCA2-Rad51 interaction that may further control HR in mammalian cells (Esashi et al., 2005).

In the S and G2 phases when both NHEJ and HR are licensed to operate, the two pathways likely contend for access to individual break sites. Indeed, cells lacking functional NHEJ proteins reveal a DSB repair bias in favor of HR while end-resection mutants show increased frequencies of NHEJ, suggesting that these pathways normally compete for DSBs (Delacote et al., 2002; Huertas et al., 2008; Lee et al., 1998; Pierce et al., 2001a; Yun and Hiom, 2009). When both NHEJ and HR are active, other factors such

as the nature and location of the break may bias the use of pathways. NHEJ can swiftly repair breaks that have low complexity and are predominantly localized in easily accessible euchromatic regions. However, repair may not be readily achieved when breaks have 'dirty', non-ligatable ends such as those generated by heavy ions and high LET radiation or when breaks are generated in compacted heterochromatic regions. In these cases, NHEJ is aborted when it fails to ensure rapid repair and the breaks are subsequently directed to the HR pathway (Jeggo et al., 2011; Shibata et al., 2011). Another instance where the nature of the break directs a preferential use of a specific repair pathway is the use of HR for restoring collapsed replication forks in S phase (Petermann and Helleday, 2010). DSBs arising during DNA replication may typically be one ended, and necessitate repair by HR as NHEJ requires two free DNA duplex ends for repair.

Despite numerous mechanistic insights into the regulation of repair pathway choice, a clear picture of how individual cells balance NHEJ and HR with cell cycle progression is still lacking. With the current progress in live cell imaging techniques and single-cell approaches it is now feasible to capture the repair process over time in the same living cell. Such observations afford a more comprehensive understanding of the dynamics and interplay of different DSB repair pathways at different stages of repair, and in diverse cellular contexts.

The connection between DNA double strand breaks and the tumor suppressor p53

A primary outcome of the DNA damage response is the activation of cellular checkpoint mechanisms that link DNA lesions with effectors of cell fate (Figure 1.1, Zhou and Elledge, 2000). The most notable cell fate regulator activated by this response is the transcription factor and tumor suppressor p53. p53 is induced by diverse stresses that impact on cellular homeostatic mechanisms that monitor and control the fidelity of DNA replication, chromosome segregation and cell division (Vogelstein et al., 2000). Active p53 can execute distinct cellular programs that effect transient cell cycle arrest and DNA repair or result in irreversible outcomes such as cellular senescence and apoptosis (Riley et al., 2008). These functions of the p53 pathway are critical to maintaining genomic integrity, limiting oncogene activation and preventing tumorigenesis, and their importance is underscored by the fact that almost all human cancers contain a dysfunctional p53 pathway that permits unregulated proliferation of severely damaged cells (Jin and Levine, 2001). Activation of p53 and its network of genes in response to cellular stress also sets into motion an elaborate network of autoregulatory positive and negative feedback loops that ensure a complete execution of the p53 program or lead to reversal if the stress stimulus has been adequately addressed (Harris and Levine, 2005).

Under normal, unstressed conditions, p53 is kept at a low level, predominantly by its interaction with its negative regulator H/Mdm2 (human/mouse double minute 2) Mdm2 is a E3 ubiquitin ligase that tags p53 for degradation by the 26s proteasome (Kruse and Gu, 2009; Wu et al., 1993). Mdm2 is also a target gene of p53, and any increase in p53

levels leads to an increased transcription and production of mdm2, which in turn serves to lower p53 levels. In response to DNA damage, both the level of p53 as well as its transcriptional activity rapidly increases. Every type of DNA lesion including SSBs, DSBs, alkylated and depurinated bases, DNA crosslinks, and alterations of the deoxyribose sugar moiety is reported to the p53 pathway (Giaccia and Kastan, 1998; Gudkov and Komarova, 2003; Oren, 2003). However, the behavior of p53 post DNA damage is perhaps best characterized in response to DNA DSBs. In the presence of DSBs, induction of p53 is achieved by activation of the upstream mediators ATM and Chk2 that introduce post-translational modifications, specifically phosphorylations, on p53 and Mdm2 (Figure 1.4a, Banin et al., 1998; Canman et al., 1998; Chehab et al., 1999; Khosravi et al., 1999; Maya et al., 2001). These modifications disrupt p53-Mdm2 interaction and improve the stability of the p53 protein. Activated p53 exhibits a remarkable dynamic behavior, where the levels of p53 exhibit a series of undamped pulses in single cells (Lahav et al., 2004). p53 pulses have been observed in several transformed and non-transformed cells in culture (Hu et al., 2007; Lev Bar-Or et al., 2000; Loewer et al., 2010), as well as in a live mouse model (Hamstra et al., 2006). These pulses are generated in an excitable manner where a transient damage signal suffices to elicit a full p53 response (Batchelor et al., 2008; Loewer et al., 2010). The shape of the pulses is regulated by a combination of two negative feedbacks - the negative feedback between p53 and Mdm2, and an additional negative feedback between p53 and its upstream modulators ATM and Chk2 (Batchelor et al., 2008). Active p53 transcribes a phosphatase WIP1 that abrogates ATM and Chk2 phosphorylation, in addition to dephosphorylating p53 and Mdm2 (Fiscella et al., 1997; Lu et al., 2007; Shreeram et al.,

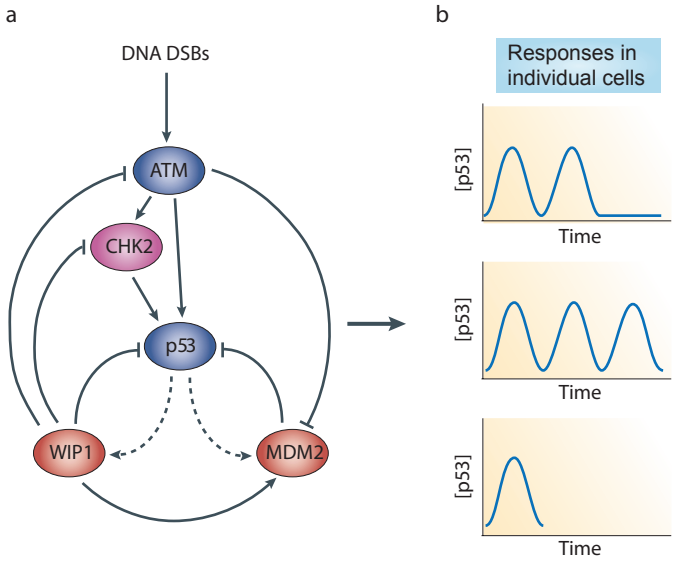

Figure 1.4: The response of p53 to DNA double-strand breaks.

(a) In response to DSBs ATM kinase is activated, and activates Chk2. Both of these kinases upregulate p53 by disrupting its interaction with one of its target genes, the E3 ubiquitin ligase Mdm2. p53 also upregulates the transcription of the phosphatase Wip1 which negatively feeds back on the entire circuit by dephosphorylating ATM, Chk2, p53 and Mdm2. Solid lines represent protein–protein interactions, dashed lines represent transcriptional activation. (b) Single cell measurements of p53 levels show a series of undamped pulses with different cells showing different numbers of pulses to the same damage dose. Figure and legend adapted from (Batchelor et al., 2009)

2006). This results in an oscillatory behavior of the ATM and Chk2 activities, which is transmitted downstream to p53 (Batchelor et al., 2008). Characterization of individual p53 pulses reveals that they have fixed amplitude and duration, which are independent of the damage dose (Lahav et al., 2004). However, the number of p53 pulses increases with greater amounts of damage. Interestingly, genetically identical cells exposed to the same DNA damage dose exhibit varying number of p53 pulses (Figure 1.4b). It is unknown whether these cell-to-cell differences in p53 behavior result from a differential sensitivity

of individual cells to the same damage stimulus or arise from differences in their p53 and/or other cellular networks. A rigorous quantitative assessment of the relationship between DSBs and p53 activation in single cells will provide insights into the sensitivity of the p53 network and enable a detailed understanding of p53 activation in response to DNA damage.

This Work

Chapter 2 (Published in Molecular Cell, 2012)

In this chapter we examine the effect of cell cycle on the rates of DNA DSB repair and the balance between NHEJ and HR in asynchronous, individual, living cells. To quantify these events in living cells, we developed a clonal U2OS cell-line that stably expresses fluorescent-tagged Geminin, 53BP1 and Rad52 that serve as markers for cell cycle stage, total number of DSBs and HR respectively. Using long-term time-lapse microscopy, we first show that cells damaged in different cell cycle stages vary in their kinetics of repair. Surprisingly, we find that cells damaged within S phase also exhibit a large variation in their rates of repair with cells damaged at mid-S repairing the slowest amongst all cells. This suggests that in S phase, the kinetics of repair are determined by the exact cell cycle position at the time of damage.

Next, we show that the levels of HR change gradually with cell cycle progression. HR is activated as cells undergo the G1/S transition, following which its levels increase and peak at mid-S and then gradually decline towards late-S and G2. High proportions of HR in mid-S correlate with slower repair and high levels of active DNA replication. HR does not capture all breaks in a cell, rather S and G2 cells utilize both NHEJ and HR for repair. Additionally, NHEJ is the predominant repair pathway in G2 cells even when HR is functional. Our results demonstrate that the choice of repair mechanism is continuously adjusted throughout the cell cycle and suggest that the extent of active replication, rather than the presence of a sister chromatid influences the balance between the two repair

pathways in human cells. This study emphasizes the importance of collecting quantitative dynamic information at a single cell resolution for understanding the complex regulation and interplay of the DNA repair pathways.

Chapter 3

In chapter 3, we investigate the quantitative relationship between DSBs and the activation of the tumor suppressor p53 in single cells. Previous studies have demonstrated that genetically identical cells exposed to the same damage stimulus are highly diverse in their p53 response, where some cells show no p53 pulse and others exhibit a varying number of pulses. We hypothesized that these differences potentially arise from cell-to-cell heterogeneity in the number of DSBs and their rates of repair. p53 may only be activated above a threshold number of DSBs or in cells that have slower repair. To monitor the number of DNA DSBs, their repair, and p53 activation in individual cells, we combined the 53BP1 reporter developed in Chapter 2 with a fluorescent reporter for p53 in a stable, clonal MCF7 breast carcinoma cell-line. We found that, in response to a uniform damage dose, individual cells indeed vary in their initial number of DSBs and their rates of repair. The probability of inducing a p53 pulse increases linearly with the number of DSBs. Surprisingly, we did not detect a clear threshold of DSBs, above which all cells unanimously initiate a p53 pulse immediately after damage. This suggests that other factors such as the rates of repair or the cell cycle phase might influence a cell's decision to pulse after damage. It is also possible that p53 pulses are generated primarily in a stochastic manner.

We explored this possibility and found that the decision to pulse is not entirely stochastic, but is potentially affected by internal cellular factors. We investigated the rates of repair as a potential factor that affects this decision. We found that the induction of p53 is insensitive to the half-life of DSBs as demonstrated by a lack of correlation between the rates of repair and the probability of generating an initial p53 pulse. Additionally, the rate of repair also did not affect the amplitude and duration of the p53 pulse. To probe this further by generating a longer delay in DSB joining, we knocked down XRCC4, a key protein in the NHEJ repair pathway. Unexpectedly, a reduced expression of XRCC4 did not significantly decrease the rates of DSB repair in our system. However, reducing the efficiency of the NHEJ pathway remarkably increased the duration of the initial p53 pulse. We are currently exploring other potential factors that affect the activation of p53 in response to DNA DSBs. Such an assessment of factors that impact on p53 behavior will offer important insights into the sensitivity of the p53 network to DNA damage.

Chapter 4

In chapter 4, I summarize and discuss the key findings from chapters 2 and 3 in the broader perspective of genomic instability and cancer. I describe how several types of cancer rely on a reduced subset of repair proteins to survive DNA damage. A comprehensive understanding of the natural balance between different repair pathways, as well as their ability to compensate for each other in altered cellular contexts is essential to grasp the beginnings of genomic instability in cancer and also for designing more selective therapies. The work described in Chapter 2 presents a step forward in this

direction. Cancer cells also exhibit remarkable heterogeneity in their response to drug treatment, such that chemotherapy only achieves a fractional killing of tumor cells. While heterogeneity in a tumor may arise directly from genetic sources, it is possible that isogenic cells also vary in their sensitivity to a chemotherapeutic agent. We explore this possibility in Chapter 3, and provide a rigorous quantitative assessment of how p53, an effector of cell fate decisions, is activated in response to DNA damage. An advanced understanding of the factors that influence the induction of p53 to mediate cell death or survival will enable the identification of drug regimes and strategies that effect maximal cell killing in tumors.

I conclude this chapter with a note on the power of live cell imaging and single cell analyses in probing the dynamic behavior of cellular signaling pathways; and discuss how these methods can be effectively applied towards answering other fundamental questions in the DNA repair field.

Attributions for Chapters 2 and 3

The work presented in Chapter 2 was done in collaboration with Ran Kafri and Alexander Loewer, postdoctoral fellows at the Department of Systems Biology at Harvard. I developed the experimental system, and designed and performed all experiments. Ran developed the image analysis software for data acquisition and analysis. Ran and I contributed equally to the data analysis and interpretation. Alexander initiated the project and also contributed to discussions regarding experimental design and data interpretation.

The work presented in Chapter 3 was done in collaboration with Alexander Loewer. Alexander initiated the project and developed the experimental system and image analysis algorithms. Alexander and I both performed experiments and contributed equally to experimental design, data acquisition, analysis and interpretation of results.

References

Aylon, Y., Liefshitz, B., and Kupiec, M. (2004). The CDK regulates repair of double-strand breaks by homologous recombination during the cell cycle. Embo J *23*, 4868-4875.

Bakkenist, C.J., and Kastan, M.B. (2003). DNA damage activates ATM through intermolecular autophosphorylation and dimer dissociation. Nature *421*, 499-506.

Banin, S., Moyal, L., Shieh, S., Taya, Y., Anderson, C.W., Chessa, L., Smorodinsky, N.I., Prives, C., Reiss, Y., Shiloh, Y.*, et al.* (1998). Enhanced phosphorylation of p53 by ATM in response to DNA damage. Science *281*, 1674-1677.

Batchelor, E., Loewer, A., and Lahav, G. (2009). The ups and downs of p53: understanding protein dynamics in single cells. Nat Rev Cancer *9*, 371-377.

Batchelor, E., Mock, C.S., Bhan, I., Loewer, A., and Lahav, G. (2008). Recurrent initiation: a mechanism for triggering p53 pulses in response to DNA damage. Mol Cell *30*, 277-289.

Bekker-Jensen, S., Lukas, C., Kitagawa, R., Melander, F., Kastan, M.B., Bartek, J., and Lukas, J. (2006). Spatial organization of the mammalian genome surveillance machinery in response to DNA strand breaks. J Cell Biol *173*, 195-206.

Bianco, P.R., Tracy, R.B., and Kowalczykowski, S.C. (1998). DNA strand exchange proteins: a biochemical and physical comparison. Front Biosci *3*, D570-603.

Block, W.D., Yu, Y., Merkle, D., Gifford, J.L., Ding, Q., Meek, K., and Lees-Miller, S.P. (2004). Autophosphorylation-dependent remodeling of the DNA-dependent protein kinase catalytic subunit regulates ligation of DNA ends. Nucleic Acids Res *32*, 4351-4357.

Boulton, S.J., and Jackson, S.P. (1996). Identification of a Saccharomyces cerevisiae Ku80 homologue: roles in DNA double strand break rejoining and in telomeric maintenance. Nucleic Acids Res *24*, 4639-4648.

Canman, C.E., Lim, D.S., Cimprich, K.A., Taya, Y., Tamai, K., Sakaguchi, K., Appella, E., Kastan, M.B., and Siliciano, J.D. (1998). Activation of the ATM kinase by ionizing radiation and phosphorylation of p53. Science *281*, 1677-1679.

Chan, D.W., Chen, B.P., Prithivirajsingh, S., Kurimasa, A., Story, M.D., Qin, J., and Chen, D.J. (2002). Autophosphorylation of the DNA-dependent protein kinase catalytic subunit is required for rejoining of DNA double-strand breaks. Genes Dev *16*, 2333-2338.

Chapman, J.R., and Jackson, S.P. (2008). Phospho-dependent interactions between NBS1 and MDC1 mediate chromatin retention of the MRN complex at sites of DNA damage. EMBO Rep *9*, 795-801.

Chehab, N.H., Malikzay, A., Stavridi, E.S., and Halazonetis, T.D. (1999). Phosphorylation of Ser-20 mediates stabilization of human p53 in response to DNA damage. Proc Natl Acad Sci U S A *96*, 13777-13782.

Ciccia, A., and Elledge, S.J. (2010). The DNA damage response: making it safe to play with knives. Mol Cell *40*, 179-204.

Cole, F., Keeney, S., and Jasin, M. (2010). Evolutionary conservation of meiotic DSB proteins: more than just Spo11. Genes Dev *24*, 1201-1207.

Couedel, C., Mills, K.D., Barchi, M., Shen, L., Olshen, A., Johnson, R.D., Nussenzweig, A., Essers, J., Kanaar, R., Li, G.C., *et al.* (2004). Collaboration of homologous recombination and nonhomologous end-joining factors for the survival and integrity of mice and cells. Genes Dev *18*, 1293-1304.

DeFazio, L.G., Stansel, R.M., Griffith, J.D., and Chu, G. (2002). Synapsis of DNA ends by DNA-dependent protein kinase. Embo J *21*, 3192-3200.

Delacote, F., Han, M., Stamato, T.D., Jasin, M., and Lopez, B.S. (2002). An xrcc4 defect or Wortmannin stimulates homologous recombination specifically induced by double-strand breaks in mammalian cells. Nucleic Acids Res *30*, 3454-3463.

Derheimer, F.A., and Kastan, M.B. (2010). Multiple roles of ATM in monitoring and maintaining DNA integrity. FEBS Lett *584*, 3675-3681.

Ding, Q., Reddy, Y.V., Wang, W., Woods, T., Douglas, P., Ramsden, D.A., Lees-Miller, S.P., and Meek, K. (2003). Autophosphorylation of the catalytic subunit of the DNA-dependent protein kinase is required for efficient end processing during DNA double-strand break repair. Mol Cell Biol *23*, 5836-5848.

Dudas, A., and Chovanec, M. (2004). DNA double-strand break repair by homologous recombination. Mutat Res *566*, 131-167.

Dudley, D.D., Chaudhuri, J., Bassing, C.H., and Alt, F.W. (2005). Mechanism and control of V(D)J recombination versus class switch recombination: similarities and differences. Adv Immunol *86*, 43-112.

Esashi, F., Christ, N., Gannon, J., Liu, Y., Hunt, T., Jasin, M., and West, S.C. (2005). CDK-dependent phosphorylation of BRCA2 as a regulatory mechanism for recombinational repair. Nature *434*, 598-604.

Feldmann, H., Driller, L., Meier, B., Mages, G., Kellermann, J., and Winnacker, E.L. (1996). HDF2, the second subunit of the Ku homologue from Saccharomyces cerevisiae. J Biol Chem *271*, 27765-27769.

Fiscella, M., Zhang, H., Fan, S., Sakaguchi, K., Shen, S., Mercer, W.E., Vande Woude, G.F., O'Connor, P.M., and Appella, E. (1997). Wip1, a novel human protein phosphatase that is induced in response to ionizing radiation in a p53-dependent manner. Proc Natl Acad Sci U S A *94*, 6048-6053.

Fukushima, T., Takata, M., Morrison, C., Araki, R., Fujimori, A., Abe, M., Tatsumi, K., Jasin, M., Dhar, P.K., Sonoda, E*., et al.* (2001). Genetic analysis of the DNA-dependent protein kinase reveals an inhibitory role of Ku in late S-G2 phase DNA double-strand break repair. J Biol Chem *276*, 44413-44418.

Giaccia, A.J., and Kastan, M.B. (1998). The complexity of p53 modulation: emerging patterns from divergent signals. Genes Dev *12*, 2973-2983.

Goldberg, M., Stucki, M., Falck, J., D'Amours, D., Rahman, D., Pappin, D., Bartek, J., and Jackson, S.P. (2003). MDC1 is required for the intra-S-phase DNA damage checkpoint. Nature *421*, 952-956.

Gottlieb, T.M., and Jackson, S.P. (1993). The DNA-dependent protein kinase: requirement for DNA ends and association with Ku antigen. Cell *72*, 131-142.

Grawunder, U., Wilm, M., Wu, X., Kulesza, P., Wilson, T.E., Mann, M., and Lieber, M.R. (1997). Activity of DNA ligase IV stimulated by complex formation with XRCC4 protein in mammalian cells. Nature *388*, 492-495.

Gu, J., Lu, H., Tsai, A.G., Schwarz, K., and Lieber, M.R. (2007). Single-stranded DNA ligation and XLF-stimulated incompatible DNA end ligation by the XRCC4-DNA ligase IV complex: influence of terminal DNA sequence. Nucleic Acids Res *35*, 5755-5762.

Gudkov, A.V., and Komarova, E.A. (2003). The role of p53 in determining sensitivity to radiotherapy. Nat Rev Cancer *3*, 117-129.

Hammond, E.M., Dorie, M.J., and Giaccia, A.J. (2003). ATR/ATM targets are phosphorylated by ATR in response to hypoxia and ATM in response to reoxygenation. J Biol Chem *278*, 12207-12213.

Hamstra, D.A., Bhojani, M.S., Griffin, L.B., Laxman, B., Ross, B.D., and Rehemtulla, A. (2006). Real-time evaluation of p53 oscillatory behavior in vivo using bioluminescent imaging. Cancer Res *66*, 7482-7489.

Hao, L.Y., Strong, M.A., and Greider, C.W. (2004). Phosphorylation of H2AX at short telomeres in T cells and fibroblasts. J Biol Chem *279*, 45148-45154.

Harper, J.W., and Elledge, S.J. (2007). The DNA damage response: ten years after. Mol Cell *28*, 739-745.

Harris, S.L., and Levine, A.J. (2005). The p53 pathway: positive and negative feedback loops. Oncogene *24*, 2899-2908.

Hartlerode, A.J., and Scully, R. (2009). Mechanisms of double-strand break repair in somatic mammalian cells. Biochem J *423*, 157-168.

Herrmann, G., Lindahl, T., and Schar, P. (1998). Saccharomyces cerevisiae LIF1: a function involved in DNA double-strand break repair related to mammalian XRCC4. Embo J *17*, 4188-4198.

Heyer, W.D., Ehmsen, K.T., and Liu, J. (2010). Regulation of homologous recombination in eukaryotes. Annu Rev Genet *44*, 113-139.

Hinz, J.M., Yamada, N.A., Salazar, E.P., Tebbs, R.S., and Thompson, L.H. (2005). Influence of double-strand-break repair pathways on radiosensitivity throughout the cell cycle in CHO cells. DNA Repair (Amst) *4*, 782-792.

Hoeijmakers, J.H. (2009). DNA damage, aging, and cancer. N Engl J Med *361*, 1475-1485.

Hu, W., Feng, Z., Ma, L., Wagner, J., Rice, J.J., Stolovitzky, G., and Levine, A.J. (2007). A single nucleotide polymorphism in the MDM2 gene disrupts the oscillation of p53 and MDM2 levels in cells. Cancer Res *67*, 2757-2765.

Huen, M.S., Grant, R., Manke, I., Minn, K., Yu, X., Yaffe, M.B., and Chen, J. (2007). RNF8 transduces the DNA-damage signal via histone ubiquitylation and checkpoint protein assembly. Cell *131*, 901-914.

Huen, M.S., Sy, S.M., and Chen, J. (2010). BRCA1 and its toolbox for the maintenance of genome integrity. Nat Rev Mol Cell Biol *11*, 138-148.

Huertas, P., Cortes-Ledesma, F., Sartori, A.A., Aguilera, A., and Jackson, S.P. (2008). CDK targets Sae2 to control DNA-end resection and homologous recombination. Nature *455*, 689-692.

Huertas, P., and Jackson, S.P. (2009). Human CtIP mediates cell cycle control of DNA end resection and double strand break repair. J Biol Chem *284*, 9558-9565.

Jackson, S.P., and Bartek, J. (2009). The DNA-damage response in human biology and disease. Nature *461*, 1071-1078.

Jazayeri, A., Falck, J., Lukas, C., Bartek, J., Smith, G.C., Lukas, J., and Jackson, S.P. (2006). ATM- and cell cycle-dependent regulation of ATR in response to DNA double-strand breaks. Nat Cell Biol *8*, 37-45.

Jeggo, P.A., Geuting, V., and Lobrich, M. (2011). The role of homologous recombination in radiation-induced double-strand break repair. Radiother Oncol *101*, 7-12.

Jensen, R.B., Carreira, A., and Kowalczykowski, S.C. (2010). Purified human BRCA2 stimulates RAD51-mediated recombination. Nature *467*, 678-683.

Jin, S., and Levine, A.J. (2001). The p53 functional circuit. J Cell Sci *114*, 4139-4140.

Kaneko, H., Igarashi, K., Kataoka, K., and Miura, M. (2005). Heat shock induces phosphorylation of histone H2AX in mammalian cells. Biochem Biophys Res Commun *328*, 1101-1106.

Kass, E.M., and Jasin, M. (2010). Collaboration and competition between DNA double-strand break repair pathways. FEBS Lett *584*, 3703-3708.

Khosravi, R., Maya, R., Gottlieb, T., Oren, M., Shiloh, Y., and Shkedy, D. (1999). Rapid ATM-dependent phosphorylation of MDM2 precedes p53 accumulation in response to DNA damage. Proc Natl Acad Sci U S A *96*, 14973-14977.

Kolas, N.K., Chapman, J.R., Nakada, S., Ylanko, J., Chahwan, R., Sweeney, F.D., Panier, S., Mendez, M., Wildenhain, J., Thomson, T.M.*, et al.* (2007). Orchestration of the DNA-damage response by the RNF8 ubiquitin ligase. Science *318*, 1637-1640.

Kruse, J.P., and Gu, W. (2009). Modes of p53 regulation. Cell *137*, 609-622.

Kultz, D., and Chakravarty, D. (2001). Hyperosmolality in the form of elevated NaCl but not urea causes DNA damage in murine kidney cells. Proc Natl Acad Sci U S A *98*, 1999-2004.

Lahav, G., Rosenfeld, N., Sigal, A., Geva-Zatorsky, N., Levine, A.J., Elowitz, M.B., and Alon, U. (2004). Dynamics of the p53-Mdm2 feedback loop in individual cells. Nat Genet *36*, 147-150.

Lander, E.S., Linton, L.M., Birren, B., Nusbaum, C., Zody, M.C., Baldwin, J., Devon, K., Dewar, K., Doyle, M., FitzHugh, W.*, et al.* (2001). Initial sequencing and analysis of the human genome. Nature *409*, 860-921.

Lavin, M.F. (2007). ATM and the Mre11 complex combine to recognize and signal DNA double-strand breaks. Oncogene *26*, 7749-7758.

Lavin, M.F. (2008). Ataxia-telangiectasia: from a rare disorder to a paradigm for cell signalling and cancer. Nat Rev Mol Cell Biol *9*, 759-769.

Lavin, M.F., and Kozlov, S. (2007). ATM activation and DNA damage response. Cell Cycle *6*, 931-942.

Lee, J.H., and Paull, T.T. (2007). Activation and regulation of ATM kinase activity in response to DNA double-strand breaks. Oncogene *26*, 7741-7748.

Lee, M.S., Edwards, R.A., Thede, G.L., and Glover, J.N. (2005). Structure of the BRCT repeat domain of MDC1 and its specificity for the free COOH-terminal end of the gamma-H2AX histone tail. J Biol Chem *280*, 32053-32056.

Lee, S.E., Moore, J.K., Holmes, A., Umezu, K., Kolodner, R.D., and Haber, J.E. (1998). Saccharomyces Ku70, mre11/rad50 and RPA proteins regulate adaptation to G2/M arrest after DNA damage. Cell *94*, 399-409.

Lees-Miller, S.P., and Meek, K. (2003). Repair of DNA double strand breaks by non-homologous end joining. Biochimie *85*, 1161-1173.

Lev Bar-Or, R., Maya, R., Segel, L.A., Alon, U., Levine, A.J., and Oren, M. (2000). Generation of oscillations by the p53-Mdm2 feedback loop: a theoretical and experimental study. Proc Natl Acad Sci U S A *97*, 11250-11255.

Li, X., and Heyer, W.D. (2008). Homologous recombination in DNA repair and DNA damage tolerance. Cell Res *18*, 99-113.

Lieber, M.R., Ma, Y., Pannicke, U., and Schwarz, K. (2003). Mechanism and regulation of human non-homologous DNA end-joining. Nat Rev Mol Cell Biol *4*, 712-720.

Lisby, M., Barlow, J.H., Burgess, R.C., and Rothstein, R. (2004). Choreography of the DNA damage response: spatiotemporal relationships among checkpoint and repair proteins. Cell *118*, 699-713.

Loewer, A., Batchelor, E., Gaglia, G., and Lahav, G. (2010). Basal dynamics of p53 reveal transcriptionally attenuated pulses in cycling cells. Cell *142*, 89-100.

Lou, Z., Minter-Dykhouse, K., Franco, S., Gostissa, M., Rivera, M.A., Celeste, A., Manis, J.P., van Deursen, J., Nussenzweig, A., Paull, T.T.*, et al.* (2006). MDC1 maintains genomic stability by participating in the amplification of ATM-dependent DNA damage signals. Mol Cell *21*, 187-200.

Lu, X., Ma, O., Nguyen, T.A., Jones, S.N., Oren, M., and Donehower, L.A. (2007). The Wip1 Phosphatase acts as a gatekeeper in the p53-Mdm2 autoregulatory loop. Cancer Cell *12*, 342-354.

Mahaney, B.L., Meek, K., and Lees-Miller, S.P. (2009). Repair of ionizing radiation-induced DNA double-strand breaks by non-homologous end-joining. Biochem J *417*, 639-650.

Mailand, N., Bekker-Jensen, S., Faustrup, H., Melander, F., Bartek, J., Lukas, C., and Lukas, J. (2007). RNF8 ubiquitylates histones at DNA double-strand breaks and promotes assembly of repair proteins. Cell *131*, 887-900.

Manolis, K.G., Nimmo, E.R., Hartsuiker, E., Carr, A.M., Jeggo, P.A., and Allshire, R.C. (2001). Novel functional requirements for non-homologous DNA end joining in Schizosaccharomyces pombe. Embo J *20*, 210-221.

Maya, R., Balass, M., Kim, S.T., Shkedy, D., Leal, J.F., Shifman, O., Moas, M., Buschmann, T., Ronai, Z., Shiloh, Y.*, et al.* (2001). ATM-dependent phosphorylation of Mdm2 on serine 395: role in p53 activation by DNA damage. Genes Dev *15*, 1067-1077.

McIlwraith, M.J., Vaisman, A., Liu, Y., Fanning, E., Woodgate, R., and West, S.C. (2005). Human DNA polymerase eta promotes DNA synthesis from strand invasion intermediates of homologous recombination. Mol Cell *20*, 783-792.

McVey, M., and Lee, S.E. (2008). MMEJ repair of double-strand breaks (director's cut): deleted sequences and alternative endings. Trends Genet *24*, 529-538.

Meek, K., Douglas, P., Cui, X., Ding, Q., and Lees-Miller, S.P. (2007). trans Autophosphorylation at DNA-dependent protein kinase's two major autophosphorylation site clusters facilitates end processing but not end joining. Mol Cell Biol *27*, 3881-3890.

Melander, F., Bekker-Jensen, S., Falck, J., Bartek, J., Mailand, N., and Lukas, J. (2008). Phosphorylation of SDT repeats in the MDC1 N terminus triggers retention of NBS1 at the DNA damage-modified chromatin. J Cell Biol *181*, 213-226.

Mills, K.D., Ferguson, D.O., Essers, J., Eckersdorff, M., Kanaar, R., and Alt, F.W. (2004). Rad54 and DNA Ligase IV cooperate to maintain mammalian chromatid stability. Genes Dev *18*, 1283-1292.

Mimitou, E.P., and Symington, L.S. (2009). DNA end resection: many nucleases make light work. DNA Repair (Amst) *8*, 983-995.

Muller, H.J. (1927). Artificial Transmutation of the Gene. Science *66*, 84-87.

Oren, M. (2003). Decision making by p53: life, death and cancer. Cell Death Differ *10*, 431-442.

Orii, K.E., Lee, Y., Kondo, N., and McKinnon, P.J. (2006). Selective utilization of nonhomologous end-joining and homologous recombination DNA repair pathways during nervous system development. Proc Natl Acad Sci U S A *103*, 10017-10022.

Paques, F., and Haber, J.E. (1999). Multiple pathways of recombination induced by double-strand breaks in Saccharomyces cerevisiae. Microbiol Mol Biol Rev *63*, 349-404.

Petermann, E., and Helleday, T. (2010). Pathways of mammalian replication fork restart. Nat Rev Mol Cell Biol *11*, 683-687.

Pierce, A.J., Hu, P., Han, M., Ellis, N., and Jasin, M. (2001a). Ku DNA end-binding protein modulates homologous repair of double-strand breaks in mammalian cells. Genes Dev *15*, 3237-3242.

Pierce, A.J., Stark, J.M., Araujo, F.D., Moynahan, M.E., Berwick, M., and Jasin, M. (2001b). Double-strand breaks and tumorigenesis. Trends Cell Biol *11*, S52-59.

Polo, S.E., and Jackson, S.P. (2011). Dynamics of DNA damage response proteins at DNA breaks: a focus on protein modifications. Genes Dev *25*, 409-433.

Ramos, W., Liu, G., Giroux, C.N., and Tomkinson, A.E. (1998). Biochemical and genetic characterization of the DNA ligase encoded by Saccharomyces cerevisiae open reading frame YOR005c, a homolog of mammalian DNA ligase IV. Nucleic Acids Res *26*, 5676-5683.

Richardson, C., Horikoshi, N., and Pandita, T.K. (2004). The role of the DNA double-strand break response network in meiosis. DNA Repair (Amst) *3*, 1149-1164.

Riley, T., Sontag, E., Chen, P., and Levine, A. (2008). Transcriptional control of human p53-regulated genes. Nat Rev Mol Cell Biol *9*, 402-412.

Rogakou, E.P., Boon, C., Redon, C., and Bonner, W.M. (1999). Megabase chromatin domains involved in DNA double-strand breaks in vivo. J Cell Biol *146*, 905-916.

Rogakou, E.P., Nieves-Neira, W., Boon, C., Pommier, Y., and Bonner, W.M. (2000). Initiation of DNA fragmentation during apoptosis induces phosphorylation of H2AX histone at serine 139. J Biol Chem *275*, 9390-9395.

Rogakou, E.P., Pilch, D.R., Orr, A.H., Ivanova, V.S., and Bonner, W.M. (1998). DNA double-stranded breaks induce histone H2AX phosphorylation on serine 139. J Biol Chem *273*, 5858-5868.

Rooney, S., Chaudhuri, J., and Alt, F.W. (2004). The role of the non-homologous end-joining pathway in lymphocyte development. Immunol Rev *200*, 115-131.

Rothkamm, K., Kruger, I., Thompson, L.H., and Lobrich, M. (2003). Pathways of DNA double-strand break repair during the mammalian cell cycle. Mol Cell Biol *23*, 5706-5715.

San Filippo, J., Sung, P., and Klein, H. (2008). Mechanism of eukaryotic homologous recombination. Annu Rev Biochem *77*, 229-257.

Sartori, A.A., Lukas, C., Coates, J., Mistrik, M., Fu, S., Bartek, J., Baer, R., Lukas, J., and Jackson, S.P. (2007). Human CtIP promotes DNA end resection. Nature *450*, 509-514.

Schar, P., Herrmann, G., Daly, G., and Lindahl, T. (1997). A newly identified DNA ligase of Saccharomyces cerevisiae involved in RAD52-independent repair of DNA double-strand breaks. Genes Dev *11*, 1912-1924.

Sedelnikova, O.A., Horikawa, I., Zimonjic, D.B., Popescu, N.C., Bonner, W.M., and Barrett, J.C. (2004). Senescing human cells and ageing mice accumulate DNA lesions with unrepairable double-strand breaks. Nat Cell Biol *6*, 168-170.

Shibata, A., Conrad, S., Birraux, J., Geuting, V., Barton, O., Ismail, A., Kakarougkas, A., Meek, K., Taucher-Scholz, G., Lobrich, M.*, et al.* (2011). Factors determining DNA double-strand break repair pathway choice in G2 phase. Embo J.

Shreeram, S., Demidov, O.N., Hee, W.K., Yamaguchi, H., Onishi, N., Kek, C., Timofeev, O.N., Dudgeon, C., Fornace, A.J., Anderson, C.W.*, et al.* (2006). Wip1 phosphatase modulates ATM-dependent signaling pathways. Mol Cell *23*, 757-764.

Shrivastav, M., De Haro, L.P., and Nickoloff, J.A. (2008). Regulation of DNA double-strand break repair pathway choice. Cell Res *18*, 134-147.

Skalka, A.M., and Katz, R.A. (2005). Retroviral DNA integration and the DNA damage response. Cell Death Differ *12 Suppl 1*, 971-978.

Spycher, C., Miller, E.S., Townsend, K., Pavic, L., Morrice, N.A., Janscak, P., Stewart, G.S., and Stucki, M. (2008). Constitutive phosphorylation of MDC1 physically links the MRE11-RAD50-NBS1 complex to damaged chromatin. J Cell Biol *181*, 227-240.

Stewart, G.S., Wang, B., Bignell, C.R., Taylor, A.M., and Elledge, S.J. (2003). MDC1 is a mediator of the mammalian DNA damage checkpoint. Nature *421*, 961-966.

Stiff, T., O'Driscoll, M., Rief, N., Iwabuchi, K., Lobrich, M., and Jeggo, P.A. (2004). ATM and DNA-PK function redundantly to phosphorylate H2AX after exposure to ionizing radiation. Cancer Res *64*, 2390-2396.

Stucki, M., Clapperton, J.A., Mohammad, D., Yaffe, M.B., Smerdon, S.J., and Jackson, S.P. (2005). MDC1 directly binds phosphorylated histone H2AX to regulate cellular responses to DNA double-strand breaks. Cell *123*, 1213-1226.

Sung, P., and Klein, H. (2006). Mechanism of homologous recombination: mediators and helicases take on regulatory functions. Nat Rev Mol Cell Biol *7*, 739-750.

Takahashi, A., Matsumoto, H., Nagayama, K., Kitano, M., Hirose, S., Tanaka, H., Mori, E., Yamakawa, N., Yasumoto, J., Yuki, K.*, et al.* (2004). Evidence for the involvement of double-strand breaks in heat-induced cell killing. Cancer Res *64*, 8839-8845.

Takahashi, A., Mori, E., Somakos, G.I., Ohnishi, K., and Ohnishi, T. (2008). Heat induces gammaH2AX foci formation in mammalian cells. Mutat Res *656*, 88-92.

Takata, M., Sasaki, M.S., Sonoda, E., Morrison, C., Hashimoto, M., Utsumi, H., Yamaguchi-Iwai, Y., Shinohara, A., and Takeda, S. (1998). Homologous recombination and non-homologous end-joining pathways of DNA double-strand break repair have overlapping roles in the maintenance of chromosomal integrity in vertebrate cells. Embo J *17*, 5497-5508.

Tashiro, S., Walter, J., Shinohara, A., Kamada, N., and Cremer, T. (2000). Rad51 accumulation at sites of DNA damage and in postreplicative chromatin. J Cell Biol *150*, 283-291.

Teo, S.H., and Jackson, S.P. (1997). Identification of Saccharomyces cerevisiae DNA ligase IV: involvement in DNA double-strand break repair. Embo J *16*, 4788-4795.

Vogelstein, B., Lane, D., and Levine, A.J. (2000). Surfing the p53 network. Nature *408*, 307-310.

Walker, J.R., Corpina, R.A., and Goldberg, J. (2001). Structure of the Ku heterodimer bound to DNA and its implications for double-strand break repair. Nature *412*, 607-614.

Weller, G.R., Kysela, B., Roy, R., Tonkin, L.M., Scanlan, E., Della, M., Devine, S.K., Day, J.P., Wilkinson, A., d'Adda di Fagagna, F.*, et al.* (2002). Identification of a DNA nonhomologous end-joining complex in bacteria. Science *297*, 1686-1689.

West, S.C. (2003). Molecular views of recombination proteins and their control. Nat Rev Mol Cell Biol *4*, 435-445.

Weterings, E., Verkaik, N.S., Bruggenwirth, H.T., Hoeijmakers, J.H., and van Gent, D.C. (2003). The role of DNA dependent protein kinase in synapsis of DNA ends. Nucleic Acids Res *31*, 7238-7246.

Wilson, S., Warr, N., Taylor, D.L., and Watts, F.Z. (1999). The role of Schizosaccharomyces pombe Rad32, the Mre11 homologue, and other DNA damage response proteins in non-homologous end joining and telomere length maintenance. Nucleic Acids Res *27*, 2655-2661.

Wu, X., Bayle, J.H., Olson, D., and Levine, A.J. (1993). The p53-mdm-2 autoregulatory feedback loop. Genes Dev *7*, 1126-1132.

Yaneva, M., Kowalewski, T., and Lieber, M.R. (1997). Interaction of DNA-dependent protein kinase with DNA and with Ku: biochemical and atomic-force microscopy studies. Embo J *16*, 5098-5112.

Yoo, S., and Dynan, W.S. (1999). Geometry of a complex formed by double strand break repair proteins at a single DNA end: recruitment of DNA-PKcs induces inward translocation of Ku protein. Nucleic Acids Res *27*, 4679-4686.

Yu, X., and Chen, J. (2004). DNA damage-induced cell cycle checkpoint control requires CtIP, a phosphorylation-dependent binding partner of BRCA1 C-terminal domains. Mol Cell Biol *24*, 9478-9486.

Yun, M.H., and Hiom, K. (2009). CtIP-BRCA1 modulates the choice of DNA double-strand-break repair pathway throughout the cell cycle. Nature *459*, 460-463.

Zhou, B.B., and Elledge, S.J. (2000). The DNA damage response: putting checkpoints in perspective. Nature *408*, 433-439.

Chapter 2: Quantitative live cell imaging reveals a gradual shift between DNA repair mechanisms and a maximal use of HR in mid-S phase

The content in this chapter was published in:
Molecular Cell (2012)

Authors: Ketki Karanam, Ran Kafri, Alexander Loewer, and Galit Lahav

Abstract

DNA double strand breaks are repaired by two main pathways: non-homologous end joining (NHEJ) and homologous recombination (HR). The choice between these pathways depends on cell cycle phase; however the continuous effect of cell cycle on the balance between them is still unclear. We used live cell imaging and fluorescent reporters for 53BP1, Rad52 and cell cycle to quantify the relative contribution of NHEJ and HR at different points of the cell cycle in single cells. We found that NHEJ is the dominant repair pathway in G1 and G2 even when both repair pathways are functional. The shift from NHEJ to HR is gradual, with the highest proportion of breaks repaired by HR in mid-S, where amount of DNA replication is highest. Higher proportions of HR also strongly correlate with slower rates of repair. Our study shows that the choice of repair mechanism is continuously adjusted throughout the cell cycle and suggests that the extent of active replication, rather than the presence of a sister chromatid influences the balance between the two repair pathways in human cells.

Introduction

DNA double strand breaks (DSBs) are potentially cytotoxic lesions generated during normal cell metabolism or by ionizing radiation and chemotherapeutic drugs. Their repair is critical for the successful maintenance and propagation of genetic information. In mammalian cells, two distinct pathways promote repair of DSBs, non-homologous end joining (NHEJ) and homologous recombination (HR). In NHEJ, the broken DNA ends

are aligned and ligated together without requiring long sequence complementarities (Lieber et al., 2003). HR requires an intact homologous sequence located on a sister chromatid, or elsewhere in the genome. It is initiated by resection of DNA at the break site to generate 3′ single-stranded DNA overhangs that invade the DNA double helix of the undamaged, homologous partner and copy information back to the break site (West, 2003). Both NHEJ and HR are essential for genome maintenance, and defects in either pathway are linked to immunodeficiency, cancer predisposition and other diseases.

A critical question is how the choice of DNA repair pathway is regulated. The current view is that cell cycle is the key regulatory factor that guides the decision between pathways (Shrivastav et al., 2008). NHEJ functions throughout the cell cycle, but is assumed to be most important in G0/G1 (Lieber et al., 2003). HR was suggested to be active only in the post-replicative stages of the cell cycle, S and G2, during which time the preferred homologous template – the sister chromatid - is available (Aylon et al., 2004; Johnson and Jasin, 2000; Kadyk and Hartwell, 1992; West, 2003). This cell cycle dependent competency for HR was suggested to be regulated by the activity of cyclin dependent kinases (CDKs), which control DSB resection, a prerequisite for HR (Aylon et al., 2004; Huertas et al., 2008; Huertas and Jackson, 2009; Ira et al., 2004; Yun and Hiom, 2009). Interestingly, the physical presence of replicated DNA did not affect the choice of repair mechanism in yeast (Aylon et al., 2004). It is unclear whether this is also the case in mammalian cells. In addition, it is unclear how individual mammalian cells transition between the two mechanisms with cell cycle progression (Figure 2.1A), whether all breaks in a cell are repaired exclusively by one mechanism, and is the choice

Figure 2.1: Experimental system for quantifying DSBs and cell cycle phase in single, living cells

(A) Potential models of the transition between NHEJ and HR with cell cycle progression. The transition can be switch like (i) where cells completely shift to HR on entering S phase; or a more gradual change (ii) where cells utilize more HR with greater progress in S and G2 as the amount of replicated homologous substrate accrues. **(B)** Schematic drawing of the Geminin reporter. **(C)** Time lapse images of a freely cycling U2OS cell expressing the Geminin-CFP reporter. Images are overlays of the phase and CFP channels. **(D)** Quantification of the average nuclear Geminin-CFP intensity in a freely cycling cell over one cell division (indicated by the sharp drop in intensity). **(E)** Heat map of Geminin-CFP intensities in individual cells over time. Each horizontal line represents a single cell; blue represents low Geminin intensity; red represents high intensity. Cells were clustered according to their time of mitosis (t_M, diagonal black line). Damage was applied at the 24h time point (t_D). Cells at the top were in G2 when damage was applied, while cells in G1 are at the bottom. The red arrow indicates the trajectory of the cell shown in (C). **(F)** Schematic drawing of the 53BP1 reporter. **(G)** Cells expressing 53BP1-YFP were fixed and stained with anti γ-H2AX antibody after damage. The overlaid image shows co-localization between 53BP1 and γ-H2AX foci (see additional examples and quantification in Figure 2.2C-E). **(H)** Time-lapse images of a cell expressing 53BP1-YFP after damage. t' is the time elapsed from the initiation of DNA damage. Images are maximum projections of z-stacks through the nucleus (see Experimental Procedures) in the YFP channel. **(I)** Example of the automated segmentation for the enumeration of 53BP1-YFP foci in a cell. Image processing was performed using the Ensemble Thresher software package developed in our lab (see experimental procedures for algorithmic details).

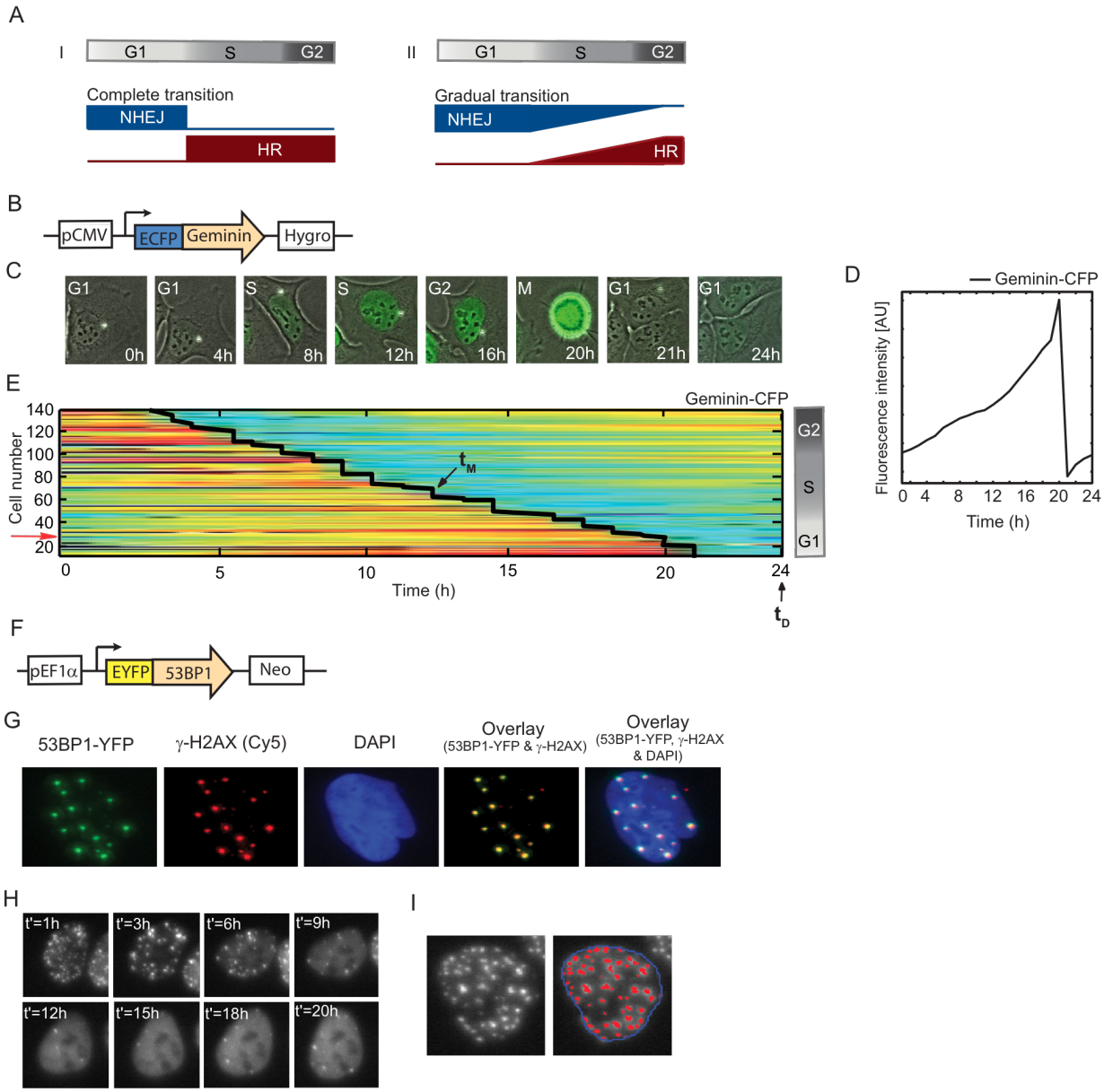

Figure 2.1 (continued)

of repair mechanism fixed at the time of damage or changed during the course of repair. Most of our knowledge about the relationship between cell cycle and the choice of repair pathway comes from measurements of fixed cells at specific times post damage. Such measurements allow estimation of cell cycle phase based on one fixed snapshot of a cell, followed by grouping of cells into three major phases G1, S and G2. However, each group includes cells that enter that phase at different times, potentially leading to large heterogeneity within each group. Direct connection between cell cycle phase and the choice of repair mechanism therefore requires quantification of these events over time in the same cell.

Here, we use long-term, time-lapse microscopy and fluorescent reporters to measure DSBs, HR and cell cycle phase in asynchronous, individual living cells, and accurately determine the relationship between cell cycle state, choice of repair mechanism and kinetics of repair. Our results show that the choice of repair pathway is not fixed at the time of damage but rather is adjusted during the course of repair. NHEJ is the exclusive repair pathway in G1; however cells damaged in late G1 show low levels of HR as they progress into S. Once HR is activated, it does not capture all breaks, and the balance between NHEJ and HR changes gradually with cell cycle progression. Specifically, S and G2 cells exhibit both HR and NHEJ with maximal use of HR in mid-S phase; during which time repair is the slowest and the amount of DNA replication is highest. Our data argue against the idea that the presence of replicated DNA determines the choice of repair, and instead suggest a direct link between the extent of active replication and HR.

Results

1. Quantifying DSB repair and cell cycle in individual living cells

We developed a fluorescent reporter system that allows quantification of cell cycle phase and DNA DSBs in individual living cells. To monitor cell cycle phase we expressed a CFP fusion of the N-terminal domain of Geminin (Figure 2.1B); which was previously shown to faithfully report APC inactivation (Sakaue-Sawano et al., 2008). Geminin-CFP slowly accumulates in cells post division; reaches maximal levels as cells enter mitosis, and then rapidly degrades during cytokinesis (Figure 2.1C, D). We imaged freely cycling cells for 24 hours prior to inducing DNA damage. During this time most cells divided at least once and their time of division was identified computationally based on the rapid drop in Geminin-CFP levels. Based on each cell's division time, we determined its cell cycle phase at the time of damage and the time that had passed since it entered that phase (see experimental procedures, Figure 2.1E, Figure 2.2A, B).

We quantify DNA DSBs in single cells using 53BP1 fused to yellow fluorescent protein (YFP; Figure 2.1F). 53BP1 is a mediator protein in the DNA damage response. It localizes to DSB sites within minutes after damage and forms sub-nuclear compartments (foci) on chromatin regions adjacent to the break (Anderson et al., 2001; Bekker-Jensen et al., 2005; Schultz et al., 2000). As previously reported, we found that the tagged 53BP1 protein forms distinct foci that co-localize with the canonical marker for DSBs, γ-H2AX (Figures 2.1G, 2.2C-E, Lobrich et al., 2010). Foci formed by DNA damage response proteins such as 53BP1 and γ-H2AX provide an indirect measurement of DSBs

Figure 2.2: Characterization of the Geminin-CFP and 53BP1-YFP reporters

(A) Average lengths of G1, S and G2 of U2OS cells as determined from their cell cycle distributions (See experimental procedures). **(B)** Time-lapse imaging setup to observe DNA repair and cell cycle phase in living cells. U2OS cells expressing 53BP1-YFP and Geminin-CFP are imaged undamaged for 24h to determine their time of division. At 24h, the same cells are damaged with NCS (200 ng/mL) without disturbing the setup and imaging is continued for 20h post damage to measure the decay in 53BP1-YFP foci numbers and obtain rates of repair in these cells. **(C)** U2OS cells expressing 53BP1-YFP were fixed and stained with anti γ-H2AX antibody at the indicated times after damage (200 ng/mL NCS). The overlaid images show co-localization of the 53BP1-YFP and γ-H2AX foci. The zoomed overlay enlarges the foci enclosed by the white box 1h post damage. **(D)** The percentage of γ-H2AX foci that co-localize with 53BP1-YFP foci was calculated for each cell and are shown as probability histograms for a population of >200 cells. On average, 92.5% of γ-H2AX foci in a cell have a corresponding, co-localized 53BP1-YFP focus. **(E)** The percentage of 53BP1-YFP foci that co-localize with γ-H2AX foci (blue) and the percentage of γ-H2AX foci that co-localize with 53BP1-YFP foci (red) as a function of cell cycle phase. Each dot represents the average percent co-localization between the two proteins for cells binned according to their cell cycle stage. Cell cycle positions were determined from DNA content measured by DAPI staining. Co-localizations were measured for a population of > 200 cells. **(F)** Examples of G1 cells showing 53BP1-YFP localized to sites of mitotic chromosomal lesions before damage and at newly generated DSBs at 1h after damage (200 ng/mL NCS). **(G)** Distributions of the number of 53BP1-YFP foci at 1h (i) and at 24h post damage (200 ng/mL NCS) in cells imaged either every hour for 24h (ii) or only at 24h (iii) post damage. **(H)** The proportion of cells in G1, S and G2 cell cycle phases in asynchronously growing populations of wild-type U2OS cells and reporter cells engineered to express the 53BP1-YFP, Rad52-mCherry and Geminin-CFP reporters showing that expression of these reporters does not affect cell cycle distribution. Cell cycle distributions were obtained by flow cytometry using propidium iodide staining.

A

Cell cycle phase	Duration (h)
G1	8.25
S	7.75
G2	4

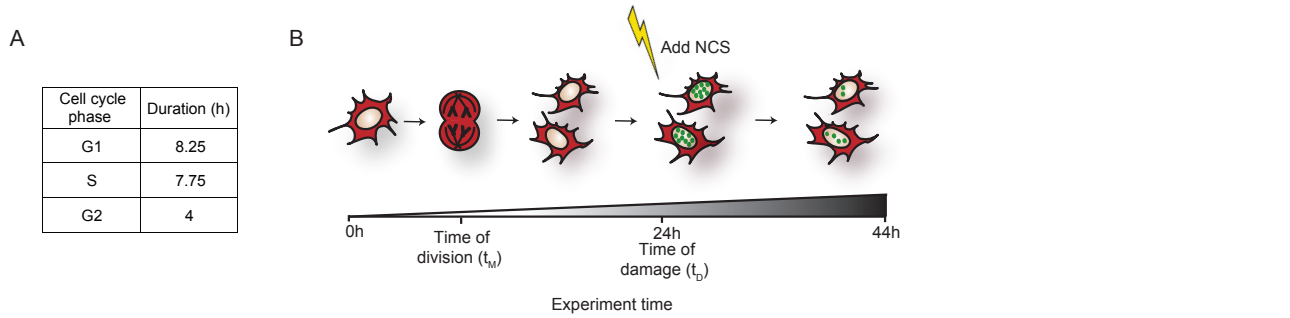

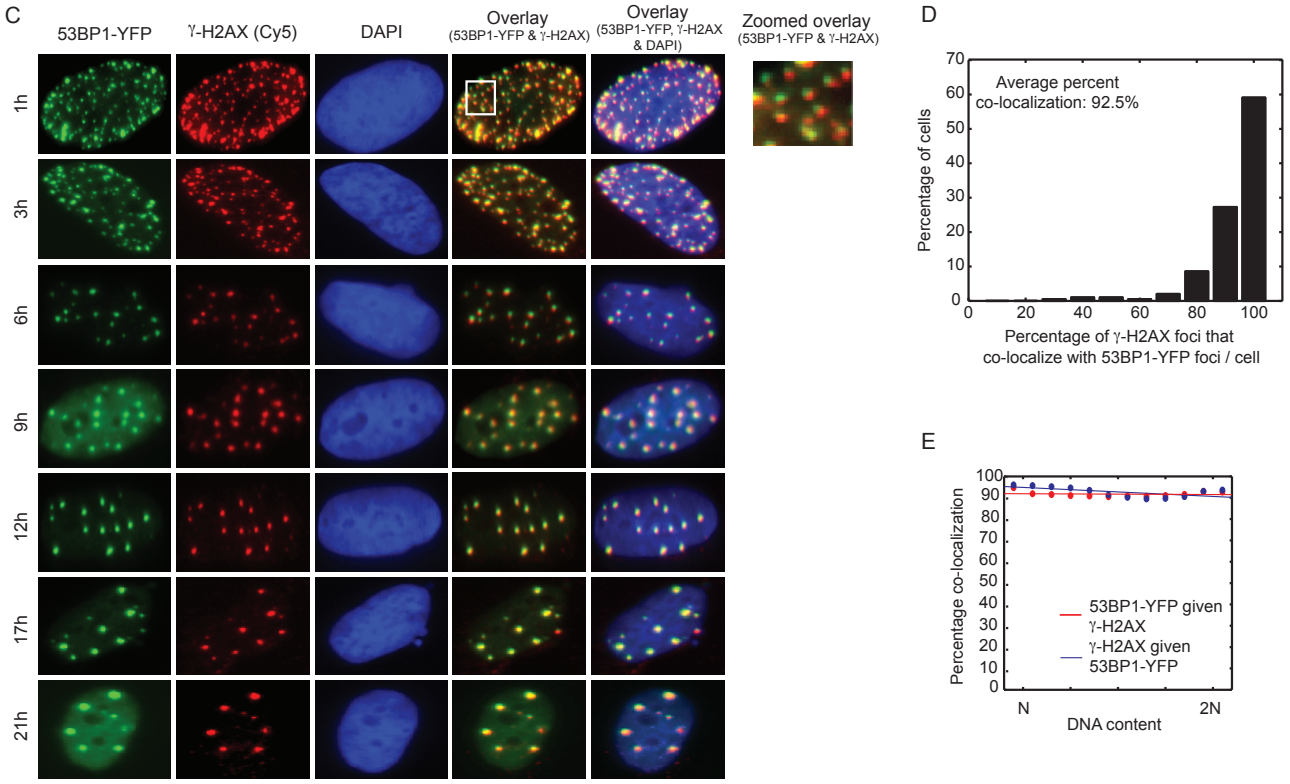

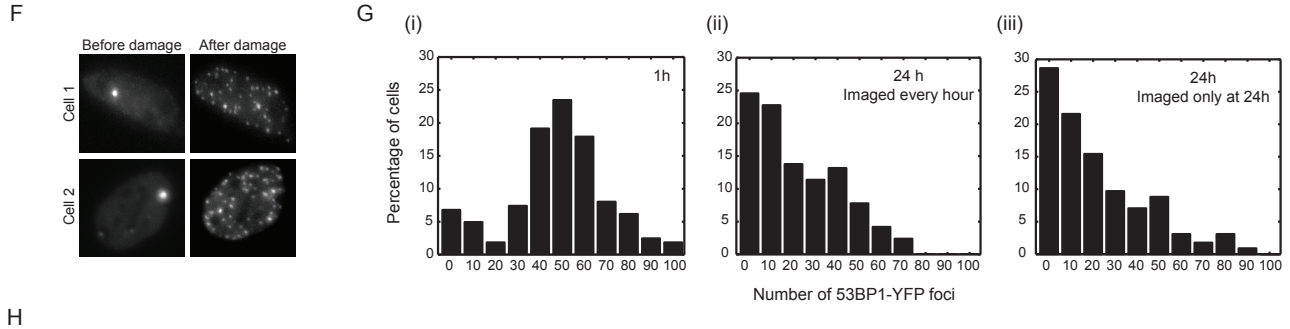

H

Cell cycle phase	Percent cells (wt U2OS)	Percent cells (Reporter cell line)
G1	52.77	50.47
S	32.28	35.74
G2	14.96	13.79

Figure 2.2 (continued)

in cells. For example, γ-H2AX and 53BP1 foci may be affected by factors that alter the signal persistence rather than the actual breaks. In addition, multiple breaks may cluster into a single focus. Despite these limitations, measurements of foci provide a sensitive, high-resolution quantification of breaks in individual cells and have been shown to faithfully reproduce results obtained from populations of fixed cells by more direct measurements of DNA breaks such as pulsed-field gel electrophoresis (Rothkamm and Lobrich, 2003). Our analysis showed that the number of 53BP1-YFP foci in a cell decreases with time (Figure 2.1H, 2.2C). Note that the number of 53BP1 foci we measure represents a balance between repair and generation of new breaks by internal cellular events such as replication. We were able to distinguish the large, high intensity 53BP1 foci, which were recently shown to form at sites of mitotic chromosomal lesions in non-damaged G1 cells (Lukas et al., 2011), from the numerous, smaller 53BP1 foci generated after damage induction by imaging the same cell before and after inducing damage (Fig. 2.2F). We also confirmed that the decay in the number of foci post damage represents repair (and not decay of the fluorescent signal due to photo bleaching), by showing that the distribution of foci at 24 hours post damage is similar between cells that were imaged frequently (every hour) and cells that were imaged only at 24 hours post damage (Figure 2.2G, p-value 0.99, Kolmogorov-Smirnov test). We generated a double reporter cell line expressing both Geminin-CFP and 53BP1-YFP and confirmed that these reporters do not alter cell cycle distribution of asynchronously growing cells (Figure 2.1H).

To induce DSBs, we used the radiomimetic drug neocarzinostatin (NCS). NCS creates a burst of DSBs and has been shown to act solely within five minutes following addition of

the drug to the cell culture medium (Shiloh et al., 1983). We chose to use NCS instead of irradiating cells because this allowed us to add the drug directly to cells on the microscope and follow the same cells before and after damage without disturbing the imaging setup and without a significant time delay in image acquisition. We verified that the kinetics of DSB repair post NCS treatment are similar to those obtained in irradiated cells (compare Figure 2.4A to Figure 2.3B). To minimize photo bleaching, we limited the imaging of cells to hourly intervals post NCS treatment. The mobility of foci and cells does not permit tracking individual foci between time points. Our measurements therefore provide the *total* numbers and intensity of foci in each cell over time.

2. Cell cycle phase at the time of damage affects the rate of DSB repair

We first asked if cells damaged in different stages of the cell cycle repair DSBs uniformly or if they vary in their kinetics of repair. Previous studies in fixed cells have suggested that DSBs are repaired with bi-phasic kinetics comprising a fast repair process (half-life of 0.5h - 2h) and a slower repair process (half-life of 12h - 24h). Since our measurements were collected at hourly intervals, the sampling of the early, rapid decay was limited to two data points. This resolution was insufficient to faithfully characterize and separate the fast repair kinetics from the overall repair trajectory, and we were able to observe clear, biphasic repair only in 12% of the cells. We therefore focused on the slow phase of repair and fit the enumerated 53BP1 foci from 2 hours post damage to an exponential decay until the net decay approached zero (Figure 2.3A). Our analysis revealed a large variation in the half-life of 53BP1 foci across cells with a peak around 4-5 hours (Figure 2.3B). To test whether these variations relate to cell cycle phase, we

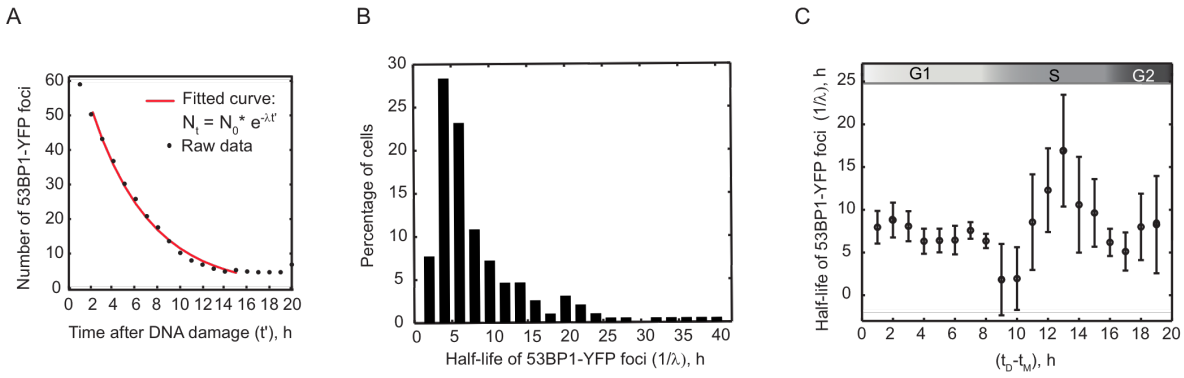

Figure 2.3: Cell cycle position at the time of damage affects kinetics of DSB repair

(A) Enumerated 53BP1-YFP foci (black dots) and the exponential fit to the raw data (red line) for the cell shown in Figure 1H). **(B)** The distribution of half-lives of 53BP1-YFP foci in an unsynchronized population (n>220 cells) and as a function of cell cycle progression **(C)**. In (C), the average half-life of 53BP1-YFP foci is plotted for cells binned according to their cell cycle position at the time of damage. The plot was calculated with a sliding window of bin size W = 2 hours. Bars represent mean ± SEM for a total population of > 220 cells.

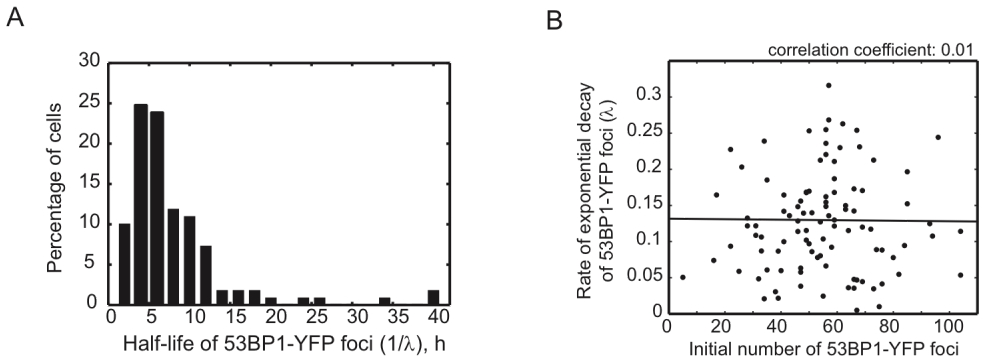

Figure 2.4: Controls related to analysis of the rate of repair

(**A**) Distribution of the half-lives of 53BP1-YFP foci across a population (~ 200 cells) after damage with 5Gy γ-irradiation. (**B**) The decay constant obtained from exponential fits to the enumerated 53BP1-YFP foci is plotted against the initial number of 53BP1-YFP foci in each cell.

binned cells according to their position in cell cycle at the time of damage and plotted the half-life of 53BP1 foci for cells in each bin (Figure 2.3C). Our results indicate a significant association ($p<0.01$, one-way ANOVA) between cell cycle phase and the rates of DSB repair. We observed that cells damaged in G1 and G2 have comparable half-lives of DSBs. In contrast, cells damaged in S phase show a large variation in their kinetics of repair. Cells at the G1/S transition attain the shortest half-lives of DSBs amongst all cells. Half-lives then gradually increase as cells enter S phase and peak in mid-S; followed by an acceleration of repair as presented by shorter half-lives in late-S and G2.

The rapid kinetics of repair at the G1/S boundary may result from changes in chromatin structure in preparation for DNA replication, promoting accessibility of repair factors to break sites. Additionally, there may be increased availability of key substrates such as dNTPs, and DNA processing enzymes that allow rapid DNA repair during this time. The accelerated kinetics of repair towards the end of the cell cycle may be important to address DNA damage in a timely manner as cells progress towards mitosis.

To ensure that the observed effect of cell cycle on repair kinetics is not merely due to differences in the initial number of DSBs, we plotted the rate of repair as a function of the initial number of breaks. We found no correlation between the initial number of breaks and the rate of repair (Figure 2.4B). At present, we cannot rule out the possibility that clustering of multiple repair sites into a single focus leads to the appearance of longer repair times.

Our results show that the dynamics of DSB repair differ significantly between cells in different cell cycle phases and even more strikingly, repair rates are not uniform for S phase cells, but rather are determined by the exact time a cell has spent in S phase at the time of damage.

3. NHEJ is the dominant repair mechanism in both G1 and G2 cells

Several factors, including the degree of chromatin compaction, level of CDK activity, and availability of nucleotide substrates could affect the rates of DSB repair through the cell cycle. Another potential factor is the balance between NHEJ and HR. It was recently suggested that NHEJ repairs breaks with faster kinetics than HR (Shibata et al., 2011). To quantify the extent of activation of the alternative repair pathways and the cell cycle dependent balance between them, we added a fluorescent reporter of Rad52 (Rad52-mCherry) to cells expressing 53BP1-YFP and Geminin-CFP (Figure 2.5A). Rad52 is a recombinase mediator protein that forms foci at DSB sites that are committed to homology dependent repair (Essers et al., 2002). Evidence in mammalian cells suggests that Rad52 functions primarily in single strand annealing (Stark et al., 2004). An *in vitro* study of the human Rad52 protein indicates that it functions to catalyze the capture of the second DSB end prior to D-loop dissociation in canonical HR reactions (McIlwraith and West, 2008). More recently, it was demonstrated that Rad52 is synthetically lethal with the recombinase mediator BRCA2, and depletion of Rad52 in BRCA2 deficient cells impairs Rad51 foci formation, (Feng et al., 2011), suggesting that Rad52 functions in an independent, alternate pathway that supports Rad51 mediated classical HR repair.

Figure 2.5: NHEJ dominates the repair of DSBs in G1 and G2 cells

(**A**) Schematic drawing of the Rad52, 53BP1 and Geminin reporters for quantifying HR, total DSBs and cell cycle phase respectively in individual cells. **(B)** U2OS cells expressing the Rad52-mCherry reporter were fixed and stained with anti-BRCA1 antibody after damage. The overlaid image shows co-localization of the Rad52-mCherry and BRCA1 foci (see additional examples and quantification in Figure S3A-C). **(C, E)** Time-lapse images of U2OS cells expressing the reporters in (A) that were damaged in the G1 (C) or S (E) cell cycle phases. The 53BP1-YFP and Rad52-mCherry images are maximum projections of z-stacks through the nucleus (see Experimental Procedures). **(D, F)** Quantification of the number of 53BP1-YFP (green) and Rad52-mCherry (red) foci in the cells shown in (C) and (E) respectively. **(G)** Heat maps of 53BP1-YFP and Rad52-mCherry foci as a function of time after damage (x-axis) and cell cycle progression (y-axis). Cells were binned to 20% full interval on both axes. Blue represents low foci numbers and red represents high foci numbers in a range of 0-120 (53BP1-YFP) or 0-100 (Rad52-mCherry) foci. Number of cells >140 **(H)** Heat map of Rad52-mCherry foci zoomed in on cells damaged in G1. The gray bars on the right indicate the average EdU content (total nuclear intensity) for cells binned into three groups A, B and C (from early to late G1) based on their cell cycle stage at the time of damage. Number of cells >40.

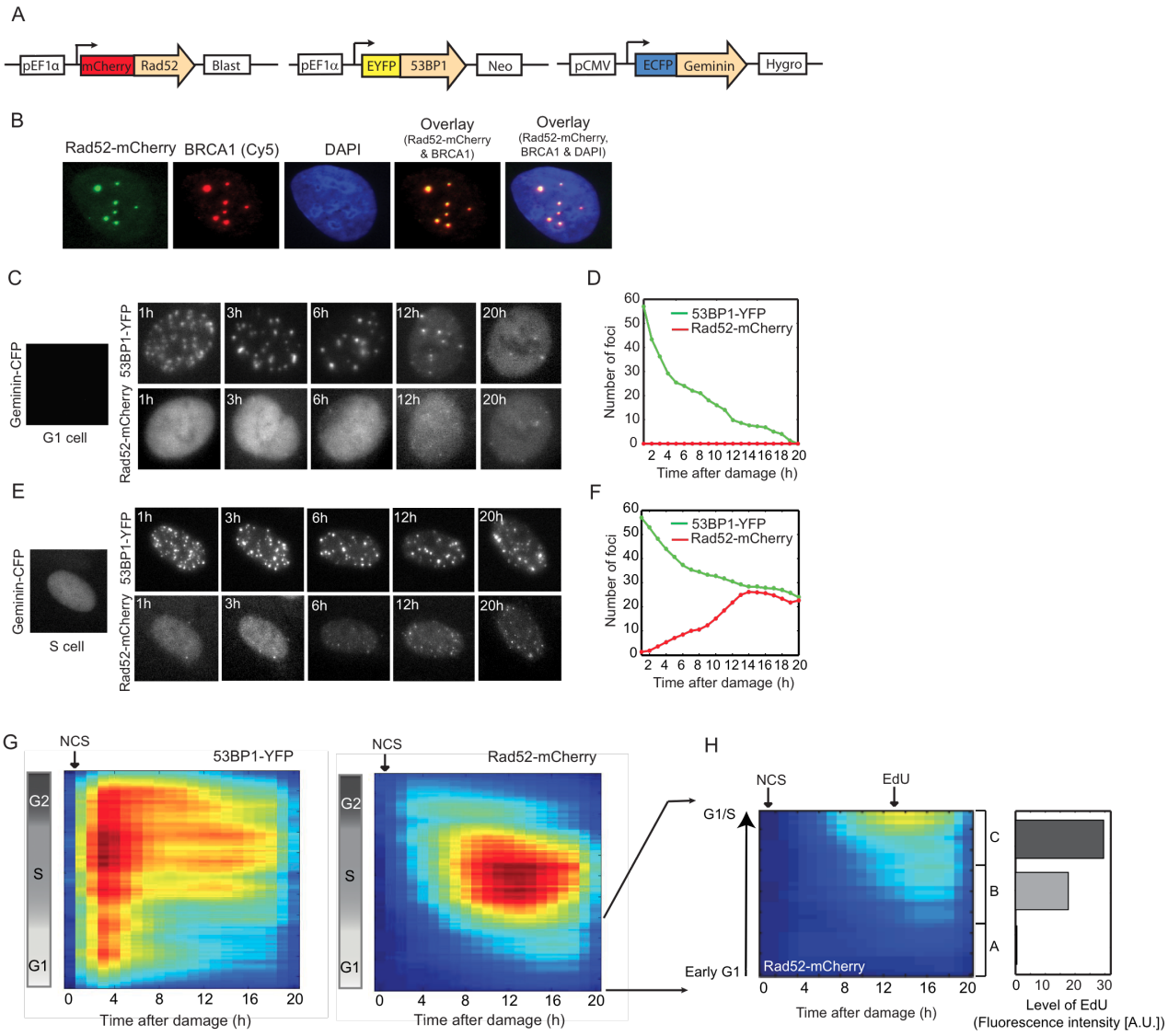

Figure 2.5 (continued)

Homology dependent repair comprises many sub-pathways, which precludes the development of a single protein reporter that can capture all homology dependent events. We chose Rad52 to report on HR since it is not a key factor for mammalian HR (Rijkers et al., 1998; van Veelen et al., 2005) and we were concerned that high expression of core HR proteins (such as Rad51 and BRCA1) may disturb the natural balance between NHEJ and HR. However, one limitation of using Rad52 as an HR marker is that it may not accompany all HR reactions in mammalian cells. To evaluate if our Rad52 reporter captures all homology dependent repair events or a specific subset of HR reactions, we performed immunofluorescence based comparisons of Rad52-mCherry foci with BRCA1, a protein that functions in DNA resection, an early, essential step for all homology dependent events. (Figure 2.5B, Figure 2.6A). We found that 93.1% of Rad52-mCherry foci in a cell had a corresponding, co-localized BRCA1 focus (Figure 2.6B). This may result from BRCA1 leaving the break before Rad52 is loaded. Interestingly, only 72% of the BRCA1 foci in a cell had a corresponding, co-localized Rad52-mCherry focus, indicating that 28% of breaks accompanied by BRCA1 are repaired by Rad52 independent HR mechanisms. Thus the Rad52 reporter underrepresents the total number of foci repaired by homology dependent repair in our experimental system. However, this underrepresentation was found to be systematic and did not depend on cell cycle phase (Figure 2.6C). This demonstrates that the Rad52 reporter is reliable for studying the effect of cell cycle on all HR reactions that utilize BRCA1 mediated DNA resection. Lastly, since fluorescent reporters may provide a risk of altering the natural balance of proteins and cellular responses, we confirmed that insertion of the triple reporters does not alter the kinetics of repair (Figure 2.6D).

Figure 2.6: Characterization of the Rad52-mCherry reporter

(A) U2OS cells expressing the Rad52-mCherry reporter were fixed and stained with anti BRCA1 antibody after damage (200 ng/mL NCS). The overlaid images show co-localization of the Rad52-mCherry and BRCA1 foci. Four cells with varying number of Rad52-mCherry foci are shown. The zoomed overlay enlarges the foci enclosed by the white box. **(B)** The percentage of Rad52-mCherry foci that co-localize with BRCA1 foci was calculated for each cell and are shown as probability histograms for a population of >200 cells. **(C)** The percentage of Rad52-mCherry foci that co-localize with BRCA1 foci (red) and the percentage of BRCA1 foci that co-localize with Rad52-mCherry foci (blue) as a function of cell cycle phase. Each dot represents the average percent co-localization between the two proteins for cells binned according to their cell cycle stage. Cell cycle positions were determined from DNA content measured by DAPI staining. Co-localizations were measured for a population of > 200 cells. **(D)** Kinetics of DSB repair in wild type U2OS cells and reporter cells engineered to express the 53BP1-YFP, Geminin-CFP and Rad52-mCherry reporters. Cells were damaged (200 ng/mL NCS), fixed and stained with anti γ-H2AX antibody at the indicated times post damage. Bars represent mean $\pm$ SEM in a population of ~ 200 cells. **(E)** Cell cycle phase at the time of damage (y-axis) was determined as described in Figure 1. Cell cycle phase at maximal HR activation (x-axis) was determined by fixing cells at 11h post damage and measuring DNA content by DAPI. Bars represent mean $\pm$ SEM for a population of > 460 cells (**F)** The average half-life of Rad52-mCherry foci in populations of cells damaged in S and G2 phases. Half-lives were calculated by fitting a single exponential decay to the enumerated Rad52-mCherry foci in individual cells. Bars represent mean $\pm$ SEM for a population of > 60 cells in each group.

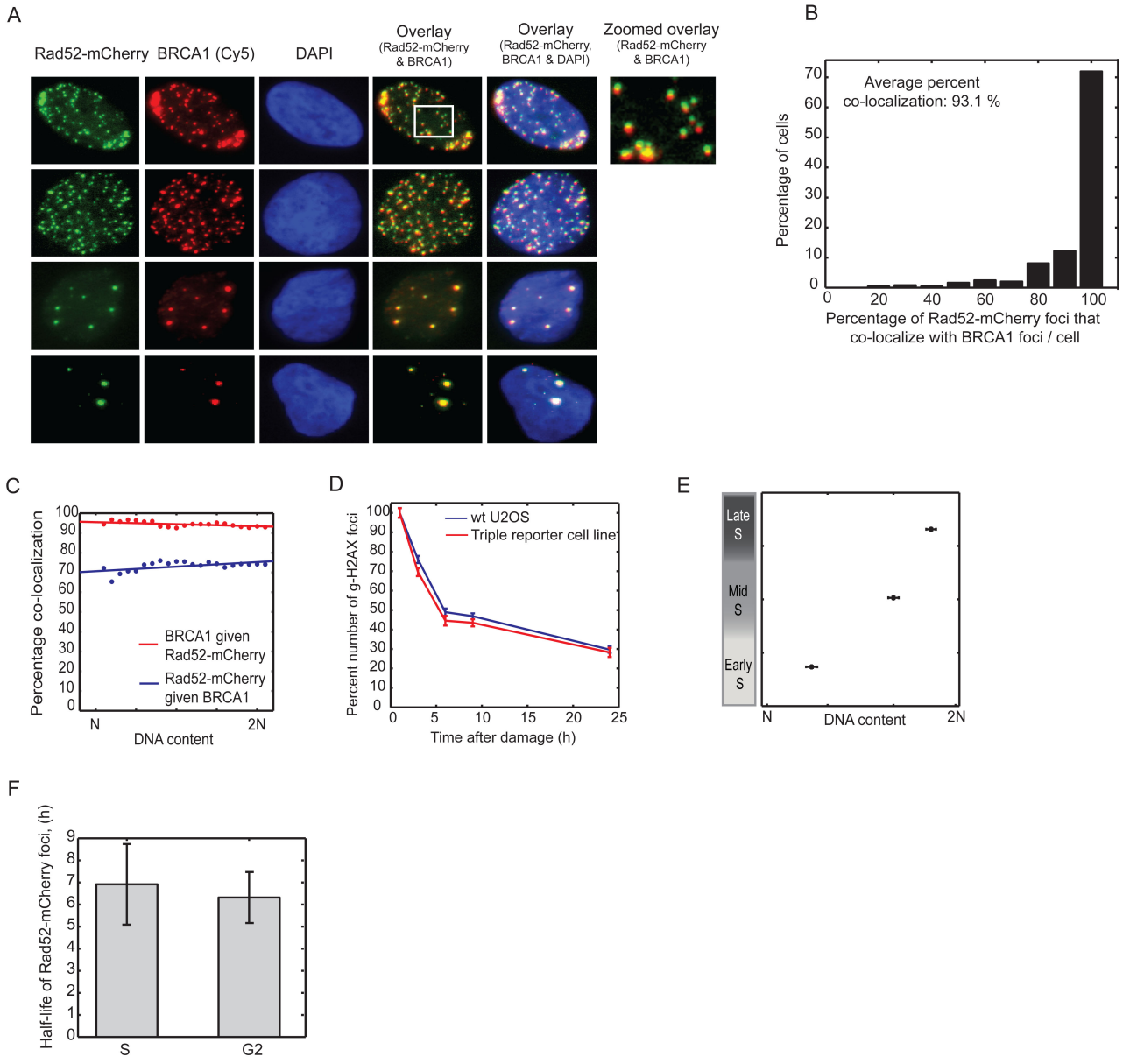

Figure 2.6 (continued)

While all cells treated with NCS showed 53BP1 foci, formation of Rad52 foci was highly dependent on cell cycle phase, in agreement with previous studies in fixed cells (Bekker-Jensen et al., 2006; Jazayeri et al., 2006; Lisby et al., 2004; Tashiro et al., 2000). S phase cells show higher numbers of Rad52 foci, while early/mid G1 cells show no Rad52 foci (Figure 2.5C-F). Interestingly, late G1 cells show low numbers of Rad52 foci at 12-16 hours post damage (Figure 2.5G). To determine if this activation of HR results from G1 cells progressing into S phase during the course of the repair, we exposed damaged G1 cells to a 40 minute pulse of the thymine analogue EdU at the time of HR activation (13 hours post damage) and analyzed their EdU content. We observed that early G1 cells that did not develop Rad52 foci also did not incorporate EdU (Figure 2.5H). Cells damaged in late G1 and at the G1/S transition incorporated higher amounts of EdU and developed Rad52 foci, indicating that they had progressed into S phase when HR was activated. This shows that the decision to activate HR in G1 cells is not fixed at the time of damage; cells in early G1 exclusively activate NHEJ for repair, however mid/late G1 cells first repair exclusively by NHEJ, but then progress into S phase and activate HR. Since NCS also leads to a small proportion of single strand breaks (SSBs, Shiloh et al., 1983), it is possible that as cells undergo the G1/S transition, SSBs may cause replication forks to collapse and generate one-ended DSBs that initiate HR repair.

Based on current literature, the precise role of HR in G2 is somewhat controversial. On one hand, studies in HR deficient cells suggested HR as the dominant repair pathway in both S and G2 (Rothkamm et al., 2003; Takata et al., 1998). On the other hand, a more recent study shows that HR deficient cells can repair up to 85% of DSBs by NHEJ in G2

(Beucher et al., 2009). It is unclear if this reflects the behavior in wild-type cells or results from the ability of NHEJ to compensate for the absence of functional HR. Our system allowed us to determine the contribution of HR and NHEJ when both mechanisms are intact in wild-type cells. We found that cells damaged in G2 show low levels of HR, comparable to the levels seen in late G1 cells (Figure 2.5G). However this activation was much earlier (4h post damage in G2 cells compared to 12h in late G1 cells). Late G2 cells show very little or no induction of HR (Figure 2.5G). Importantly, G2 cells that divided after damage were eliminated from this analysis to ensure that the predominant NHEJ observed in this phase did not result from G2 cells progressing into G1 phase during the course of repair. Thus NHEJ is the dominant repair mechanism in both G1 and G2 cells even in the presence of a functional HR pathway.

4. The balance between HR and NHEJ changes gradually with highest activation of HR in mid-S

What fraction of DSBs is repaired by HR in S and G2 cells? To answer this we divided the number of Rad52 foci by the number of 53BP1 foci induced post damage (Figure 2.7A). We observed that the proportion of HR gradually increases as cells progress from early S towards mid-S phase, followed by a decrease as cells progress to late-S and G2 (Figure 2.7A). The same pattern was observed when the maximum proportion of HR in individual cells (calculated as the ratio between the maximum number of Rad52 foci to the total number of 53BP1 foci induced post damage), and the rates of Rad52 foci accumulation were plotted against cell cycle position (Figure 2.7B, C). Our data demonstrate that cells do not show an immediate and complete activation of HR on

Figure 2.7: Contribution of HR to DSB repair changes gradually with cell cycle progression and is highest in mid-S.

(**A**) Heat map showing the proportion of DSBs channeled to the HR repair pathway over time post damage, calculated as the ratio between Rad52-mCherry foci to 53BP1-YFP foci. The ratio is shown as a function of the time elapsed from the induction of DSBs and cell cycle progression (indicated by the reference bar on the left). Cells were binned to 20% full interval on both axes. Blue represents low ratios and red indicates a higher proportion of HR. **(B)** The maximum proportion of HR in individual cells post damage is plotted against their cell cycle progression at the time of damage indicated by the reference bar on top. The median (black line), 25^{th} and 75^{th} percentile (dashed blue lines) of the population (n> 220 cells) are shown. **(C)** The rate at which Rad52-mCherry foci accumulate in individual cells post damage is plotted against their cell cycle progression at the time of damage. The median (black line), 25^{th} and 75^{th} percentile (dashed blue lines) of the population (n> 220 cells) are shown. **(D)** The rate of repair as a function of HR usage is plotted for cells binned according to their maximum Rad52-mcherry/53BP1-YFP foci ratio. Cells are binned according to a bin size of 0.03. Bars represent mean $\pm$ SEM. Population of n>220 cells. **(E, F)** The amount of DNA replication as a function of S phase progression was measured by pulse labeling cells with EdU. Levels of EdU fluorescence are shown as a function of the DAPI fluorescence (E) for a non-synchronized population of cells. The level of DNA replication is quantified as the average EdU intensity per cell. To avoid bias from non-replicating cells, (F) was calculated from cells in the window shown in (E). **(G)** A new model for the transition between NHEJ and HR with cell cycle progression. Cells in G1 repair DSBs exclusively by NHEJ. Cells then increase their use of HR gradually as they progress from G1 to early S. Following a peak in mid-S, HR decreases gradually as cells move towards late S and G2, with late G2 cells repairing DSBs almost entirely by NHEJ.

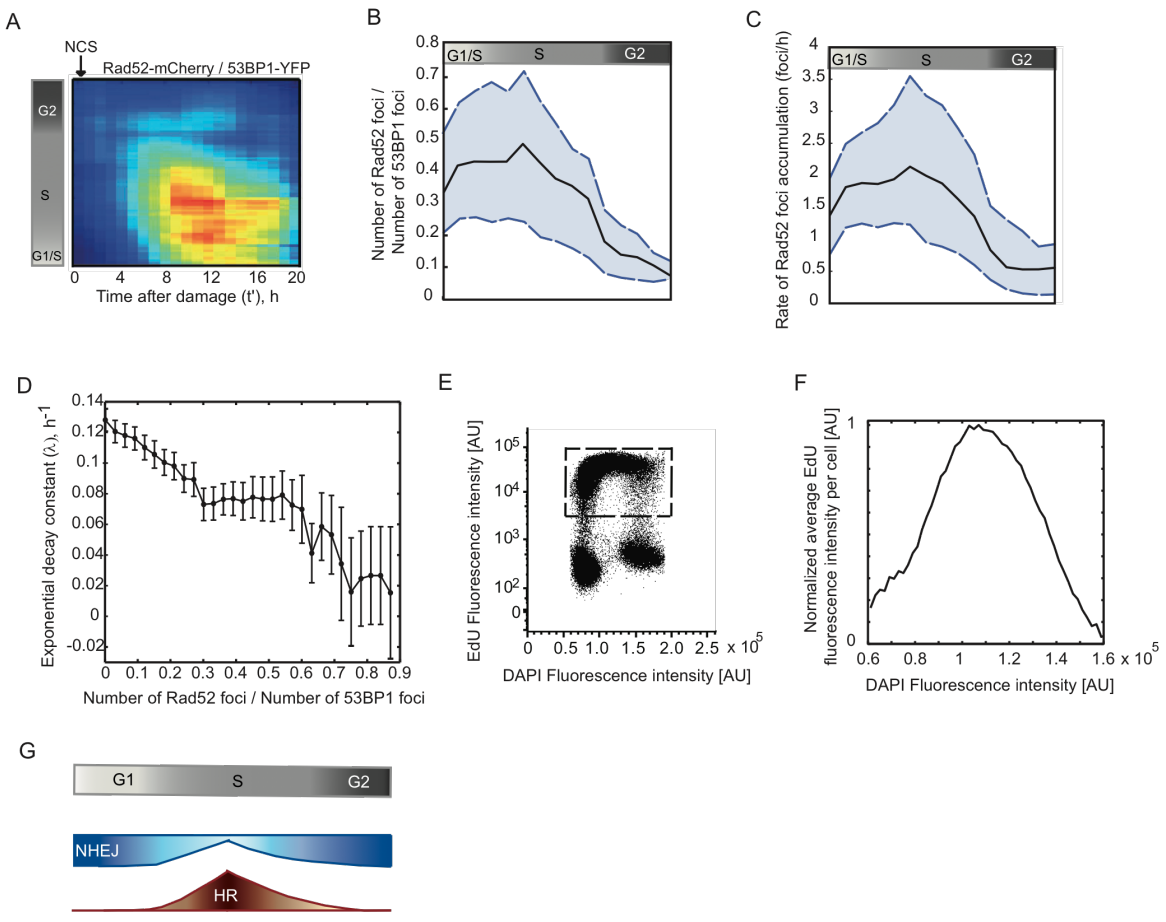

Figure 2.7 (continued)

entering S phase. Instead, the level of HR increases gradually as cells progress from early to mid-S phase, followed by a gradual decrease when they progress to late-S and G2. We confirmed that the relative position of cells in S (early, mid, late) at the time of damage had not changed when they showed maximal activation of HR (11h post damage; Figure 2.6E).

The observation that mid-S phase cells attain the greatest proportions of HR (Figure 2.7A, B) and exhibit the longest half-lives of DSBs (Figure 2.3C) suggests a potential correlation between the choice of repair pathway and the kinetics of repair. To investigate this further, we plotted the average decay constant obtained from exponential fits to the enumerated 53BP1-YFP foci for cells binned according to their proportions of HR post damage (Figure 2.7D). Indeed, a strong correlation was observed; the rates of repair declined with increasing contribution of HR to total DSB repair, supporting the idea that HR mediated DSB joining proceeds at a slower rate than NHEJ mediated repair. We also calculated the half-lives of Rad52 foci in cells damaged in S and G2, and found no significant difference (Figure 2.6F, p-value 0.2379, t-test), suggesting that the 5 – 10 hour variation in the half-life of DSBs observed between S and G2 results mainly from the choice of repair mechanism and not from differences in the kinetics of HR. Interestingly, there were several regimes in which an increase in HR did not produce a proportional change in repair rates (Figure 2.7D), supporting that, in addition to the extent of HR, other factors such as chromatin compaction and cyclin-CDK activity affect the kinetics of DSB repair.

5. Increased levels of HR in mid-S correlate with high levels of DNA replication

When damaged cells replicate their DNA, SSBs and blocking lesions on the DNA may cause active replication forks to stall and collapse, resulting in one-ended DSBs. One-ended DSBs breaks are repaired exclusively by HR (Helleday et al., 2007), as NHEJ requires two free DNA duplex ends for repair. The proportion of HR in S phase therefore, might depend on the level of active DNA replication. DNA does not replicate uniformly throughout S phase, rather different regions of the genome are replicated at distinct rates and times during S phase. In yeast, the highest replication origin firings occur near mid-S (Raghuraman et al., 2001). Even though replication timing is less well characterized in human cells, studies indicate that replication rates are highest around mid-S (Woodfine et al., 2004). To measure the level of DNA replication, we exposed an asynchronously growing population to a 20 minute pulse of EdU and quantified its content by flow cytometry. Within such a short time interval, the number of cells entering or exiting S phase is negligible and EdU fluorescence per cell is indicative mainly of level of EdU incorporation (i.e. amount of DNA replication). We found that cells in mid-S amassed the highest quantities of EdU (Figure 2.7E, F). This indicates that DNA replication was greatest in mid-S, correlating with the high proportions of HR observed during this time. This suggests that in mammalian cells, HR is most important for repair of DSBs created during active DNA replication.

Discussion

With recent advances in imaging techniques and single cell analyses, it has become clear that variability in internal states leads to remarkable heterogeneity in the behavior of isogenic cells exposed to a uniform stimulus (Snijder and Pelkmans, 2011). Studying how basal states affect individual cellular behavior is crucial for our ability to understand and predict cellular responses and for developing efficient drugs. In this study, we used fluorescent reporters for 53BP1, Geminin and Rad52 to assess how variations in cell cycle state impact the kinetics of DSB repair and the balance between alternate repair pathways in individual cells. Although an analysis of the rates of repair has been previously undertaken in populations of fixed cells (Shibata et al., 2011), our live cell system allowed us to develop a more comprehensive picture of how the kinetics of repair vary throughout the cell cycle and within each phase. We show that not only do the rates of repair differ between cells damaged in different cell cycle phases, but individual cells damaged in the same phase also vary significantly in the kinetics of repair. This heterogeneity is most pronounced for S phase cells; cells damaged closer to the G1/S transition attain the highest rates of repair amongst all cells, following which the rates decrease as cells progress to mid-S and then increase towards late S and G2. Based on these findings, we argue that the rates of DSB repair are fine tuned according to the exact time each cell has spent in a phase.

Next, we show that the rate of repair strongly correlates with the contribution of HR to DSB repair, which also varies continuously with cell cycle progression. HR is absent in

cells damaged in early G1, following which it increases gradually and peaks at mid-S then declines towards late S and G2 (Fig. 2.7G). This shows that cells do not initiate a maximal use of HR immediately on entering S phase, nor do they show maximal HR at the end of S and in G2 when replication is complete. Our data therefore do not favor the idea that the presence of sister chromatids control the level of HR in the post replicative phases in mammalian cells.

Our analysis also provided a measure of the variation between cells. We found that the proportion and rates of active HR vary widely even between individual cells damaged at the exact cell cycle position. For example, the proportion of breaks repaired by HR in cells at the G1/S transition (~ 8 h post division) vary from approximately 20% to 65% (Figure 2.7B). This suggests that the choice between NHEJ and HR is influenced by additional factors such as the nature of the break (one-ended or two-ended); chromatin complexity; or dose of DNA damage (Beucher et al., 2009; Shibata et al., 2011).

One explanation for the high proportions of HR observed in mid-S is that NHEJ is unable to compete with HR for break sites during this phase. It is known that HR plays an exclusive role in the repair of one-ended DSBs that arise when replication forks stall at nicks in the DNA template and collapse in S phase (Helleday et al., 2007). When cells are damaged during peak DNA replication, nicks created on the DNA template may cause collapse of several active forks and create substrate that can only be addressed by HR mediated repair. We observe that in our cells; the highest amount of DNA replication occurs in mid-S, correlating well with increased proportions of HR observed during this

time. It is further tempting to speculate that a close association between replication machinery and HR factors leads to the gradual transition between NHEJ and HR as cells enter or exit S phase. The interaction of CtIP, a protein essential for DNA resection in the HR pathway, with PCNA, provides some evidence for this hypothesis (Gu and Chen, 2009). G2 cells demonstrate a reduced efficiency of DNA resection compared to S phase cells that may further allow an increased channeling of DSBs into NHEJ as cells progress into G2 (Zierhut and Diffley, 2008). Additionally, while both cyclins A and B can activate the resection machinery, differences in their individual efficiencies could lead to a decline in HR with a gradual decrease in cyclin A activity as cells progress towards mitosis. Future studies employing conditional replication defective cell lines and perturbations that uncouple DNA replication from cyclin activity will help consolidate the relationship between active DNA replication, cyclin levels and HR repair.

In this study we used U2OS cells, which lack a stable G1/S checkpoint. This allows cells damaged in G1 to progress into S phase and activate HR during the course of repair (Figure 2.5H). As in the case of U2OS, many cancers arise due to mutations in key regulators of the G1/S checkpoint and hence understanding how cells with disabled checkpoints repair DNA damage in response to chemotherapy is of clinical relevance. In addition, recent work has uncovered substantial limitations to the G1/S checkpoint even in damaged normal cells (Deckbar et al., 2010). First, the G1/S checkpoint is not fully initiated until several hours post damage, during which time many G1 cells enter S phase with unrepaired breaks. Second, at high doses of damage most cells undergo a permanent G1/S arrest, but a small fraction of cells escape arrest and enter S phase with DSBs. It

would be important to determine the choice and kinetics of repair in additional cancer and primary cells.

The quantitative analysis presented here was made possible due to the use of fluorescent reporters in live cells. Previous studies that have used similar approaches provided important insights about the complex mechanisms that function to preserve genomic integrity in response to DNA damage. For example, fluorescent tagged 53BP1, Mdc1 and NBS1 provided a detailed understanding of the spatiotemporal sequence of events initiated on DSB generation and the causal relationship between them (Bekker-Jensen et al., 2005; Lukas et al., 2004). In addition, using fluorescent H2B and probes that bind to an *ISce1* induced break led to the discovery that free DNA ends at DSB sites have limited local movement and that damaged chromatin does not undergo large-scale movements (Kruhlak et al., 2006; Soutoglou et al., 2007). Therefore, fluorescent reporters that bind DSBs present a powerful tool for dissecting signaling kinetics and cellular decisions in individual cells.

Ultimately, measurements using DNA damage and repair reporters in live cells will enable us to address additional long-standing, fundamental questions in this field. For example, reporters for NHEJ and HR in altered cellular states can teach us about their ability to compensate for each other under selective drug action. Reporters for the different sub-pathways of homology dependent repair can provide insights into their interplay and balance at different stages of repair. Such reporters can also help determine the timing at which commitment to a specific repair pathway occurs and the factors

leading to these decisions. Live cell reporters also enable the observation of time separated events in the same cells such as repair, cell cycle checkpoints and activation of tumor suppressor proteins. Such analyses in cellular backgrounds where key DNA response proteins are mutated have the promise of providing a comprehensive understanding of how specific mutations or polymorphisms lead to carcinogenesis.

Experimental procedures

Cell culture

U2OS cells were grown in McCoy′s 5A medium supplemented with 10% fetal calf serum, 100 U/mL penicillin, 100 μg/mL streptomycin and 250 ng/mL fungizone (Gemini Bio-Products). When required, the medium was supplemented with selective antibiotics (400 μg/mL G418, 5 μg/mL blasticidin, 50 μg/mL hygromycin). When indicated, medium was replaced with fresh medium supplemented with 200 ng/mL Neocarzinostatin (National Cancer Institute) during experiments. Cell cycle distributions were analyzed by flow cytometry using propidium iodide or DAPI staining as indicated. DNA replication was measured by incorporation of EdU using the Click-iT EdU kit (Invitrogen).

Cell Line Construction

The original pCMV-EGFP-53BP1 construct was kindly provided by Prof. Yasuhisa Adachi (Jullien et al., 2002). We generated our pEF1a-EYFP-53BP1 plasmid by replacing GFP with YFP and combining this fluorescent protein-cDNA fragment with the

EF1a promoter in a vector harboring a neomycin resistance cassette using standard molecular biology techniques. This plasmid was stably transfected into U2OS cells using FuGENE6 (Roche), which were maintained in selective media and sorted into single cells using fluorescence activated cell sorting to generate a clonal population.

Our pEF1a-mCherry-Rad52 plasmid was generated similarly from the original pCMV-EGFP-Rad52 construct kindly provided by Prof. Roland Kanaar (Essers et al., 2002). The GFP tag was replaced with mCherry and the fluorescent protein-cDNA fragment was combined with the EF1a promoter in a vector harboring a blasticidin resistance cassette. Stable, clonal cell lines were established as described above.

The pCMV-ECFP-Geminin construct was generated by PCR amplification of the sequence coding for the 110 amino acid N-terminus of Geminin from genomic DNA isolated from human cells. The PCR product was combined with the CMV promoter and CFP tag in a lentiviral vector harboring a hygromycin resistance cassette by Multisite Gateway cloning (Invitrogen). This plasmid was transfected into 293T cells to generate replication-defective viral particles using standard protocols, which were used to stably infect our engineered U2OS cell line.

In silico mapping of cell cycle progression in individual cells

We first established the average cell cycle duration of our cell line by imaging undamaged, freely cycling cells for 48h. During this time most cells underwent at least two successive divisions, which were identified from the Geminin-CFP reporter. The

time between successive divisions was measured and averaged for ~100 cells to establish the average cell cycle. For *in silico* mapping of cell cycle progression of individual cells at the time of damage, we imaged cells for 24h prior to addition of NCS (Figure S1B). This allowed most cells to divide at least once prior to damage; and we isolated trajectories where the time of division could be clearly determined. To relate elapsed time after division to cell cycle phase and progression, we measured the distribution of DNA content in an asynchronously growing culture by flow cytometry using propidium iodide staining. These distributions were fit using a modification of the Dean-Jett model (Dean and Jett, 1974) to determine the amount of cells in G1, S and G2 phases; and were subsequently translated to the time spent in various cell cycle phases using a previously published model (Toettcher et al., 2009). These durations were then mapped to the time since last cell division before damage was applied for individual cells to establish their cell cycle progression at the time of damage.

Time-Lapse Microscopy

24h prior to microscopy, cells were plated in RMPI lacking riboflavin and phenol red in poly-D-lysine coated glass-bottom plates (MatTek Corporation). The medium was supplemented with 10% fetal calf serum, 100 U/mL penicillin, 100 mg/mL streptomycin, 250 ng/mL fungizone (Gemini Bio-Products) and 10 mM HEPES. Cells were imaged on a Nikon Eclipse Ti inverted microscope with a 40X plan apo objective (NA 0.95), Hamamatsu Orca ER camera and a Perfect Focus System. The microscope was surrounded by a custom enclosure to maintain constant temperature and atmosphere. The filter sets used were CFP - 436/20 nm; 455 nm; 480/40 nm (excitation; beam splitter;

emission filter), YFP - 500/20 nm; 515 nm; 535/30 nm; and mCherry - 560/40 nm; 585 nm; 630/75 nm (Chroma). Images were acquired every 20 mins in the phase and CFP channels and every 60 mins in the YFP and mCherry channels. We acquired 6 z-sections with a step size of 0.75 μm in the YFP and mCherry channels. Image acquisition was controlled by MetaMorph software (Molecular Devices).

Image Analysis

Image analysis was done by Matlab (MathWorks) based custom written software. Cell boundaries were calculated by two complementary approaches. (i) Cells were separated from background by thresholding a Top-Hat transform of the original image. Top-Hat transformation was used to remove trends that are spatially wider than cell diameters. (ii) Boundaries between adjacent, touching cells were identified by seed based watershedding. Seeds were calculated as the regional maxima of the Gaussian smoothed image. To eliminate bias to regional maxima by bright foci, images were first pre-processed by morphological closing with a structure smaller than cell diameter but larger than foci. Foci were identified by taking advantage of their small size. Images were first transformed with Top-Hat to remove all intensities that are spatially larger that 10% of cell diameter. This transformation resulted in an image with a strongly intensified foci signal. Foci were then segmented by regional thresholding followed by seed-based watershedding (Figure 2.8). Similar to cell boundaries, seeds were calculated as the

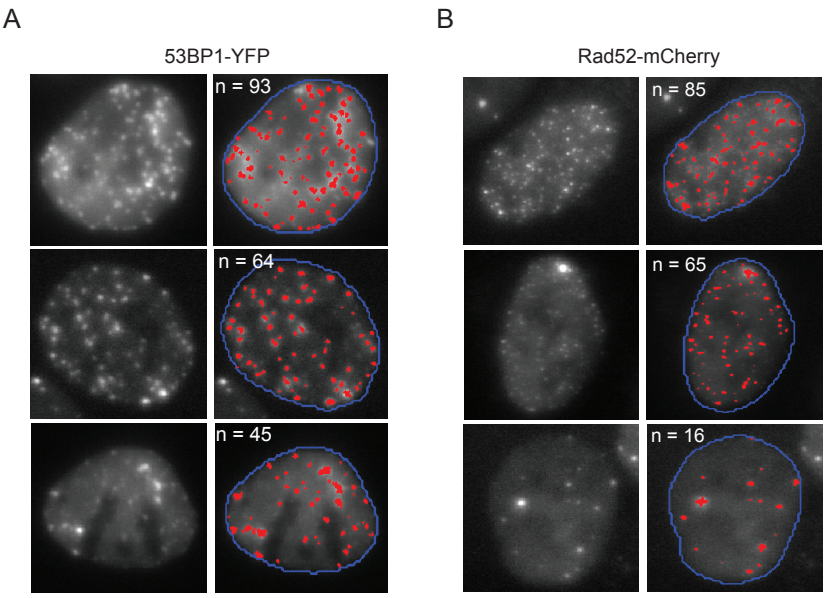

Figure 2.8: Examples of automated foci segmentation

Examples of automated foci segmentation in three cells with different 53BP1-YFP (A) or Rad52-mCherry (B) foci numbers and intensities. Image processing was performed using the Ensemble Thresher software package developed in our lab. See experimental procedures for algorithmic details.

---

regional maxima of the fluorescence intensity. The image analysis algorithm was separately optimized to identify 53BP1-YFP foci and Rad52-mCherry foci, which differed in size and intensity.

Immunofluorescence

Cells were grown on number 1.5 glass coverslips coated with poly-L-lysine (Sigma-Aldrich). They were fixed with 2% paraformaldehyde, permeabilized with 0.2% Triton/PBS and blocked with 5% goat serum supplemented with 1% bovine serum albumin. Cells were treated with primary antibody to detect γ-H2AX (mouse

monoclonal JBW301, Upstate, 1:700 dilution) or BRCA1 (mouse monoclonal D-9, Santa Cruz, 1:100 dilution), washed and treated with secondary antibody conjugated with Alexa Fluor 647 (Molecular Probes). After washing, cells were stained with Hoechst (Molecular Probes) and embedded in Prolong Antifade (Invitrogen). Immunofluorescence preparations were imaged on the microscope described for live cell imaging and automated segmentation was performed in Matlab (MathWorks) with algorithms from CellProfiler (Carpenter et al., 2006).

Acknowledgements

We thank Sara Thiebaud and Michal Mekel for early contribution to this work. We thank Roy Kishony, Tim Mitchison, Dipanjan Chowdhury, Rebecca Ward and all members of the Lahav lab for comments and discussions. We thank the Nikon Imaging Center at Harvard Medical School for assistance with microscopy. This research was supported by the National Institute of Health grant GM083303, the Kaneb foundation, Hoffman-La Roche and fellowships from the German Research Foundation and the Charles King trust to A.L.

References

Anderson, L., Henderson, C., and Adachi, Y. (2001). Phosphorylation and rapid relocalization of 53BP1 to nuclear foci upon DNA damage. Mol Cell Biol *21*, 1719-1729.

Aylon, Y., Liefshitz, B., and Kupiec, M. (2004). The CDK regulates repair of double-strand breaks by homologous recombination during the cell cycle. Embo J *23*, 4868-4875.

Bekker-Jensen, S., Lukas, C., Kitagawa, R., Melander, F., Kastan, M.B., Bartek, J., and Lukas, J. (2006). Spatial organization of the mammalian genome surveillance machinery in response to DNA strand breaks. J Cell Biol *173*, 195-206.

Bekker-Jensen, S., Lukas, C., Melander, F., Bartek, J., and Lukas, J. (2005). Dynamic assembly and sustained retention of 53BP1 at the sites of DNA damage are controlled by Mdc1/NFBD1. J Cell Biol *170*, 201-211.

Beucher, A., Birraux, J., Tchouandong, L., Barton, O., Shibata, A., Conrad, S., Goodarzi, A.A., Krempler, A., Jeggo, P.A., and Lobrich, M. (2009). ATM and Artemis promote homologous recombination of radiation-induced DNA double-strand breaks in G2. Embo J *28*, 3413-3427.

Carpenter, A.E., Jones, T.R., Lamprecht, M.R., Clarke, C., Kang, I.H., Friman, O., Guertin, D.A., Chang, J.H., Lindquist, R.A., Moffat, J.*, et al.* (2006). CellProfiler: image analysis software for identifying and quantifying cell phenotypes. Genome Biol *7*, R100.

Dean, P.N., and Jett, J.H. (1974). Mathematical analysis of DNA distributions derived from flow microfluorometry. J Cell Biol *60*, 523-527.

Deckbar, D., Stiff, T., Koch, B., Reis, C., Lobrich, M., and Jeggo, P.A. (2010). The limitations of the G1-S checkpoint. Cancer Res *70*, 4412-4421.

Essers, J., Houtsmuller, A.B., van Veelen, L., Paulusma, C., Nigg, A.L., Pastink, A., Vermeulen, W., Hoeijmakers, J.H., and Kanaar, R. (2002). Nuclear dynamics of RAD52 group homologous recombination proteins in response to DNA damage. Embo J *21*, 2030-2037.

Feng, Z., Scott, S.P., Bussen, W., Sharma, G.G., Guo, G., Pandita, T.K., and Powell, S.N. (2011). Rad52 inactivation is synthetically lethal with BRCA2 deficiency. Proc Natl Acad Sci U S A *108*, 686-691.

Gu, B., and Chen, P.L. (2009). Expression of PCNA-binding domain of CtIP, a motif required for CtIP localization at DNA replication foci, causes DNA damage and activation of DNA damage checkpoint. Cell Cycle *8*, 1409-1420.

Helleday, T., Lo, J., van Gent, D.C., and Engelward, B.P. (2007). DNA double-strand break repair: from mechanistic understanding to cancer treatment. DNA Repair (Amst) *6*, 923-935.

Huertas, P., Cortes-Ledesma, F., Sartori, A.A., Aguilera, A., and Jackson, S.P. (2008). CDK targets Sae2 to control DNA-end resection and homologous recombination. Nature *455*, 689-692.

Huertas, P., and Jackson, S.P. (2009). Human CtIP mediates cell cycle control of DNA end resection and double strand break repair. J Biol Chem *284*, 9558-9565.

Ira, G., Pellicioli, A., Balijja, A., Wang, X., Fiorani, S., Carotenuto, W., Liberi, G., Bressan, D., Wan, L., Hollingsworth, N.M.*, et al.* (2004). DNA end resection, homologous recombination and DNA damage checkpoint activation require CDK1. Nature *431*, 1011-1017.

Jazayeri, A., Falck, J., Lukas, C., Bartek, J., Smith, G.C., Lukas, J., and Jackson, S.P. (2006). ATM- and cell cycle-dependent regulation of ATR in response to DNA double-strand breaks. Nat Cell Biol *8*, 37-45.

Johnson, R.D., and Jasin, M. (2000). Sister chromatid gene conversion is a prominent double-strand break repair pathway in mammalian cells. Embo J *19*, 3398-3407.

Jullien, D., Vagnarelli, P., Earnshaw, W.C., and Adachi, Y. (2002). Kinetochore localisation of the DNA damage response component 53BP1 during mitosis. J Cell Sci *115*, 71-79.

Kadyk, L.C., and Hartwell, L.H. (1992). Sister chromatids are preferred over homologs as substrates for recombinational repair in Saccharomyces cerevisiae. Genetics *132*, 387-402.

Kruhlak, M.J., Celeste, A., Dellaire, G., Fernandez-Capetillo, O., Muller, W.G., McNally, J.G., Bazett-Jones, D.P., and Nussenzweig, A. (2006). Changes in chromatin structure and mobility in living cells at sites of DNA double-strand breaks. J Cell Biol *172*, 823-834.

Lieber, M.R., Ma, Y., Pannicke, U., and Schwarz, K. (2003). Mechanism and regulation of human non-homologous DNA end-joining. Nat Rev Mol Cell Biol *4*, 712-720.

Lisby, M., Barlow, J.H., Burgess, R.C., and Rothstein, R. (2004). Choreography of the DNA damage response: spatiotemporal relationships among checkpoint and repair proteins. Cell *118*, 699-713.

Lobrich, M., Shibata, A., Beucher, A., Fisher, A., Ensminger, M., Goodarzi, A.A., Barton, O., and Jeggo, P.A. (2010). gammaH2AX foci analysis for monitoring DNA double-strand break repair: strengths, limitations and optimization. Cell Cycle *9*, 662-669.

Lukas, C., Melander, F., Stucki, M., Falck, J., Bekker-Jensen, S., Goldberg, M., Lerenthal, Y., Jackson, S.P., Bartek, J., and Lukas, J. (2004). Mdc1 couples DNA double-strand break recognition by Nbs1 with its H2AX-dependent chromatin retention. Embo J *23*, 2674-2683.

Lukas, C., Savic, V., Bekker-Jensen, S., Doil, C., Neumann, B., Pedersen, R.S., Grofte, M., Chan, K.L., Hickson, I.D., Bartek, J*., et al.* (2011). 53BP1 nuclear bodies form around DNA lesions generated by mitotic transmission of chromosomes under replication stress. Nat Cell Biol *13*, 243-253.

McIlwraith, M.J., and West, S.C. (2008). DNA repair synthesis facilitates RAD52-mediated second-end capture during DSB repair. Mol Cell *29*, 510-516.

Raghuraman, M.K., Winzeler, E.A., Collingwood, D., Hunt, S., Wodicka, L., Conway, A., Lockhart, D.J., Davis, R.W., Brewer, B.J., and Fangman, W.L. (2001). Replication dynamics of the yeast genome. Science *294*, 115-121.

Rijkers, T., Van Den Ouweland, J., Morolli, B., Rolink, A.G., Baarends, W.M., Van Sloun, P.P., Lohman, P.H., and Pastink, A. (1998). Targeted inactivation of mouse RAD52 reduces homologous recombination but not resistance to ionizing radiation. Mol Cell Biol *18*, 6423-6429.

Rothkamm, K., Kruger, I., Thompson, L.H., and Lobrich, M. (2003). Pathways of DNA double-strand break repair during the mammalian cell cycle. Mol Cell Biol *23*, 5706-5715.

Rothkamm, K., and Lobrich, M. (2003). Evidence for a lack of DNA double-strand break repair in human cells exposed to very low x-ray doses. Proc Natl Acad Sci U S A *100*, 5057-5062.

Sakaue-Sawano, A., Kurokawa, H., Morimura, T., Hanyu, A., Hama, H., Osawa, H., Kashiwagi, S., Fukami, K., Miyata, T., Miyoshi, H.*, et al.* (2008). Visualizing spatiotemporal dynamics of multicellular cell-cycle progression. Cell *132*, 487-498.

Schultz, L.B., Chehab, N.H., Malikzay, A., and Halazonetis, T.D. (2000). p53 binding protein 1 (53BP1) is an early participant in the cellular response to DNA double-strand breaks. J Cell Biol *151*, 1381-1390.

Shibata, A., Conrad, S., Birraux, J., Geuting, V., Barton, O., Ismail, A., Kakarougkas, A., Meek, K., Taucher-Scholz, G., Lobrich, M.*, et al.* (2011). Factors determining DNA double-strand break repair pathway choice in G2 phase. Embo J.

Shiloh, Y., van der Schans, G.P., Lohman, P.H., and Becker, Y. (1983). Induction and repair of DNA damage in normal and ataxia-telangiectasia skin fibroblasts treated with neocarzinostatin. Carcinogenesis *4*, 917-921.

Shrivastav, M., De Haro, L.P., and Nickoloff, J.A. (2008). Regulation of DNA double-strand break repair pathway choice. Cell Res *18*, 134-147.

Snijder, B., and Pelkmans, L. (2011). Origins of regulated cell-to-cell variability. Nat Rev Mol Cell Biol *12*, 119-125.

Soutoglou, E., Dorn, J.F., Sengupta, K., Jasin, M., Nussenzweig, A., Ried, T., Danuser, G., and Misteli, T. (2007). Positional stability of single double-strand breaks in mammalian cells. Nat Cell Biol *9*, 675-682.

Stark, J.M., Pierce, A.J., Oh, J., Pastink, A., and Jasin, M. (2004). Genetic steps of mammalian homologous repair with distinct mutagenic consequences. Mol Cell Biol *24*, 9305-9316.

Takata, M., Sasaki, M.S., Sonoda, E., Morrison, C., Hashimoto, M., Utsumi, H., Yamaguchi-Iwai, Y., Shinohara, A., and Takeda, S. (1998). Homologous recombination and non-homologous end-joining pathways of DNA double-strand break repair have overlapping roles in the maintenance of chromosomal integrity in vertebrate cells. Embo J *17*, 5497-5508.

Tashiro, S., Walter, J., Shinohara, A., Kamada, N., and Cremer, T. (2000). Rad51 accumulation at sites of DNA damage and in postreplicative chromatin. J Cell Biol *150*, 283-291.

Toettcher, J.E., Loewer, A., Ostheimer, G.J., Yaffe, M.B., Tidor, B., and Lahav, G. (2009). Distinct mechanisms act in concert to mediate cell cycle arrest. Proc Natl Acad Sci U S A *106*, 785-790.

van Veelen, L.R., Essers, J., van de Rakt, M.W., Odijk, H., Pastink, A., Zdzienicka, M.Z., Paulusma, C.C., and Kanaar, R. (2005). Ionizing radiation-induced foci formation of mammalian Rad51 and Rad54 depends on the Rad51 paralogs, but not on Rad52. Mutat Res *574*, 34-49.

West, S.C. (2003). Molecular views of recombination proteins and their control. Nat Rev Mol Cell Biol *4*, 435-445.

Woodfine, K., Fiegler, H., Beare, D.M., Collins, J.E., McCann, O.T., Young, B.D., Debernardi, S., Mott, R., Dunham, I., and Carter, N.P. (2004). Replication timing of the human genome. Hum Mol Genet *13*, 191-202.

Yun, M.H., and Hiom, K. (2009). CtIP-BRCA1 modulates the choice of DNA double-strand-break repair pathway throughout the cell cycle. Nature *459*, 460-463.

Zierhut, C., and Diffley, J.F. (2008). Break dosage, cell cycle stage and DNA replication influence DNA double strand break response. Embo J *27*, 1875-1885.

Chapter 3: The relationship between DNA repair and p53 dynamics in single cells

Authors: Ketki Karanam, Alexander Loewer, and Galit Lahav

Abstract

The tumor suppressor p53 is activated by DNA DSBs and initiates transcriptional programs that promote repair, cell cycle arrest or terminal cell fates. The threshold of damage required for p53 activation is unclear. Using fluorescent reporters to quantify DSBs and p53 in single cells, we show that there is no distinct number of breaks above which all damaged cells induce p53 accumulation. The amount of DNA damage rather determines the probability of a p53 response. The decision to activate p53 is influenced by other cell-specific factors in addition to the number of DSBs. We also present evidence that the rates of DSB repair do not affect the probability of activating p53 or its dynamical behavior in response to DNA damage.

Introduction

The tumor suppressor p53 mediates the cellular response to DNA damage by triggering DNA repair and cell cycle arrest or by evoking cellular senescence and apoptosis. These functions of p53 are essential for preserving genomic integrity and preventing neoplastic transformation, and loss of p53 activity either by functional inactivation of its pathway or by gene mutation is a frequent event in the onset and progression of many human malignancies (Jin and Levine, 2001; Levine, 1997). p53 function is also critical to the efficacy of cancer therapies that generate DNA lesions, such as radiation and chemotherapy, and defects in p53 are often associated with therapy resistance (Jiang et al., 2009; Vousden and Lane, 2007). In order to gain a full appreciation of how p53

potentiates genomic stability, as well as to enable its clinical manipulation for maximal therapeutic benefit, it is essential to determine the sensitivity of the p53 pathway to various DNA lesions and identify factors that regulate its activation in response to genotoxic insult.

Within cells, levels of p53 are tightly controlled by several autoregulatory feedback loops that direct the stability and degradation of its protein. Noteworthy in this regard, is the interaction between p53 and its negative regulator, the E3 ubiquitin ligase Mdm2. p53 transcriptionally activates Mdm2 expression and Mdm2 targets p53 for degradation (Barak et al., 1993; Haupt et al., 1997; Kubbutat et al., 1997; Wu et al., 1993). This interaction keeps p53 levels low under unstressed conditions. In response to cellular stress such as DNA damage, p53 is activated through upstream mediators that induce post-translational modifications that disrupt the p53-Mdm2 interaction and allow p53 to stably accumulate in the nucleus. In particular, DNA DSBs induce rapid phosphorylation and activation of the ataxia-telangiectasia mutated (ATM) and checkpoint kinase 2 (Chk2) kinases (Ahn et al., 2000; Bakkenist and Kastan, 2003; Matsuoka et al., 2000). Activated ATM and Chk2 subsequently phosphorylate and stabilize p53, which shows a series of highly regulated, undamped pulses in single cells. The amplitude and duration of p53 pulses is independent of the damage dose, whereas the number of pulses increases with higher damage (Lahav et al., 2004). In addition, these pulses are generated in an excitable manner, where both a transient or sustained input triggers a complete p53 pulse (Batchelor et al., 2008; Loewer et al., 2010). Remarkably, identical cells in a uniformly damaged population exhibit a large heterogeneity in their p53 response. A fraction of

cells do not activate p53, while other cells induce one or more p53 pulses (Lahav et al., 2004). It is likely that this variation arises from differences in the cells' number of breaks and rates of repair, and p53 may only be active in cells where the damage exceeds a threshold number of DSBs.

Although much insight has been gained into the molecular mechanisms that regulate p53 pulses in response to DNA DSBs, little is known about the threshold of damage necessary for p53 activation. Immunoblots for ATM and Chk2 phosphorylation in irradiated cells suggested that these kinases are activated in a highly sensitive manner. Damage doses estimated to generate one or two DSBs were sufficient for a partial activation of ATM, and doses that generated less than twenty DSBs evoked a complete ATM and Chk2 response (Bakkenist and Kastan, 2003; Buscemi et al., 2004). However, since these measurements averaged over a population of cells, it is unclear if all irradiated cells uniformly activated ATM, or, if the partial activation of ATM resulted from averaging between distinct subpopulations that either received a high number of breaks and generated a full ATM response or received no or few breaks and did not respond. Other measurements of the sensitivity of the p53 pathway were obtained by introducing restriction enzymes or linearized double-stranded DNA molecules into cells that were subsequently assayed for p53 function. Based on serial dilutions of the introduced substrates, it was estimated that a solitary DSB might suffice to activate a p53 response (Huang et al., 1996; Wahl et al., 1997). However, these estimates were limited by the lack of a direct observation of the number of DSBs in each cell, which raises the possibility that not all cells received exactly one DSB or uniformly activated a p53

response. In order to gain a clear quantitative understanding of the relationship between the number of DSBs, their rates of repair and p53 activation, it is therefore necessary to observe these events in the same living cell.

In this study we quantify the number of DSBs and the induction of a p53 response in individual living cells by using fluorescent reporters. We show that the probability of inducing a p53 pulse increases with the amount of damage. However, there is no fixed threshold number of DSBs above which all cells trigger a p53 response. We demonstrate that a cell's decision to activate a p53 pulse, as well as the dynamical properties of the pulse, are independent of the rates of DSB repair. Our findings suggest that in addition to the number of DSBs, other cellular factors potentially influence the activation of p53 in response to DNA damage.

Results

4. Quantifying DNA DSBs and rates of repair in individual living cells

We quantify DNA DSBs in single cells using a fluorescent reporter expressing mouse 53BP1 fused to mCherry (Figure 3.1A). 53BP1 is a mediator protein in the DNA damage response. It localizes to chromatin regions adjacent to the break within minutes after damage, and forms discernable foci that serve as markers for the number and location of DSBs (Anderson et al., 2001; Bekker-Jensen et al., 2005; Jullien et al., 2002; Schultz et al., 2000). We established a clonal MCF7 breast carcinoma cell line that stably expressed

Figure 3.1 Experimental system for quantifying DNA DSBs in single, living cells

(A) Schematic drawing of the 53BP1 reporter. **(B)** Cells expressing 53BP1- mCherry were fixed and stained with anti γ-H2AX antibody 30 mins after 5Gy γ-irradiation. The overlaid image, and the measured intensities of both 53BP1-mCherry and γ-H2AX staining across a random line in the nucleus **(C)** show co-localization between 53BP1 and γ-H2AX foci. **(D)** Time-lapse images of two cells expressing 53BP1- mCherry after 5Gy γ-irradiation. Images are maximum projections of z-stacks through the nucleus (see Experimental Procedures) in the mCherry channel. **(E)** Example of the automated segmentation for the enumeration of 53BP1-mCherry foci in a cell. Images are pseudo colored to improve visualization and segmented foci are shown in red. Image processing was performed using custom written Matlab based software (see Experimental Procedures for algorithmic details). **(F)** Enumerated 53BP1-mCherry foci (dots) and the exponential fits to the raw data (dashed lines) for the two cells shown in (C). **(G)** Time-lapse images of two cells that were pre-treated with a small molecule inhibitor of DNA-PK prior to 10 Gy γ-irradiation. The images show that foci decay more slowly when repair is inhibited. **(H)** The average half-life of 53BP1 foci after 10Gy γ-irradiation in a control population and in cells that were pre-treated with a small molecule inhibitor of DNA-PK. Half-lives were calculated by fitting a single exponential decay to the enumerated 53BP1-mCherry foci in individual cells. Bars represent mean $\pm$ sd for a population of 97 cells in the 10 Gy control and 81 cells in the 10 Gy + Inhibitor treatment **(I)** Distributions of the number of 53BP1-mCherry foci at 18hr post damage in cells imaged every hour for 18hr (i) or imaged only once at 18hr (ii) post damage. No of cells = ~140 for each condition. **(J)** Average number of 53BP1 foci in cells treated with 0Gy, 5Gy and 10Gy γ-irradiation at 1hr post irradiation. Bars represent mean $\pm$ sd. No of cells, n = 89 (0Gy IR), 97 (5Gy IR) and 65 (10Gy IR). **(K)** Distribution of the initial number and half-life **(L)** of 53BP1 foci in a population of cells treated with 5 Gy γ-irradiation.

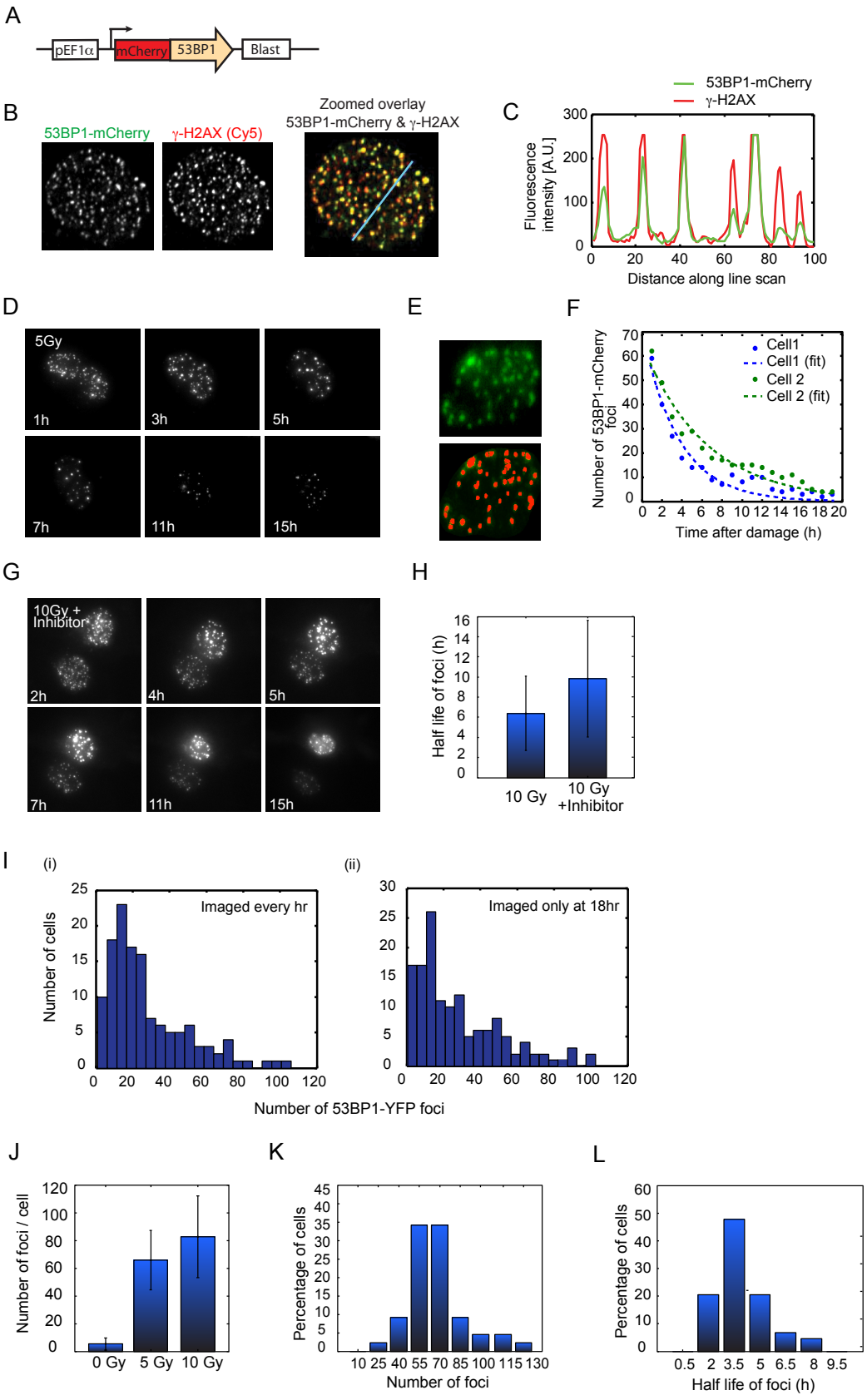

Figure 3.1 (continued)

the 53BP1 reporter, and verified that foci formed by the tagged mouse 53BP1 proteins co-localize with the canonical marker for DSBs, γ-H2AX (Figure 3.1B, C). Our analysis showed that the number of 53BP1-mCherry foci in a cell decreases with time (Figure 3.1D-F). We calculated the half-life of foci by fitting the enumerated foci with an exponential model. To confirm that the decay in the number of foci represents repair (and not loss of signal due to photobleaching), we treated cells with a specific small molecule inhibitor of DNA-PK (NU7026) and showed that their disappearance slows (Figure 3.1G, H). Additionally, we showed that the distribution of the number of foci at 18hr post irradiation is similar between cells that were imaged frequently (every hr) and cells that were imaged only at 18hr post irradiation (Figure 3.1I, p-value 0.41, Kolmogorov-Smirnov test).

We first characterized how individual cells in an irradiated population develop and repair DSBs. As expected, we find that the initial number of 53BP1 foci formed in cells immediately after damage increases with the irradiation dose (Figure 3.1J). Individual cells in a uniformly irradiated population acquire different initial numbers of 53BP1 foci and also vary in their kinetics of repair (Figure 3.1K, L). This shows that there is a large heterogeneity in the response of identical cells exposed to the same damage dose.

2. Is there a threshold number of DSBs required for p53 activation?

Next, we investigated if there is a threshold number of DSBs required to initiate a p53 pulse in damaged cells. To quantify p53 levels in single cells, we added a fluorescent

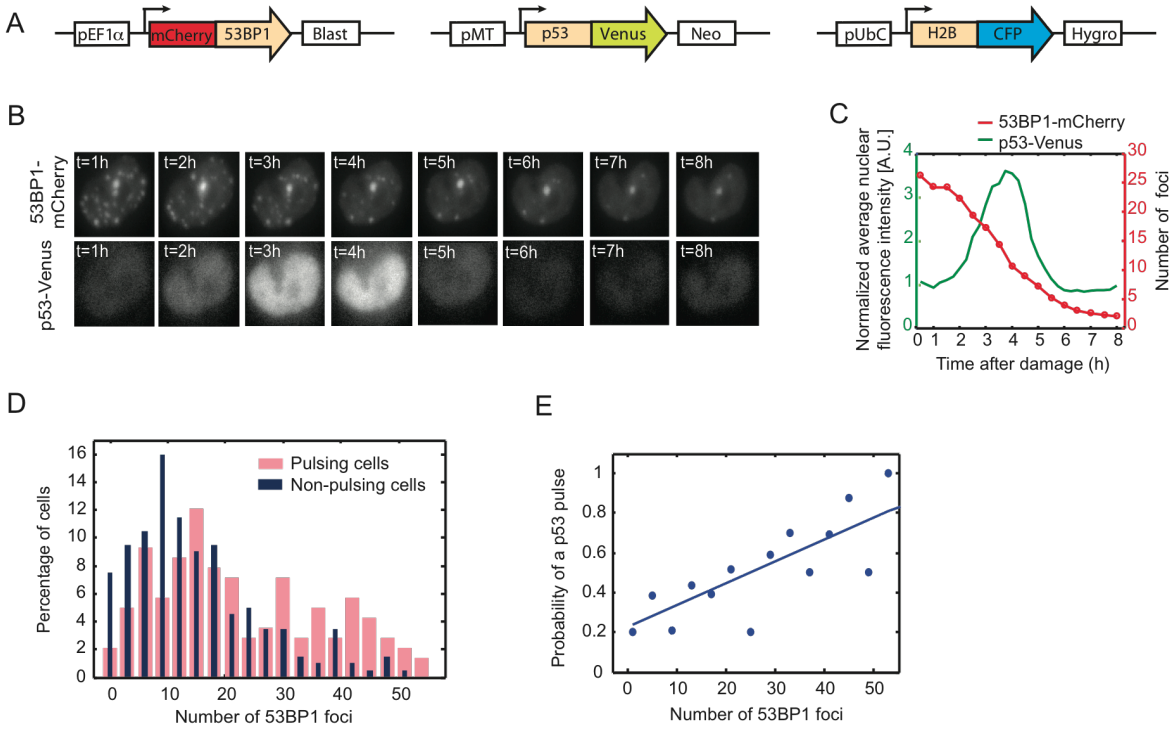

Figure 3.2: Quantifying the threshold number of DSBs required to activate a p53 pulse

(A) Schematic drawing of the 53BP1 and p53 and H2B reporters. **(B)** Time-lapse images of MCF7 cells expressing the reporters in (A) after damage (50 ng/ml NCS). The 53BP1- mCherry images are maximum projections of z-stacks through the nucleus (see Experimental Procedures). **(C)** Quantification of the number of 53BP1-mCherry foci (red) and the normalized average nuclear p53-Venus intensity (green) for the cell shown in (B). **(D)** Distribution of the initial numbers of 53BP1 foci in cells that show a p53 pulse (pink) or do not pulse (blue) after damage. Cells were damaged with a range of NCS concentrations (12.5 ng/ml – 100 ng/ml) to generate a wide distribution of the number of DSBs. Number of cells = ~ 360. **(E)** The probability of inducing a p53 pulse after damage is plotted for cells binned according to their initial number of 53BP1 foci after damage. Bins were calculated with a bin size W = 2 foci and the probability of pulsing is calculated as the fraction of cells that show a pulse in each bin (blue dots). The blue line shows a robust, regression fit to all datapoints. Number of cells = ~ 360.

---

reporter of p53 (p53-Venus) to cells expressing the 53BP1 reporter (Figure 3.2A-C). Our p53-Venus reporter has been previously described (Batchelor et al., 2008; Loewer et al., 2010). In addition, we added a fluorescent reporter for histone H2B (H2B-CFP) to obtain

a uniform nuclear signal that aided the automated segmentation of nuclei for image analysis.

We treated cells expressing the triple reporters with a range of damage doses to generate a wide distribution of initial numbers of DSBs. To induce DSBs, we used the radiomimetic drug neocarzinostatin (NCS), instead of irradiating cells because this allowed us to add the drug directly to cells on the microscope and quantify DSBs before and immediately after damage without a significant time delay in image acquisition. We have previously shown that the kinetics of DSB repair following NCS treatment are similar to those in irradiated cells (Karanam et al., 2012). We found that the distributions of the initial numbers of DSBs for cells that do not pulse and cells that show a p53 pulse immediately after damage differed significantly (p-value 1.19×10^{-05}, Kolmogorov-Smirnov test, Figure 3.2D). However, there was still a large overlap between these distributions, indicating that there is no distinct threshold number of DSBs, below which cells do not activate p53 and above which all damaged cells uniformly generate a p53 pulse. We observed that a higher percentage of cells in the non-pulsing population exhibited low numbers of DSBs compared to cells that induced a p53 pulse. To investigate this further, we binned damaged cells according to their number of DSBs and plotted the probability of inducing a p53 pulse (calculated as the fraction of cells that pulse) for each bin (Figure 3.2E). A linear relationship was observed; with the probability of activating a p53 pulse increasing with the number of DSBs. Our results indicate that a cell's decision to activate p53 after damage is weighted by the number of DSBs, however, other factors potentially influence this decision.

4. Is the decision to activate a p53 pulse stochastic or controlled by cell-specific factors?

Based on the observation that only a fraction of cells in a population with a similar number of DSBs activate a p53 response (for example, only ~50% of cells with ~20 DSBs exhibit a p53 pulse, Figure 3.2E), we speculated that the induction of pulses might either be stochastic, or be influenced by other internal cellular factors such as the cell cycle phase or the status of the repair pathways or p53 network in a cell. To distinguish between these two possibilities, we treated cells with an initial low dose of damage and allowed them time to recover from this treatment. We then re-damaged cells with the same damage dose (Figure 3.3A). If p53 pulses are generated in a stochastic manner, we expect a cell's response to the second treatment to be independent of its response to the first damage insult. Therefore, the population of cells that pulse in response to the second treatment should not be biased in how they responded to the first damage dose. We found that on average, 85% of the cells that pulsed in response to the second damage treatment had also activated a p53 pulse in response to the first damage dose (Figure 3.3B). This suggests that the generation of a p53 pulse in response to a distinct number of DSBs is not entirely stochastic but is potentially influenced by other internal cellular factors.

3. *How do the rates of DSB repair affect the p53 response?*

One potential factor that may affect a cell's decision to pulse after damage is the activity of its DNA repair machinery, which is reflected in its kinetics of repair. Cells that achieve rapid recognition and repair of DSBs may not initiate a p53 pulse in response to damage,

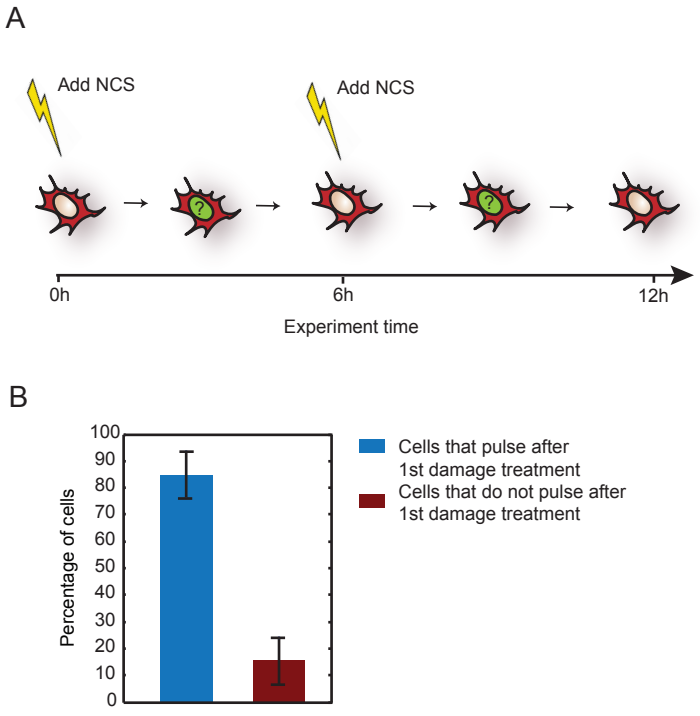

Figure 3.3: Activation of p53 in response to DNA DSBs is influenced by internal cellular factors
(A) Schematic representation of the experimental design to investigate if the decision to activate a p53 pulse is stochastic or determined by cell-specific factors. Cells were damaged with a low dose of NCS and analyzed for the activation of a p53 pulse. The same cells were re-damaged with the same dose of NCS 6h after the first damage treatment, and assessed for the induction of a p53 pulse in response to the second damage treatment. **(B)** The percentage of cells in a population that induced a p53 pulse in response to the second damage treatment, that had activated a p53 pulse (blue) or did not pulse (red) in response to the first damage treatment. Bars represent mean + sd.

---

while cells that are slower in their response to DNA DSBs may activate p53 to induce cell-cycle arrest and allow additional time for repair. To test this hypothesis, we plotted the distributions of the half-lives of 53BP1 foci for cells categorized into two groups based on whether they pulse or do not pulse after damage (Figure 3.4A). We observed that the distributions were similar between the two groups (p-value 0.1071, Kolmogorov-

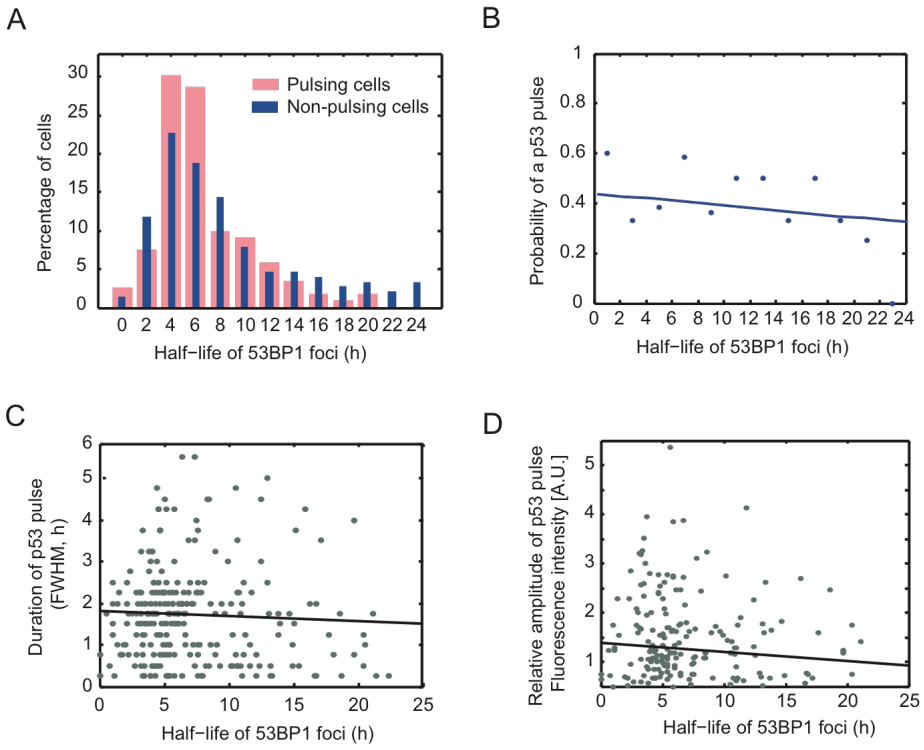

Figure 3.4: Quantifying the effect of the rates of DSB repair on the p53 response

(A) Distribution of the half-life of 53BP1 foci for cells that show a p53 pulse (pink) or do not pulse (blue) after damage (12.5 ng/ml – 100 ng/ml NCS). Number of cells = ~ 360. **(B)** The probability of inducing a p53 pulse after damage is plotted for cells binned according to their half-life of 53BP1 foci after damage. Bins were calculated with a bin size W = 2 hours and the probability of pulsing is calculated as the fraction of cells that show a pulse in each bin (blue dots). The blue line shows a robust, regression fit to all datapoints. Number of cells = ~ 360. **(C)** The duration of the p53 pulse, calculated as the full-width at half-maximal amplitude is plotted against the initial number of 53BP1 foci for a population of ~360 cells. **(D)** The amplitude of the p53 pulse, calculated from the normalized p53 trajectories is plotted against the initial number of 53BP1 foci for a population of ~360 cells. In (C) and (D), the black line shows the least-squares fit to the datapoints.

Smirnov test), suggesting that the rates of repair do not affect the decision to activate p53 after damage. A plot of the probability of inducing a p53 pulse for cells binned according to their half-lives of DSBs further confirmed the lack of a significant correlation between the rates of repair and the probability of activating p53 post damage (Figure 3.4B).

While the rate of DSB repair does not affect the decision to activate p53 after damage, it might still influence the dynamical properties of the pulse, such as its period and amplitude, in cells that activate p53. To explore this, we plotted the duration of the p53 pulse against the half-life of DSBs for individual cells (Figure 3.4C). No correlation was observed indicating that the rate of repair does not affect the period of the p53 pulse in damaged cells. Similarly, the amplitude of the p53 pulse did not correlate strongly with the rates of repair in individual cells, showing that the levels of active p53 are also independent of the speed at which DSBs are repaired (Figure 3.4D).

Intrigued by the above findings, we wondered if altering the rates of repair beyond the normal variance observed in a damaged population would affect the p53 dynamics in these cells. To generate a significant delay in the rates of DSB repair, we attempted to knock down XRCC4, a key protein in the nonhomologous end-joining pathway of DSB repair. XRCC4 in complex with DNA ligase IV functions in the final step of DSB repair where the processed DNA ends are ligated together to generate an intact molecule. We infected our reporter cell line with a virus expressing a shRNA specific for XRCC4, and found that this treatment was effective in reducing XRCC4 gene expression to 4% of its normal cellular level (Figure 3.5A). However, this knock down only resulted in an approximately 50% reduction in the XRCC4 protein level three days after infection (Figure 3.5B, C). Using immunofluorescence analysis, we verified that the 50% reduction in protein levels observed on the immunoblot resulted from a uniform knock down of XRCC4 in all cells of the infected population (Figure 3.5D).

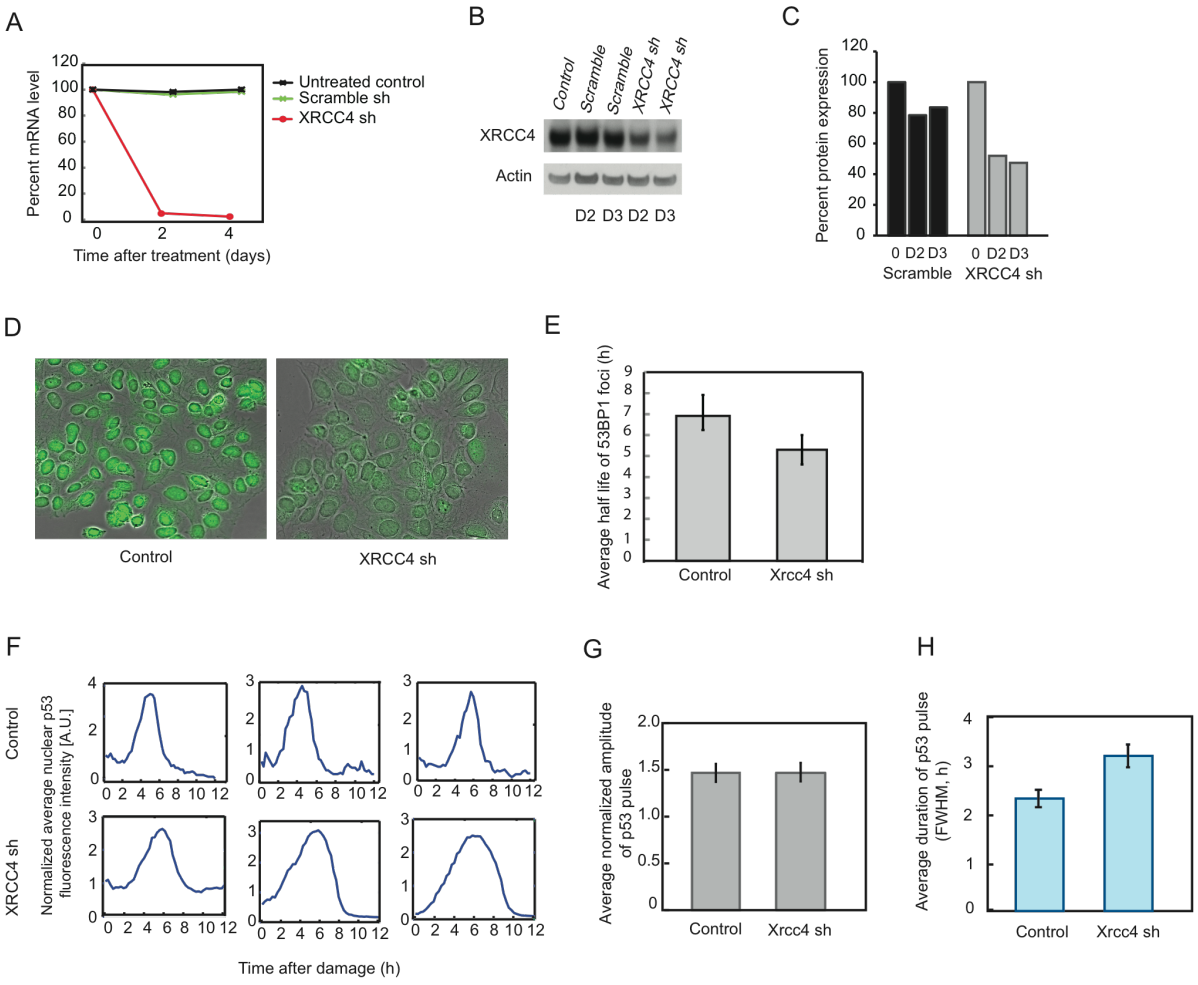

Figure 3.5: Effect of reduced XRCC4 expression on the p53 response

(A) Quantification of the level of XRCC4 mRNA expression in an untreated control (black) and in cells treated with a non-specific scramble shRNA (green) or specific XRCC4 shRNA (red). mRNA levels were measured by quantitative PCR. **(B)** Immunoblot of XRCC4 in an untreated control and in cells treated with scramble shRNA or XRCC4 shRNA. Cells were harvested on day 2 (D2) or day 3 (D3) after treatment. **(C)** Protein quantification of the blot in (B) normalized to Actin and the control. **(D)** Untreated control and cells treated with XRCC4 shRNA were fixed on day 3 after treatment and immunostained to visualize XRCC4. Images show a uniform reduction in XRCC4 protein levels in all treated cells. Images are overlays of the phase channel and the Cy5 channel used for visualizing the staining. **(E)** The average half-life of 53BP1 foci after damage (100 ng/ml NCS) in a control population and in cells treated with XRCC4 shRNA. **(F)** Trajectories of normalized p53 levels after damage (100 ng/ml NCS) for three control cells (top row) and three cells treated with XRCC4 shRNA (bottom row). **(G)** Average amplitude of the p53 pulse after damage (100 ng/ml NCS) for control cells and cells treated with XRCC4 shRNA. **(H)** Average duration of the p53 pulse after damage (100 ng/ml NCS) for control cells and cells treated with XRCC4 shRNA. The duration of the pulse was calculated as the full-width at half-maximal amplitude. In (E) – (H), cells were damaged on day 3 after treatment with XRCC4 shRNA. Bars represent mean $\pm$ SEM for a population n=130 for knock down cells and n=180 for controls.

We damaged cells treated with the XRCC4 shRNA and analyzed their rates of DSB joining. We found that a 50% reduction in XRCC4 protein levels did not generate a delay in DSB repair. Rather, we were surprised to find that the half-life of 53BP1 foci was shorter, indicating faster repair, in the knock down cells compared to normal controls (Figure 3.5E). At present we cannot explain why a reduction in XRCC4 protein levels increases the rates of DSB repair.

We analyzed how the reduced XRCC4 expression affects the dynamical properties of the p53 pulse in response to DNA DSBs. We found no difference in the amplitude of the p53 pulse between cells treated with the XRCC4 shRNA and normal controls (Figure 3.5F, G). However, the duration of the p53 pulse significantly increased in the knock down cells compared to normal controls (Figure 3.5F, H, p-value 0.007, t-test). The wider p53 pulses observed in the knock down cells are qualitatively similar to those observed in response to UV treatment, where p53 is primarily activated by the upstream kinase ATR (Ataxia telangiectasia and Rad3 related). We hypothesize that abatement of XRCC4 protein levels might prevent the effective ligation of a few DSBs in damaged cells. A failure to ligate DNA ends potentially promotes an increased resection of DNA at these break sites in an attempt to improve the annealing between the DNA strands and promote re-ligation. The resected ssDNA strands may then recruit and activate ATR, which subsequently modifies p53 and increases the duration of its pulse. Future work employing specific ATR inhibitors will aid the investigation of this hypothesis.

Future studies also comprise an investigation of other methods to perturb the kinetics of DSB repair to determine if altering the rates of repair affects the decision to induce p53, as well as its dynamic behavior after DNA damage. This includes knocking down other DNA repair proteins such as Ku70/80 or DNA Ligase IV in the NHEJ pathway or BRCA1, BRCA2 or Rad51 in the HR pathway by using shRNA against these proteins or inhibiting their activity by using specific small molecular inhibitors. Future work also includes an exploration of other factors that influence the activation of p53 in response to DSBs. One potential factor that may affect a cell's decision to pulse is its cell cycle phase. Previous work from our group has demonstrated that cells show spontaneous pulses of p53 in basal, undamaged conditions. These pulses occur in cell cycle phases that are associated with low levels of intrinsic DNA damage. It is possible that spontaneous p53 pulses are followed by a refractory period during which a cell is unable to initiate a new pulse even if it is damaged. Observations of cells for several hours prior to damage to obtain their cell cycle stage and p53 history will determine if any of these potential factors influence p53 activation.

Furthermore, it is possible that the p53 response to DNA DSBs is highly deregulated in cancer cells such as the MCF7 cells we used in this study. It will be important to establish our fluorescent reporter system in primary cells or in a non-transformed cell line such as the MCF10A breast epithelial cell line to investigate if normal cells are more uniform in their response to DNA damage. Similar investigations carried out in multiple tumor cell lines will determine how different cancers activate p53 in response to DNA DSBs.

Experimental procedures

Cell culture

Human breast cancer epithelial MCF7 cells were grown in RPMI 1640 medium supplemented with 10% fetal calf serum, 100 U/mL penicillin, 100 μg/mL streptomycin and 250 ng/mL fungizone (Gemini Bio-Products). When required, the medium was supplemented with selective antibiotics (400 μg/mL G418, 5 μg/mL blasticidin, 50 μg/mL hygromycin). When indicated, medium was replaced with fresh medium supplemented with Neocarzinostatin (National Cancer Institute) or with the DNA-PK inhibitor NU7026 (used at 10 μM, Sigma) during experiments. Irradiation treatments were carried out in a ^{60}Co irradiator.

Cell Line Construction

The original pCMV-EGFP-53BP1 construct was kindly provided by Prof. Yasuhisa Adachi (Jullien et al., 2002). We generated our pEF1α-mCherry-53BP1 plasmid by replacing GFP with mCherry and combining this fluorescent protein-cDNA fragment with the EF1α promoter in a vector harboring a blasticidin resistance cassette using standard molecular biology techniques. This plasmid was stably transfected into MCF7 cells using FuGENE6 (Roche), which were maintained in selective media and sorted into single cells using fluorescence activated cell sorting to generate a clonal population. Our pMT-p53-Venus plasmid has been previously reported (Batchelor et al., 2008). Stable, clonal cell lines were established as described above.

For constructing the pUbC-H2B-CFP vector, the H2B coding sequence was amplified by PCR from the vector pBOS-H2BGFP (BD Bioscience). Using Multiside Gateway technology (Invitrogen), the PCR product was combined with the UbC promoter and CFP tag in a lentiviral vector harboring a hygromycin resistance cassette. This plasmid was transfected into 293T cells together with the corresponding packaging plasmids to generate replication-defective viral particles using standard protocols, which were used to stably infect the engineered MCF7 cell line.

To generate XRCC4 knock-down cells, XRCC4 shRNA (TRCN40114) was obtained from OpenBiosystems. Lentiviral particles expressing XRCC4 shRNA or non-specific scramble shRNA (TRCN130036) were produced in 293T cells. MCF7 cells expressing all three reporters (53BP1-mCherry, p53-Venus and H2B-CFP) were infected with 1 ml of cell supernatant collected from the 293T cells.

Analysis of gene expression

Cells were harvested and total RNA was extracted using the RNeasy protocol (Qiagen). RNA concentrations were quantified by measuring absorbance at 260 nm. Equal RNA levels were used to generate complementary DNA using the high-capacity cDNA reverse transcription protocol (Applied Biosystems). Quantitative PCR was then performed using reaction mixtures of 8.4 ng total RNA, 100 nM primer (XRCC4 forward: CTG AAA TGA CTG CTG ACC GAG ATC C; XRCC4 reverse: TTA CAG CAG CTG AAG CCA ACC CAG AG; GAPDH forward: CAT GTT CGT CAT GGG TGT GAA CCA; GAPDH reverse: AGT GAT GGC ATG GAC TGT GGT CAT), and SYBR Green

reagent (Applied Biosystems). Reactions were set up in triplicate and run on a iCycler iQ PCR machine (BioRad).

Western Blot Analysis

Harvested cells were lysed in the presence of protease and deacetylase inhibitors. Total protein levels were quantified using the BCA assay (Pierce). Equal protein amounts were separated by electrophoreses on a 4%–12% Bis-Tris gradient gel (Invitrogen) and transferred to a PVDF membrane by electroblotting. The membrane was blocked with 5% nonfat dried milk and incubated overnight with primary antibody (anti-XRCC4 rabbit polyclonal, Abcam ab145, 1:1000 dilution). The membrane was washed and incubated with secondary antibody coupled to peroxidase, and protein levels were detected with chemoluminiscence (ECL plus, Amersham) after additional washing steps. XRCC4 levels were quantified by normalizing to total β-actin (Sigma).

Time-Lapse Microscopy

24h prior to microscopy, cells were plated in RMPI lacking riboflavin and phenol red in poly-D-lysine coated glass-bottom plates (MatTek Corporation). The medium was supplemented with 10% fetal calf serum, 100 U/mL penicillin, 100 μg/mL streptomycin, 250 ng/mL fungizone (Gemini Bio-Products) and 10 mM HEPES. Cells were imaged on a Nikon Eclipse Ti inverted microscope with a Plan Apo 60X oil objective (NA 1.4), Hamamatsu Orca ER camera and a Perfect Focus System. The microscope was surrounded by a custom enclosure to maintain constant temperature and atmosphere. The filter sets used were CFP - 436/20 nm; 455 nm; 480/40 nm (excitation; beam splitter;

emission filter), YFP - 500/20 nm; 515 nm; 535/30 nm; and mCherry - 560/40 nm; 585 nm; 630/75 nm (Chroma). Images were acquired every 15 mins in the phase, YFP and CFP channels and every 30 mins in mCherry channel for 8-12 hrs. We acquired 7 z-sections with a step size of 1 μm in the mCherry channel. Image acquisition was controlled by MetaMorph software (Molecular Devices).

Image Analysis

53BP1 foci were analyzed using custom written algorithms in Matlab (Mathworks). In brief, image stacks were first enhanced using blind deconvolution (AutoQuant), and were then converted to 2D maximum projections. Nuclei were segmented the H2B-CFP signal. For each nucleus, the background signal was first reduced by a Tophat transformation, following which the edges were detected using the Canny method. Foci were determined from the edges using morphological transformations and thresholding. Touching foci were then separated by a marker-directed watershed algorithm. We analyzed p53 trajectories in single cells using previously described algorithms (Loewer et al., 2010).

Immunofluorescence

Cells were grown on number 1.5 glass coverslips coated with poly-L-lysine (Sigma-Aldrich). They were fixed with 2% paraformaldehyde, permeabilized with 0.2% Triton/PBS and blocked with 5% goat serum supplemented with 1% bovine serum albumin. Cells were treated with primary antibody to detect γ-H2AX (mouse monoclonal JBW301, Upstate, 1:700 dilution) or XRCC4 (rabbit polyclonal ab145, Abcam, 1:500 dilution), washed and treated with secondary antibody conjugated with

Alexa Fluor 647 (Molecular Probes). After washing, cells were stained with Hoechst (Molecular Probes) and embedded in Prolong Antifade (Invitrogen). Immunofluorescence preparations were imaged on the microscope described for live cell imaging and automated segmentation was performed in Matlab (MathWorks) with algorithms from CellProfiler (Carpenter et al., 2006).

References

Ahn, J.Y., Schwarz, J.K., Piwnica-Worms, H., and Canman, C.E. (2000). Threonine 68 phosphorylation by ataxia telangiectasia mutated is required for efficient activation of Chk2 in response to ionizing radiation. Cancer Res *60*, 5934-5936.

Anderson, L., Henderson, C., and Adachi, Y. (2001). Phosphorylation and rapid relocalization of 53BP1 to nuclear foci upon DNA damage. Mol Cell Biol *21*, 1719-1729.

Bakkenist, C.J., and Kastan, M.B. (2003). DNA damage activates ATM through intermolecular autophosphorylation and dimer dissociation. Nature *421*, 499-506.

Barak, Y., Juven, T., Haffner, R., and Oren, M. (1993). mdm2 expression is induced by wild type p53 activity. Embo J *12*, 461-468.

Batchelor, E., Mock, C.S., Bhan, I., Loewer, A., and Lahav, G. (2008). Recurrent initiation: a mechanism for triggering p53 pulses in response to DNA damage. Mol Cell *30*, 277-289.

Bekker-Jensen, S., Lukas, C., Melander, F., Bartek, J., and Lukas, J. (2005). Dynamic assembly and sustained retention of 53BP1 at the sites of DNA damage are controlled by Mdc1/NFBD1. J Cell Biol *170*, 201-211.

Buscemi, G., Perego, P., Carenini, N., Nakanishi, M., Chessa, L., Chen, J., Khanna, K., and Delia, D. (2004). Activation of ATM and Chk2 kinases in relation to the amount of DNA strand breaks. Oncogene *23*, 7691-7700.

Carpenter, A.E., Jones, T.R., Lamprecht, M.R., Clarke, C., Kang, I.H., Friman, O., Guertin, D.A., Chang, J.H., Lindquist, R.A., Moffat, J.*, et al.* (2006). CellProfiler: image analysis software for identifying and quantifying cell phenotypes. Genome Biol *7*, R100.

Haupt, Y., Maya, R., Kazaz, A., and Oren, M. (1997). Mdm2 promotes the rapid degradation of p53. Nature *387*, 296-299.

Huang, L.C., Clarkin, K.C., and Wahl, G.M. (1996). Sensitivity and selectivity of the DNA damage sensor responsible for activating p53-dependent G1 arrest. Proc Natl Acad Sci U S A *93*, 4827-4832.

Jiang, H., Reinhardt, H.C., Bartkova, J., Tommiska, J., Blomqvist, C., Nevanlinna, H., Bartek, J., Yaffe, M.B., and Hemann, M.T. (2009). The combined status of ATM and p53 link tumor development with therapeutic response. Genes Dev *23*, 1895-1909.

Jin, S., and Levine, A.J. (2001). The p53 functional circuit. J Cell Sci *114*, 4139-4140.

Jullien, D., Vagnarelli, P., Earnshaw, W.C., and Adachi, Y. (2002). Kinetochore localisation of the DNA damage response component 53BP1 during mitosis. J Cell Sci *115*, 71-79.

Karanam, K., Kafri, R., Loewer, A., and Lahav, G. (2012). Quantitative Live Cell Imaging Reveals a Gradual Shift between DNA Repair Mechanisms and a Maximal Use of HR in Mid S Phase. Mol Cell *47*, 320-329.

Kubbutat, M.H., Jones, S.N., and Vousden, K.H. (1997). Regulation of p53 stability by Mdm2. Nature *387*, 299-303.

Lahav, G., Rosenfeld, N., Sigal, A., Geva-Zatorsky, N., Levine, A.J., Elowitz, M.B., and Alon, U. (2004). Dynamics of the p53-Mdm2 feedback loop in individual cells. Nat Genet *36*, 147-150.

Levine, A.J. (1997). p53, the cellular gatekeeper for growth and division. Cell *88*, 323-331.

Loewer, A., Batchelor, E., Gaglia, G., and Lahav, G. (2010). Basal dynamics of p53 reveal transcriptionally attenuated pulses in cycling cells. Cell *142*, 89-100.

Matsuoka, S., Rotman, G., Ogawa, A., Shiloh, Y., Tamai, K., and Elledge, S.J. (2000). Ataxia telangiectasia-mutated phosphorylates Chk2 in vivo and in vitro. Proc Natl Acad Sci U S A *97*, 10389-10394.

Schultz, L.B., Chehab, N.H., Malikzay, A., and Halazonetis, T.D. (2000). p53 binding protein 1 (53BP1) is an early participant in the cellular response to DNA double-strand breaks. J Cell Biol *151*, 1381-1390.

Vousden, K.H., and Lane, D.P. (2007). p53 in health and disease. Nat Rev Mol Cell Biol *8*, 275-283.

Wahl, G.M., Linke, S.P., Paulson, T.G., and Huang, L.C. (1997). Maintaining genetic stability through TP53 mediated checkpoint control. Cancer Surv *29*, 183-219.

Wu, X., Bayle, J.H., Olson, D., and Levine, A.J. (1993). The p53-mdm-2 autoregulatory feedback loop. Genes Dev *7*, 1126-1132.

Chapter 4: Discussion and Future Perspectives

Defective DNA repair is both the origin and the weakness of many cancer cells. Several tumors arise from a perturbed DNA damage response that generates mutations in genes that regulate cell growth and division. Tumor cells also depend on DNA repair to survive cancer treatments that induce DNA DSBs, such as radiation and chemotherapy. Their reduced repair capacity makes them particularly sensitive to inhibition of the remaining repair proteins, offering the possibility that using DNA repair inhibitors in combination with treatments that generate DNA damage or trap cells in states with an increased requirement for specific repair pathways, will be more effective in removing tumors with minimal toxicity to the surrounding healthy cells. In order to exploit this inherent vulnerability of cancer cells effectively, it is first necessary to develop a comprehensive understanding of the coordinated behavior of the alternate DSB repair pathways and their ability to compensate for each other in different basal conditions and cellular circumstances. DNA repair is also intimately interconnected with pathways that regulate cell fate decisions such as cell cycle arrest, senescence or cell death. Knowledge of how DNA repair synergizes with the activation of cell fate regulators for the execution of specific cellular outcomes is vital to gain a full appreciation of the processes that prevent transformation and for the intelligent design of cancer therapies.

My research focused on developing a detailed, quantitative understanding of how the kinetics of repair and the balance between the alternate DSB repair pathways changes with cell cycle, and on characterizing the relationship between DSBs, repair, and the activation of the tumor suppressor p53 in human cells. DNA repair and the activation of cell fate regulators in response to damage are inherently dynamic processes and time

separated events; hence to precisely characterize the relationship between them as well as connect their behavior with cell state prior to damage, it is necessary to follow these events over time in the same cell. We therefore developed fluorescent reporters to quantify DSBs, HR, cell cycle and p53 accumulation in individual, living cells.

We first established a cell line that stably expressed our DSB, HR and cell cycle reporters and determined how the rates of repair and the activation of HR change throughout the cell cycle. We found that the kinetics of DSB repair vary with cell cycle phase at the time of damage. We measured the balance between NHEJ and HR in unperturbed, wild type cells and showed that NHEJ is the dominant repair pathway in G1 and in G2 phase when HR is functional. We found that S and G2 cells use both NHEJ and HR for repair and higher use of HR correlates with slower repair. Further, we demonstrated that the balance between NHEJ and HR changes gradually as cells enter or exit S phase and maximal use of HR occurs in mid-S at the peak of DNA replication. Our data therefore suggests that the level of active DNA replication influences the use of HR in human cells. To further consolidate this finding, it is essential to disentangle the effect of cyclin activity and the presence of replicating DNA on the choice of repair. No perturbation is currently known to affect one and not the other in mammalian cells, hence, a definitive conclusion will first require the identification and characterization of new perturbations that prohibit DNA replication but allow cells to progress through S phase. One potential perturbation is to knock down or inhibit essential proteins of the pre-replication complexes that regulate the firing of replication origins. Cdc7, Dbf4 and the Mcm proteins are some candidates that can be explored for this perturbation.

Additionally, future studies also include knocking down or inhibiting various repair proteins in both DSB repair pathways to investigate how perturbing the pathways affects the balance between them. Such analyses will provide insights into the ability of the two repair pathways to compensate for each other under altered conditions of repair. It is likely that inhibition of some repair proteins will lead to an increased use of the alternate DSB repair pathway, while knocking down other proteins may prevent DSB joining by both repair pathways. For example, knocking down CtIP or BRCA1 that function in the DNA resection step of the HR pathway may allow an increased processing of DSBs by NHEJ, while knocking down HR proteins that function after DNA resection (for example Rad51, BRCA2) may prevent DSB joining by both HR and NHEJ. Similar measurements of the balance between NHEJ and HR in multiple cancer cell lines that lack different repair proteins, as well as in normal cells, are critical for understanding the coordinated behavior of the repair pathways in different tissues and cellular contexts. Further, many cancer cells also have disabled checkpoints; for example, the U2OS cells we used in our study lack a stable G1/S arrest. This allows damaged G1 cells to enter S phase and activate HR for repair. It will be important to determine how tumors with different checkpoint profiles activate and balance NHEJ and HR and to compare their behavior with non-transformed cells. Collectively, such analyses will enable the design of more selective and efficacious cancer treatments.

In our study, we imaged cells at hourly intervals post DNA damage. This provided snapshots of the total numbers of DSBs over time in each cell; however, it did not allow tracking individual foci between time points. Development of techniques that permit

tracking discrete foci will enable observations of individual repair events over time in the same cell. Such observations are essential to determine if individual breaks in a cell switch between the two repair pathways during the course of repair and the timing when this occurs. They will also enable an investigation of the possibility that S phase cells repair more slowly due to new damages being created in this phase during DNA replication.

Next, we explored the connection between the number and repair of DNA DSBs and the activation of the tumor suppressor p53. We combined our reporter for DSBs with the fluorescent reporter for p53 to quantify the level of damage and the activation of p53 in the same, living cell. We showed that there is a linear correlation between the number of DSBs and the probability of activating a p53 pulse. However, there is no clear threshold of damage above which all damaged cells unanimously induce a p53 response. We found that the decision to activate a p53 pulse is potentially influenced by cell-specific factors. Further, we eliminate the rates of DSB repair as a factor that affects this decision. We also demonstrated that the dynamical properties of the p53 pulse are independent of the speed with which breaks are repaired. Remarkably, perturbing the NHEJ repair pathway by reducing XRCC4 protein levels did not decrease the rates of DSB repair. However, this perturbation increased the duration of the p53 pulse. Future studies comprise knocking down or inhibiting additional repair proteins in both pathways by using shRNA or small molecule inhibitors, in order to generate a longer delay in the rates of DSB repair. This will allow measurements of how altering the kinetics of repair beyond the normal variation observed in a damaged population affects the decision to activate p53 in

response to DNA damage. Perturbations to different repair proteins will also determine if the alteration in p53 dynamics occur exclusively in response to abatement of XRCC4 levels. Recent work from our group has shown that the dynamical behavior of p53 in response to DSBs encodes critical cell-fate decisions; hence understanding how perturbations of key repair proteins alter the p53 response will provide new and important insights for the treatment of tumors with different genetic profiles and repair deficiencies.

Future studies also include an exploration of other factors that potentially influence a cell's decision to activate a p53 pulse in response to DNA DSBs. One potential factor is the expression level of key proteins of the p53 pathway such as wip1, mdm2 and p53 itself. The stimulus provided by low numbers of DSBs may not be sufficient to initiate p53 accumulation in cells that express very low levels of p53 or high levels of its negative regulators wip1 or mdm2. Another factor that might affect a cell's decision to activate a p53 pulse, is its cell cycle stage. Cells damaged in different cell cycle phases may differ in their threshold of DSBs required for p53 activation. Moreover, undamaged cells show spontaneous p53 pulses in cell cycle phases that are associated with low levels of intrinsic DNA damage. It is possible that these spontaneous pulses are followed by a refractory period during which a cell is unable to initiate a new pulse even if it is damaged. Observations of the cell cycle stage and p53 behavior of cells prior to damage will determine if any of these potential factors influence p53 activation.

Our analyses showed that some cells do not activate p53 even at high levels of DNA damage. One possibility is that the induction of p53 in response to DSBs is highly

deregulated in cancer cells such as the MCF7 cells we used in our study. It will be important to determine if normal, non-transformed cells are more uniform in their p53 response, and activate p53 at a low number of DSBs. Additionally, measurements of the number of DSBs and p53 activation in multiple cancer cell lines will enable an understanding of their potential to uniformly induce p53 in response to DNA damage, and will provide insights into their sensitivity to radiation and chemotherapeutic treatments.

Finally, the use of fluorescent reporters to measure DNA damage responses in live cells, combined with the quantitative, single cell techniques developed in this work present powerful tools for addressing additional long-standing, fundamental questions in the DNA damage and repair field. For example, studies using reporters for different sub-pathways of homology dependent repair can provide insights into their interplay and balance at different stages of repair. Similar analyses of different mediator and repair proteins will help determine the timing at which commitment to a specific repair pathway occurs and the factors leading to these decisions. Additionally, investigations combining reporters for repair and checkpoint regulators with indicators of cell fates will instruct us on how the rates and mechanisms of repair correlate with time through the checkpoints and with the execution of specific cellular outcomes. Such analyses afford an integrated, systems-level understanding of the complex interrelationships between the myriad signaling and repair pathways that comprise the DNA damage response in mammalian cells.